1984

Influence of the bcc to tetragonal transformation on superconductivity in "La3X4"(X = S or Se)

Ying-Cheun Spring Yeh
Iowa State University

INFORMATION TO USERS

This reproduction was made from a copy of a document sent to us for microfilming. While the most advanced technology has been used to photograph and reproduce this document, the quality of the reproduction is heavily dependent upon the quality of the material submitted.

The following explanation of techniques is provided to help clarify markings or notations which may appear on this reproduction.

1. The sign or "target" for pages apparently lacking from the document photographed is "Missing Page(s)". If it was possible to obtain the missing page(s) or section, they are spliced into the film along with adjacent pages. This may have necessitated cutting through an image and duplicating adjacent pages to assure complete continuity.

2. When an image on the film is obliterated with a round black mark, it is an indication of either blurred copy because of movement during exposure, duplicate copy, or copyrighted materials that should not have been filmed. For blurred pages, a good image of the page can be found in the adjacent frame. If copyrighted materials were deleted, a target note will appear listing the pages in the adjacent frame.

3. When a map, drawing or chart, etc., is part of the material being photographed, a definite method of "sectioning" the material has been followed. It is customary to begin filming at the upper left hand corner of a large sheet and to continue from left to right in equal sections with small overlaps. If necessary, sectioning is continued again—beginning below the first row and continuing on until complete.

4. For illustrations that cannot be satisfactorily reproduced by xerographic means, photographic prints can be purchased at additional cost and inserted into your xerographic copy. These prints are available upon request from the Dissertations Customer Services Department.

5. Some pages in any document may have indistinct print. In all cases the best available copy has been filmed.

University Microfilms International
300 N. Zeeb Road
Ann Arbor, MI 48106

Yeh, Ying-Cheun Spring

INFLUENCE OF THE BCC TO TETRAGONAL TRANSFORMATION ON SUPERCONDUCTIVITY IN "LANTHANUM(3)X(4)" (X = SULFUR OR SELENIUM)

Iowa State University PH.D. 1984

PLEASE NOTE:

In all cases this material has been filmed in the best possible way from the available copy. Problems encountered with this document have been identified here with a check mark __✓__.

1. Glossy photographs or pages _____
2. Colored illustrations, paper or print _____
3. Photographs with dark background _____
4. Illustrations are poor copy _____
5. Pages with black marks, not original copy _____
6. Print shows through as there is text on both sides of page _____
7. Indistinct, broken or small print on several pages __✓__
8. Print exceeds margin requirements _____
9. Tightly bound copy with print lost in spine _____
10. Computer printout pages with indistinct print _____
11. Page(s) _____ lacking when material received, and not available from school or author.
12. Page(s) _____ seem to be missing in numbering only as text follows.
13. Two pages numbered _____. Text follows.
14. Curling and wrinkled pages _____
15. Dissertation contains pages with print at a slant, filmed as received _____
16. Other _____

_____

_____

University
Microfilms
International

Influence of the bcc to tetragonal transformation on superconductivity in "La_3X_4" (X = S or Se)

by

Ying-Cheun Spring Yeh

A Dissertation Submitted to the
Graduate Faculty in Partial Fulfillment of the
Requirements for the Degree of
DOCTOR OF PHILOSOPHY

Department: Materials Science and Engineering
Major: Metallurgy (Physical Metallurgy)

Approved:

Signature was redacted for privacy.

In Charge of Major Work

Signature was redacted for privacy.

For the Major Department

Signature was redacted for privacy.

For the Graduate College

Iowa State University
Ames, Iowa

1984

TABLE OF CONTENTS

I. INTRODUCTION

Lanthanum selenide La_3Se_4 has been known to be a superconductor with a transition temperature (T_c) of 7 - 8.6 K.[1-5] It has bcc-Th_3P_4 structure type[2,6-8] which extends in a solid solution system to La_2Se_3 with a little change in lattice parameter. It undergoes a structural phase transformation at 65 K from a cubic to a tetragonally distorted unit cell.[3-5,9,10] Superconducting La_3S_4[1,3-5,11-13] which has the same crystal structure and undergoes the same structural phase transformation,[3-5,9,10,12-14] has been extensively studied by several investigators. The phase transformations in La_3Se_4 and LaS_x alloys ($1.333 \leq x \leq 1.362$) have been found in the measurements of (1) the lattice parameters,[9,13] (2) the electrical resistivity,[3,12,15] (3) the magnetic susceptibility,[12,13] and (4) the elastic stiffness constants[4,14] as a function of temperature.

In bcc-Th_3P_4 structure type of LaX_x (X= S or Se, $1.333 \leq x \leq 1.500$) system, there are four molecules per unit cell. The X atoms occupy the 16(c) positions and the La atoms and vacancies randomly occupy the 12(a) positions of the space group $I\bar{4}3d$ in the International Table. The La atom or vacancy is surrounded by eight X atoms forming a distorted eight-vertex polyhedron. The X atom is surrounded by six La atoms or vacancies forming a distorted octahedron. In La_3X_4

alloy, La atoms (also X atoms) zigzag alternately up and down forming infinite chains along some certain directions. In La_3X_4 ($x = 1.333$) alloy, there are no vacancies in the structure. As x is varied continuously from 1.333 to 1.500, the concentration of vacancies (N_v) changes. The concentration of conduction electrons (N_e) likewise varies. When $x = 1.5$, $N_e = 0$ and the alloy $LaX_{1.5}$ is an insulator or a semiconductor. When $x < 1.5$, the LaX_x alloy has some conduction electrons and eventually, with decreasing x, LaX_x becomes metallic. The constancy of structure with changes in electron and vacancy concentrations makes the LaX_x systems interesting for investigating the dependences of some physical properties, in particular superconductivity and structural phase transformation, on material parameters.

Recently, the works by Ikeda et al.[15,16] have shown that the optimum superconducting properties in LaS_x alloys exist for the composition, x_c, at which the structural phase transition is just suppressed. The x_c has been determined to be 1.362. With $1.362 \leq x \leq 1.500$, the bcc structure is stable at low temperatures down to 0 K. The superconducting transition temperature and the upper critical magnetic field at 0 K ($H_{c2}(0)$) increase with decreasing x. For $1.333 < x < 1.362$, the tetragonal phase becomes stable below T_M. As x decreases to 1.333, T_M increases, T_c remains almost constant and $H_{c2}(0)$ decreases. The results of the heat capacity and

electrical resistivity measurements for LaS_x alloys taken from Refs. 15 and 16 are given in Fig. 1. The dashed lines are the expected values if the cubic phase did not transform to the tetragonal phase. Thus, it suggests that the cubic phase if stabilized should have higher values of T_c, γ, $H_{c2}(0)$ and ρ_r. The rapid rise in T_c with pressure[3,5] in La_3S_4 and La_3Se_4 also suggests that the metastable bcc phase existing under pressure has a higher T_c value. Previous works by several investigators have also shown that a high T_c alloy or a non-superconducting alloy which is predicted to have a high T_c often distorts to a lower symmetry structure with temperature.[17-27]. The values of T_c and γ are induced or enhanced if such phase transformation did not occur.[19,21-23,25-27] The high temperature phase can be preserved by different preparation methods,[19,22] alloying with a third element,[24] or applying pressures.[25-27]

The mechanism (mechanisms) of the structural phase transformation in LaX_x system is (are) unknown. The band Jahn-Teller model has been employed by Westerholt et al.[10,28] to explain this phase transformation based on the magnetic field dependence of the structural phase transformation temperature[10] and the correlation of the density of states ($N(\epsilon_F)$) and the tetragonal distortion parameter (c/a).[28] Hence, conduction electrons may play a role to drive the transformation within this model. Ford et al.[14] based on the

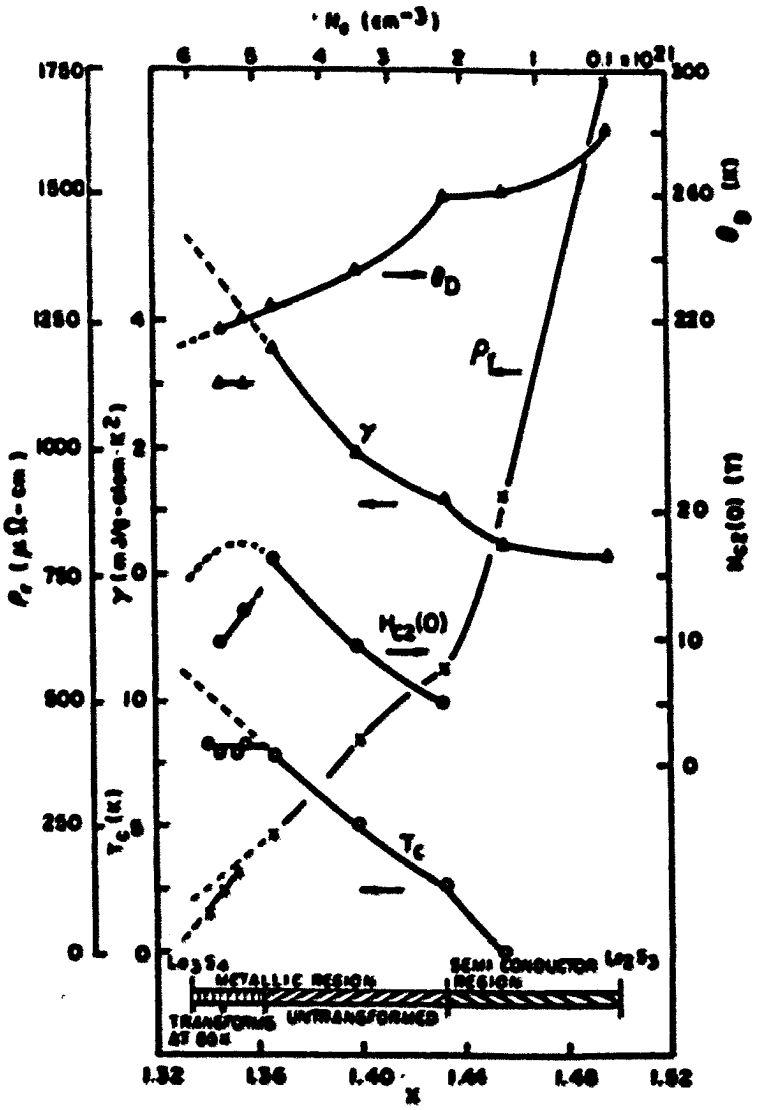

Figure 1. Summary of the results of the heat capacity and electrical resistivity measurements for the LaS_x ($1.333 \leq x \leq 1.500$) alloys taken from Ref. 16. The dashed lines are the expected values if the alloys remained cubic at low temperatures

small tetragonal distortion (maximum a/c is 1.016 in La_3S_4) from the bcc-Th_3P_4 type and no change in the number of formula units per unit cell has suggested that the transition is elastic in nature. Detailed phonon dispersion curves are needed to confirm this latter model.

In this paper, the studies are emphasized on (1) the compositional (or N_e and N_v) dependences of T_M, T_c and $H_{c2}(0)$ in the $LaSe_x$ solid solution system, (2) the alloying effects on T_M, T_c, and $H_{c2}(0)$ of the pseudobinary sulfide system by substitution of up to six percent Mg, Ca, Y, Ce or Th metals for La, (3) the effect of Se/S ratios on T_M, T_c and $H_{c2}(0)$ in the $La(S_{1-y}Se_y)_x$ solid solution system, and (4) the influence of the lattice instability on superconductivity in "La_3X_4" (X = S or Se). The experiments mainly include dc-electrical resistivity measurements, low temperature heat capacity measurements in magnetic fields, and low magnetic field low frequency a. c. magnetic susceptibility measurements. In addition to these experiments a great deal of care has been taken in (1) the preparation of La_3X_4 base alloys to insure that the alloys are homogeneous and well-characterized; and (2) the calibration of the germanium resistance thermometer (GRT), which is used in the heat capacity measurements in magnetic fields.

II. BACKGROUND THEORY

A. Electrical Resistivity

There are excellent text books[29,30] for the subjects of the electrical resistivity, heat capacity and superconductivity of the metals and alloys. Here, only a brief review of the theory is given.

For a conductor of uniform cross-sectional area A and length ℓ in which a current I flows, a voltage V between its ends will be developed and is given by the relation

$$V = I \rho \ell / A = I R \qquad (2\text{-}1)$$

where $\rho = R A / \ell$ is the electrical resistivity which is characteristic of that particular conductor and R is the electrical resistance. Eq. (2-1) is an expression of Ohm's Law. The measured resistivity $\rho(T)$ can be separated into two parts, commonly known as Matthiessen's rule,[29] which is written as

$$\rho(T) = \rho_r + \rho_i(T) \qquad (2\text{-}2)$$

where ρ_r is the residual resistivity determined at the absolute zero temperature, $\rho_i(T)$ is the intrinsic or ideal resistivity and T is the temperature. The quantity ρ_r arises from the scattering of conduction electrons by impurities, defects or strains in the metal lattice. The quantity $\rho_i(T)$

is caused by the interaction of the conduction electrons with the thermal vibrations of the ions of the lattice, normally knowns as phonons. For a magnetic metal, there is another contribution, called $\rho_m(T)$, to the electrical resistivity for the temperature below the magnetic transition temperature. The measured resistivity $\rho(T)$ is then written as

$$\rho(T) = \rho + \rho_i(T) + \rho_m(T) \qquad (2\text{-}3)$$

The $\rho_m(T)$ is due to scattering from the disordered spin arrangements.

To a fair approximation at least, the ρ_r term is independent of the temperature and the $\rho_i(T)$ term is linear in temperature for most metals above $\Theta_R/2$. Θ_R is a temperature characteristic of the metals' lattice resistivity in the same way as the Debye temperature (Θ_D) is a characteristic of a solids' lattice specific heat. Θ_R value is close to that of the Θ_D. At low temperatures, i.e. below $\Theta_R/4$, the $\rho_i(T)$ roughly varies as T^3 in many metals and as T^5 in several others. The $\rho_m(T)$ term is of the form

$$\rho_m(T) = b\,T^2 \qquad (2\text{-}4a)$$

or

$$\rho_m(T) = b\,T^2 \exp(-\Delta/kT) \qquad (2\text{-}4b)$$

where b is a constant, k is the Boltzmann constant and Δ is an energy gap representing the minimum energy to excite a spin

wave. The exponential term is included in Eq. (2-4b) to take into account of the magnetic anisotropy in some metals.

In this study, the selenides and sulfides are non-magnetic so that there is no $\rho_m(T)$ term in the measured resistivity values. Since we are interested in the crystallographic phase transformations in the selenides and sulfides, the resistivity measurements have been made to see such phase changes upon cooling. For a change to a different crystal structure, the electron-phonon interaction is modified and this results in a different proportionality constant in the $\rho_i(T)$ term. This is revealed in a change of the slope in the measured $\rho(T)$ vs. T plot.

B. Heat Capacity and Superconductivity

For a non-magnetic conductor, the observed heat capacity is of the form

$$C = C_e + C_{latt} \tag{2-5}$$

where C_e and C_{latt} are the electronic and lattice heat capacities respectively. The C_e term varies linearly with temperature as given by

$$C_e = \gamma T \tag{2-6}$$

where γ is called the electronic heat capacity constant. In the free electron model, the γ is related to the density of

states at the Fermi energy at 0 K (N(0)) and the relationship is given as

$$\gamma = 2 \pi^2 k^2 N(0) / 3 \qquad (2\text{-}7)$$

where k is the Boltzmann constant. Note that the electronic term measures merely an averaged density of states at the Fermi surface. The electron-phonon interaction will enhance γ by a factor of $(1+\lambda)$ where λ is called the electron-phonon coupling parameter. Now γ is related to N(0) as

$$\gamma = 2 \pi^2 k^2 N(0) (1+\lambda) / 3 \qquad (2\text{-}8)$$

In dilute alloys, especially of elements which have similar electronegativities and atomic radii, the metal added goes into solid solution with no change of the crystal structure. The rigid-band model assumes that the band structure remains unchanged and only the number of available electrons or the Fermi energy is altered. For alloying a metal with a higher valent metal, the extra electrons fill the band to a higher energy level. While lower valent metal added will decrease the Fermi energy. The observed variation of the γ value may then be attributed to the variation in N(0).

At low temperatures for which $T \leq \theta_D/50$, the lattice contribution to the heat capacity (C_{latt}) in terms of the Debye model can be expressed as

$$C_{latt} = \beta T^3$$

$$= 1.944 \times 10^6 \, T^3 / \Theta_D^3 \qquad (2\text{-}9)$$

where Θ_D is the Debye temperature which is characteristic of the phonon spectrum and the units of C_{latt} are in mJ/g-atom K.

From Eqs. (2-5), (2-6) and (2-9), a plot of C/T against T^2 should therefore be a straight line. The expression for C/T is given as

$$C/T = \gamma + \beta \, T^2 \qquad (2\text{-}10)$$

The intercept at 0 K gives γ value while the slope of the line gives β value from which Θ_D can be calculated.

The above discussion applies to the normal conductors. When a metal becomes superconducting at temperatures below T_c, the lattice heat capacity is assumed unchanged since no structural changes are involved but the electronic heat capacity is altered. The electronic heat capacity in the superconducting state (C_{es}) can be determined from the relation

$$C_{es} = C_s - C_n + \gamma \, T \qquad (2\text{-}11)$$

where s and n indicate the superconducting and normal states respectively. Experimentally, it has been found that C_{es} varies as

$$C_{es}/(\gamma T_c) = a \exp(-b \, T_c / T) \qquad (2\text{-}12)$$

The exponential variation of the heat capacity indicates the existence of an energy, 2Δ, separating the normal and superconducting electrons.

The BCS theory predicts that

$$C_{es}/\gamma T_c = 8.5 \exp(-1.44\ T_c / T) \quad \text{for } 2.5 < T_c/T < 6$$

$$= 26 \exp(-1.62\ T_c / T) \quad \text{for } 7 < T_c/T < 12 \qquad (2\text{-}13)$$

and the energy gap, 2Δ, is related to T_c by means of the relation

$$2\Delta = 3.52\ k\ T_c \qquad (2\text{-}14)$$

Another prediction of the BCS theory is that the jump in heat capacity at T_c ($\Delta C(T_c)$) is given as

$$\Delta C(T_c) = C_s(T_c) - C_n(T_c)$$

$$= C_{es}(T_c) - C_{en}(T_c)$$

$$= 1.43\ \gamma\ T_c \qquad (2\text{-}15)$$

where s and n denote superconducting and normal states respectively.

The thermodynamic functions derived from the heat capacity results are given below. The entropy at any temperature T may be uniquely expressed as

$$S_i(T) = \int_0^T C_i(T)/T \, dT \qquad (2\text{-}16)$$

where i is s or n for superconducting or normal state respectively. At $T = T_c$, $S_s = S_n$, i.e. the entropy values are equal for both states. The Gibbs free energy at any temperature can be expressed as

$$G_i(T) = U_i + (P\,V)_i - \int_0^T S_i(T) \, dT \qquad (2\text{-}17)$$

where i is s or n, U is the internal energy and PV is the product of the pressure and volume.

In a magnetic field H, the Gibbs free energy in the superconducting state ($G_s(T,H)$) is given as

$$G_s(T,H) = G_s(T) - 1/2\, M\, H \qquad (2\text{-}18)$$

where $G_s(T)$ denotes the superconducting Gibbs free energy in zero field and M is the induced moment given as

$$M = - H\, V / (4\,\pi) \qquad (2\text{-}19)$$

where V is the volume. On the equilibrium curve, i.e. $H = H_c$, the free energies of both states must be equal and so

$$\begin{aligned} G_n(T,H_c) &= G_s(T,H_c) \\ &= G_s(T) - 1/2\, M\, H_c(T) \\ &= G_s(T) + H_c^2(T)\, V / (8\,\pi) \end{aligned} \qquad (2\text{-}20a)$$

or

$$G_n(T,H_c) - G_s(T) = H_c^2(T)\ V\ /\ (8\ \pi) \qquad (2\text{-}20b)$$

where $H_c(T)$ is called the critical thermodynamic field. From Eq. (2-17) and with the assumption that the first two terms have same values in the normal and superconducting states, Eq. (2-20b) becomes

$$\begin{aligned} G_n(T,H_c) - G_s(T) &= -\int_0^T S_n(T,H_c)\ dT + \int_0^T S_s(T)\ dT \\ &= \int_T^{T_c} [\ S_n(T,H_c) - S_s(T)\ ]\ dT \\ &= H_c^2(T)\ V\ /\ (8\ \pi) \end{aligned} \qquad (2\text{-}20c)$$

The values of the $H_c(T)$ are related to the T empirically as

$$H_c(T) = H_o\ [\ 1 - (T\ /\ T_c)^2\ ] \qquad (2\text{-}21)$$

where H_o is the $H_c(T)$ value at 0 K.

The BCS theory explains the behavior of type I superconductors quite well and the above thermodynamic relations are obeyed. For a type II superconductor, the superconductivity is destroyed at a much higher field, called $H_{c2}(T)$. The $H_{c2}(T)$ is related to the $H_c(T)$ in the theory proposed by Maki.[31] He introduced the parameters κ_1, κ_2 and κ defined as

$$\kappa_1 = H_{c2}(T)\ /\ (\sqrt{2}\ H_c(T)) \qquad (2\text{-}22)$$

$$(dM/dH)_{H=H_{c2}} = 1\ /\ (4\ \pi\ \beta_A\ (2\ \kappa_2^{\ 2} - 1)) \qquad (2\text{-}23)$$

and

$$\kappa = \kappa_1(T_c) = \kappa_2(T_c) \qquad (2\text{-}24)$$

where $(dM/dH)_{H=H_{c2}}$ is the slope of the magnetization curve at $H_{c2}(T_H)$ and β_A is equal to 1.16 for a triangular lattice which is more stable than the square lattice near H_{c2}. According to Goodman,[32] dM/dH at $H_{c2}(T_H)$ can be obtained from the relation :

$$\Delta C(H) \,/\, (V\, T_H) = (dM \,/\, dH)_{\text{at } H_{c2}} \times (dH_{c2} \,/\, dT)^2_{\text{at } T_H} \qquad (2\text{-}25)$$

where $\Delta C(H)$ is the jump in heat capacity in field H and T_H is the superconducting temperature in that field. From Eqs. (2-23) and (2-25), the values of $\kappa_2(T)$ can be calculated.

According to Kim <u>et al</u>.[33] the upper critical field in Tesla at 0 K for type II superconductors can be calculated by using

$$H_{c2}(0) = 3.11\, \gamma\, \rho_r\, T_c \,/\, V \qquad (2\text{-}26)$$

where ρ_r is the normal state residual resistivity in ohm-cm, γ and V are in cgs units.

III. EXPERIMENTAL PROCEDURE

A. Sample Preparation

The metals used in this study, La, Th, Y, Ce, Mg and Ca, were purified at the Ames Laboratory. The La metal was purified to ~ 99.8 %. The analyses are shown in Table 1 for all the impurity elements in La metal. The sulfur was in powder form and the selenium was in pellet form about 2 mm in diameter. They were 99.999 % pure obtained from the American Smelting and Refining Company. The La, Th, Y, and Ce metals were electropolished before use. For additions of up to six percent Th, Y, or Ce metals into La metal, the two metals were co-melted in an arc-melting furnace under an atmosphere of purified argon using a non-consumable W electrode. The buttons were inverted at least six times to ensure homogeneity. For an addition of three percent Mg or Ca to La, the two metals were sealed in a tantalum crucible which was then heated to above the La melting temperature in an induction furnace.

The La or La-M alloy was either rolled into a thin strip with a roller or cut into thin strips with a diamond saw. The metal strips were then combined with either S or Se in stoichiometric ratio and were sealed in double quartz tubes under some He gas. The constituents were reacted in the furnace at about 600-650 C until all the S or Se had reacted.

Table 1. Analyses of the La metal in atomic ppm (weight ppm in parentheses)

Element[a]	La metal	Element	La metal
H	1237 (9)	Al	5
O	573(66)	Nb	10
N	89 (9)	Si	< 3
C	139(12)	Cr	2
F	102(14)	Y	24
Fe	10 (4)	Ce	10
Cl	4	Pr	1
Cs	20	Nd	2.2
Ea	3	Gd	15
Cu	7	Tb	1

[a]All metallic impurity elements except Fe were determined by mass spectrometry (those not listed were present in quantities less than 1 ppm); H, O and N by vacuum fusion method; C by combustion-chromatography method; Fe by atomic absorption method; and F by the formation distillation and spectrophotometric determination of fluosilicic acid method.

The inner tube wall would look clean at this time. Then, the furnace temperature was raised to about 910 C which was slightly below the melting point of La metal, 920 C. If the temperature was raised above 920 C there was danger of the reaction of liquid La metal with the quartz tube. The reaction at 910 C took several days and was checked for completion by leaving one end of the tube outside the furnace. For a complete reaction, no S or Se vapor condensed at the cold end of the tube. After chemical reactions were completed, the reaction product was sealed in a tungsten crucible and melted in an induction furnace at 2000-2150 C. After melting, the alloy was heat-treated at 1700-1750 C for one to three weeks in a resistance furnace to ensure homogeneity. The single-phase alloy was bluish black. The presence of second phase LaS or LaSe, which usually occurred at the top and bottom surfaces of the sample, was quite evident from their gold color.

Optical metallography of the alloys were taken to check any second phases. The results are listed in Table 2. The X-ray Debye-Scherrer powdered patterns were taken to detect any second phases and to determine the lattice parameters, a_0. No second phase was seen in any pattern which indicated less than 5 % of a second phase was present. Optical metallography was much more reliable in this regard. A computer calculation which employed the Nelson and Riley extrapolation method was used to find a_0. The a_0 values are also listed in Table 2.

Table 2. The results of the optical metallography and the lattice parameters of the sulfides and selenides

Alloy[a]	Amount of second phase[b]	a_o (A)
$LaSe_{1.334}$	none[c]	9.0506
$LaSe_{1.348}$	——[d]	9.0528
$LaSe_{1.360}$	none	9.0553
$LaSe_{1.367}$	none	9.0484
$LaSe_{1.387}$	——	9.0503
$LaSe_{1.402}$	——	9.0479
$La(S_{.898}Se_{.102})_{1.358}$	none	8.7553
$La(S_{.51}Se_{.49})_{1.373}$	——	8.8936
$La(S_{.11}Se_{.89})_{1.377}$	——	9.0202
$La_{.98}Th_{.02}S_{1.333}$	large[e]	8.7124
$La_{.97}Th_{.03}S_{1.333}$[f]	large	8.7143
$La_{.96}Th_{.04}S_{1.333}$	large	8.7118
$La_{.98}Th_{.02}S_{1.341}$	small[g]	8.7163
$La_{.96}Th_{.04}S_{1.341}$	small	8.7144

$La_{.94}Th_{.06}S_{1.341}$	large	8.7090
$La_{.98}Th_{.02}S_{1.351}$	small	8.7182
$La_{.96}Th_{.04}S_{1.351}$	large	8.7165
$La_{.94}Th_{.06}S_{1.351}$	large	8.7129
$La_{.97}Th_{.03}S_{1.360}$	none	8.7167
$La_{.98}Y_{.02}S_{1.339}$	none	8.7145

---

[a]The chemically determined compositions are used for all the $La(S_{1-y}Se_y)_x$ alloys; and $LaSe_x$ alloys for x = 1.348, 1.360 and 1.367. The nominal compositions are used for all other pseudobinary alloys.

[b]For $LaSe_{1.334}$, $La_{.96}Th_{.04}S_{1.333}$ and $La_{.98}Y_{.02}S_{1.339}$, second phases of LaSe and LaS were seen on the outer surfaces of the samples after about 1720 C heat treatment. Optical metallography was taken for the central portion of each alloy.

[c]No second phase is visible at 100 X optical metallography.

[d]Optical metallography was not available.

[e]The amount of second phases is between 1 to 5 %.

[f]The alloy after first heat treatment at 1725 C for one week had two peaks in the heat capacity plot. It was given a second heat-treatment at 1700 C for three weeks. Then, the heat capacity plot had only one peak indicating that the alloy was homogeneous.

[g]The amount of second phase is visible but is less than 1 %.

B. Electrical Resistivity Measurements

The sample resistance was measured by the standard dc four-probe current reversal method over the temperature range 4 to 300 K. The apparatus belonged to Dr. S. Legvold in the Physics Department and was described in detail in the theses of D. W. Mellon[34] and T. A. Vyrostek.[35] Fig. 2 shows the heat leak chamber and the sample holder used in the experiment. Fig. 3 gives an enlarged view of the sample holder area. The sample was cut into a rectangular rod shape by a diamond saw. It was then glued to a flat surface of a stainless steel grinding device and ground on a sand paper set on another parallel hard surface. Since the alloys were brittle, those with visible micro-cracks were simply ground by holding them with hand against the sand paper. The rectangular sample was then glued by a silver paste to metal clamps through which the current passed. Two sharpened phosphor-bronze strips stycasted to a brass block were used as a voltage probe. The voltage probe was set in place and held down over the sample with a tantalum spring. The spring was set in the radial notch located in the sample holder.

The electronic circuits mainly consisted of three parts : one to measure the voltage developed between two known points on the sample, and the second to measure the temperature of the sample and the third to control the temperature of the sample. A constant-current source was used to supply a

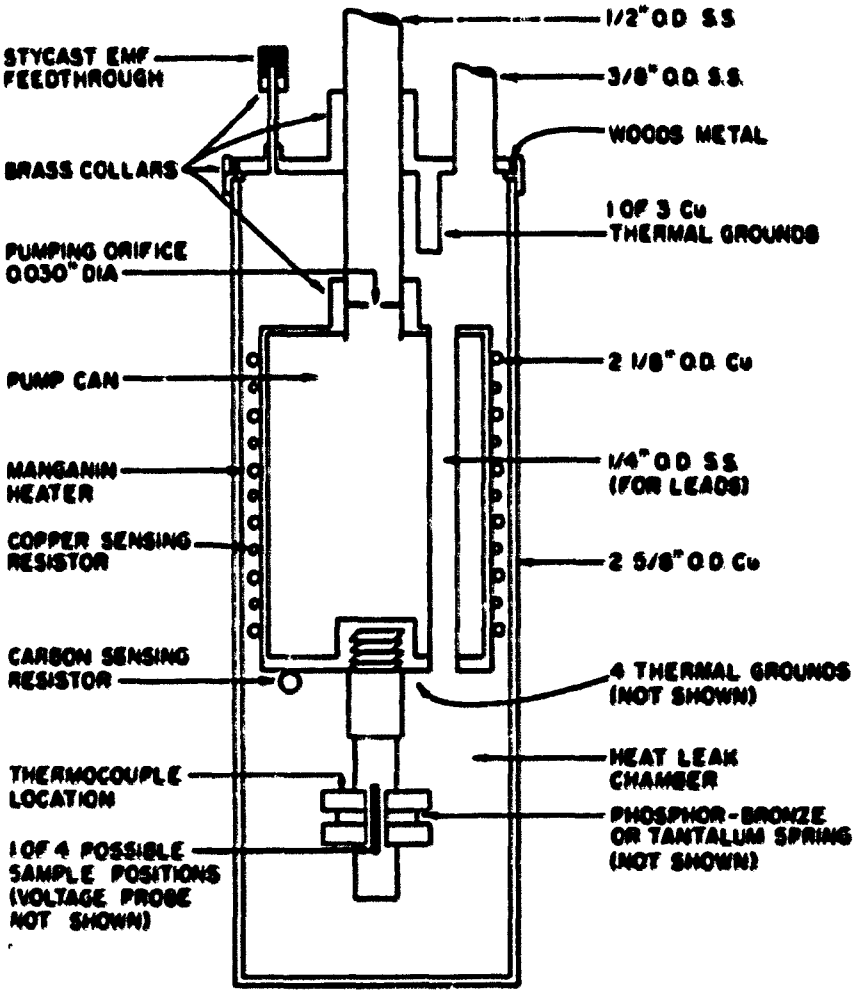

Figure 2. The heat leak chamber and the sample holder in the electrical resistivity measurement

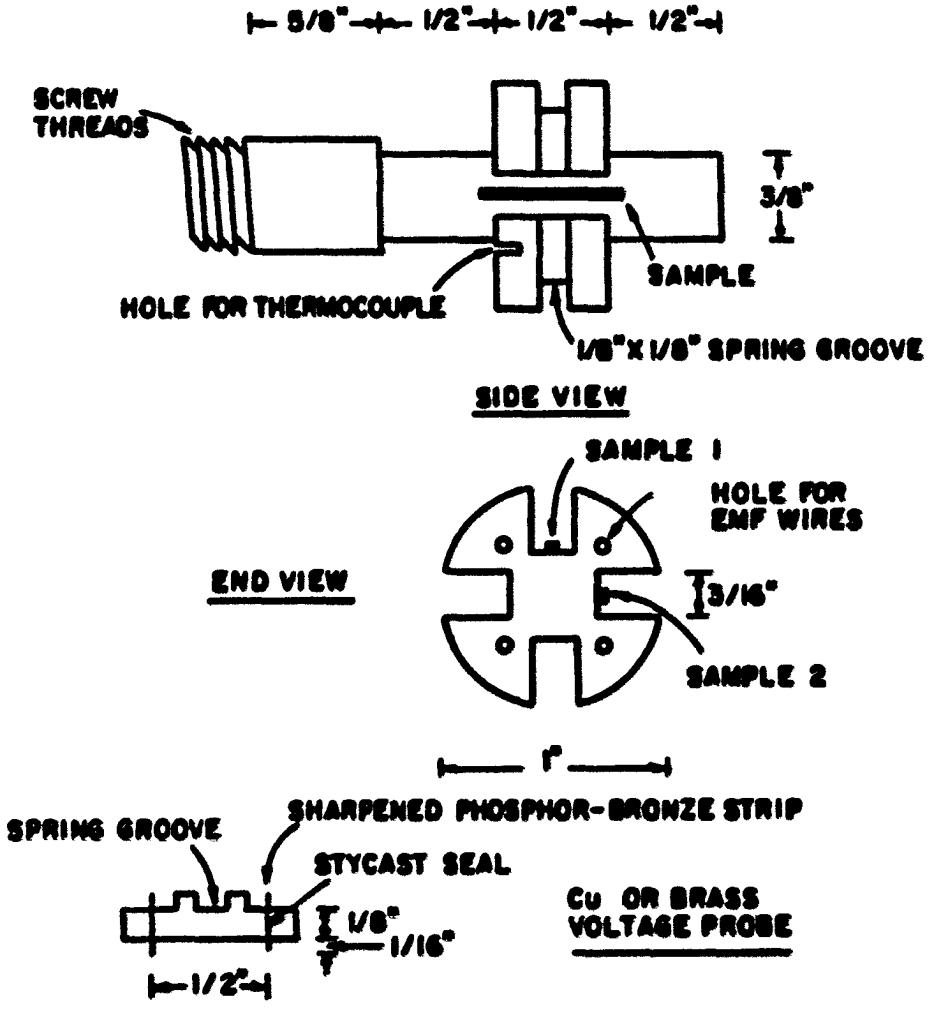

Figure 3. An enlarged picture of the sample holder area shown in Figure 2

current through the sample. The current was determined by measuring the voltage drop across a 1 Ω standard resistor.

The voltage, also called the emf, across the standard resistor or the sample voltage probe was initially measured by a Honeywell 0.01 microvolt potentiometer and later by a Keithley 181 digital nanovoltmeter. With the potentiometer, the out of balance signal was amplified by a Guildline nanovolt amplifier whose output was fed into a Guildline secondary galvanometer and then the potentiometer reading was adjusted to obtain a null reading in the galvanometer. A low thermal emf rotary switch was used to reverse the direction of the sample current. The resistance, R, and the resistivity, ρ, of the sample was calculated from Eq. (2-1). The distance between the phosphor-bronze strips making contacts with the sample was measured with a micrometer.

The second main component of the electronics was used for the temperature measurement. The temperature was determined by measuring the voltage of two types of thermocouples with a Leeds and Northrup K-5 potentiometer and a null detector. For temperatures above 77 K, a constantan vs. Cu thermocouple was used. For temperatures below 77 K, a Au-0.03 % Fe vs. Cu thermocouples was used. These thermocouples had been calibrated by earlier users. The Au-Fe vs. Cu thermocouple was checked at the liquid helium temperature to be accurate within 0.4 K.

The third component of the electronics was the temperature control unit. It was described in details in T. A. Vyrostek thesis.[35] As seen in Fig. 2, the temperature control centered around a 2 1/8" O.D. Cu pump can. The temperature was controlled by passing an appropriate current through a No. 34 manganin wire which was wound non-inductively on the pump can. A proportional temperature controller[34] was used to control the heater current. The controller was sensitive to the out-of-balance signal from a Wheatstone bridge. For temperatures above 30 K, one leg of the bridge was a non-inductively wound Cu sensing coil that was wound on the pump can underneath the manganin heater wire. For temperatures below 30 K, the leg of the bridge was a 56 Ω carbon resistor rather than Cu sensing coil. The carbon resistor was stycasted to the bottom of the pump can to make a thermal contact. A variable resistor in another leg of the Wheatstone bridge was used to balance the signal and therefore control the temperature.

Fig. 2 also shows the basic design of the cryostat. It consisted of an evacuated heat leak or sample chamber, heaters and temperature sensing elements. The sample chamber was put in a liquid He dewar which was surrounded by a liquid N_2 dewar. For cooling from 300 to 77 K, the liquid He dewar was filled with liquid N_2 to help cooling. The sample chamber was in vacuum at high temperatures and filled with some He gas

below about 180 K. Below 77 K, liquid helium was transferred to the liquid He dewar. For temperatures above 30 K, the pump can was evacuated to limit thermal conduction from the sample chamber to the liquid He dewar. Below 30 K, the pump can was filled with He gas to help cooling. Both cooling and heating data were recorded in the experiment. For a heating cycle above 77 K, no liquid N_2 was needed in the liquid He dewar.

C. A. C. Magnetic Susceptibility Measurements

The a. c. magnetic susceptibility measurements were made using Dr. D. K. Finnemore's apparatus which employed a modified a. c. Hartshorn bridge. J. R. Hopkin's thesis[36] described the details of the experimental system. The specimen was placed in the middle of a primary coil. A secondary coil was scatter wound astatically on the primary coil. An a. c. current was supplied to the primary coil. Above T_c or the magnetic ordering temperature (Curie temperature T(C) for a ferromagnetic sample or T(N) for a antiferromagnetic sample), magnetic flux penetrates the sample. The resistive and the inductive components of the voltage from the secondary were balanced by other elements in the bridge and displayed as null in a dual-phase lock-in detector. When the specimen was cooled below its T_c, T(C) or T(N), a voltage is induced in the secondary due to the change of the magnetic flux in the sample. For a superconductor at

temperatures below T_c, the magnetic flux is repelled from the sample. For a magnetic material at temperatures below its T(C) (or T(N)), the spins align with (or against) the magnetic field and will enhance (or diminish) the flux in the sample. In each of these cases, the inductance of the secondary was changed and the in-phase resistive and out-of-phase inductive components of the voltage were displayed on the dual-phase lock-in detector. The resistance component of the voltage was fed into the Y input of an X-Y recorder. A germanium resistance thermometer (GRT) supplied with a 10 μA current was used to determine the temperature. The voltage across the GRT was fed into the X input of the X-Y recorder. Since the LaX_x alloy is non-magnetic, the temperature at which a large amount of flux changes (there is always a slight flux change with temperature) is the superconducting temperature. The T_c value was taken from the midpoint of the transition curve recorded on the chart. For a homogeneous single phase alloy, the transition curve was sharp ($\Delta T_c \sim \pm 0.15$ K).

D. GRT Calibration in Magnetic Fields

A germanium resistance thermometer was used in the calorimeter for the temperture measurements from 1.4 to 20 K. It had been calibrated in zero magnetic field in Dr. C. A. Swenson group at the Ames Laboratory. The resistance (R) vs. temperature (T) values were fitted in two temperature ranges

by a least-squares method to the following equation

$$\ln T = \sum_{i=0}^{9} A_i (\ln R)^i \qquad (3\text{-}1)$$

where A_i's (i=0-9) are the constants listed in Appendix A. One set of the A_i's was generated for each of the two temperature ranges. One range was from 0.8 to 6.5 K and the other 4.0 to 21 K. In magnetic fields, the GRT calibration was done by using a capacitance thermometer (CT). The temperature dependence of the capacitance does not change under magnetic fields. This feature makes it suitable to be a temperature standard.

The CT was set close to the GRT in the calorimeter. The CT output was measured by balancing a capacitance bridge and the balance was displayed by a dual phase lock-in detector. In each magnetic field of 0.00, 2.50, 5.39, 7.62 and 9.98 T, the capacitance and the voltage across the GRT were recorded at the same time. A constant-current source from Lake Shore Cryotronics, Inc. supplied a current of magnitude 1-100 μA through the GRT. The current was determined by measuring the voltage drop across a 10 kΩ standard resistor. This voltage and the voltage across the GRT were measured with a Leeds and Northrup K-5 potentiometer. The out of balance signal was measured by a Keithley 150B microvoltmeter. Its output signal

was amplified and fed into a strip chart recorder. In this manner, the drift in temperature could be recorded. The thermal emf was determined by reversing the direction of the current flow.

Fig. 4 shows the capacitance vs. temperature from 1.4 to 20 K in zero magnetic field. The capacitance (CAP) vs. temperature (T) and T vs. CAP were fitted by a least-squares method over three temperature ranges : 1.5 - 5.1 K, 4.0 - 8.0 K, and 7.0 - 20.2 K to the following equations

$$T = \sum_{i=0}^{n} a_i \, CAP^i \tag{3-2}$$

and

$$CAP = \sum_{i=0}^{m} b_i \, T^i \tag{3-3}$$

where n = 3, 2, 5 and m = 5, 3, 5 for the respective temperature ranges. The constants a_i's and b_i's are given in Appendix A.

Although the capacitance did not change with magnetic field, there was a day-to-day variations in capacitance value. The capacitance value was pinned at the liquid He temperature each day before the magnetic field was applied. The difference between the capacitance before applying the magnetic field and the capacitance in zero field at the liquid

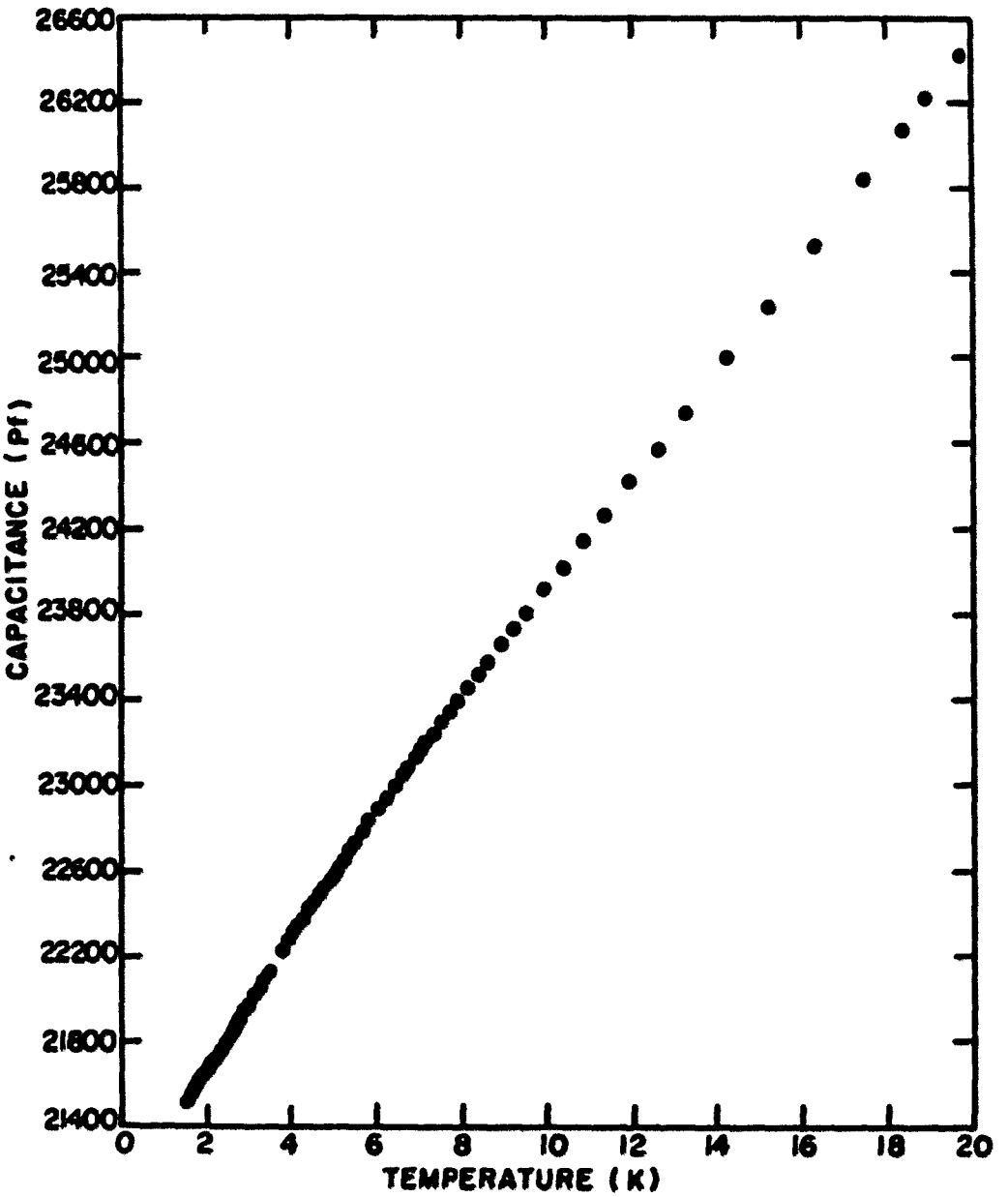

Figure 4. The plot of the capacitance of the capacitance thermometer vs. temperature in zero magnetic field

He temperature determined by Eq. (3-3) gave the offset to pin the capacitance. Now, the temperature in magnetic fields could be found from Eq. (3-2) to be

$$T = \sum_{i=0}^{n} a_i \, (CAP - \Delta CAP)^i \qquad (3\text{-}2a)$$

where ΔCAP was the offset in two CAP vs. T curves in zero magnetic field measured on different days. Fig. 5 shows schematically the meaning of the ΔCAP.

The resistance and the temperature values in magnetic fields were fitted to Eq. (3-1) by a least-squares method, except that the summation was over 9 coefficients (0 to 8 inclusive) over two temperature ranges : 1.6 - 6.5 and 4 - 21 K. The constants of B_i's (derived in the same manner as A_i's in Eq. (3-1)) are also listed in Appendix A. The GRT thermometry is shown in Fig. 6. The thermometry was checked by the heat capacity measurements of the Cu-reference standard and a high purity Sn sample. This will be discussed in the next section (E).

E. Calorimetry

The low temperature calorimeter was constructed in 1977 - 1978 by Dr. U. Atzmony and Mr. J. O. Moorman. The construction was in principle similar to the one built by W. E. Kienzle in the Deparment of Physics.[37] However, the

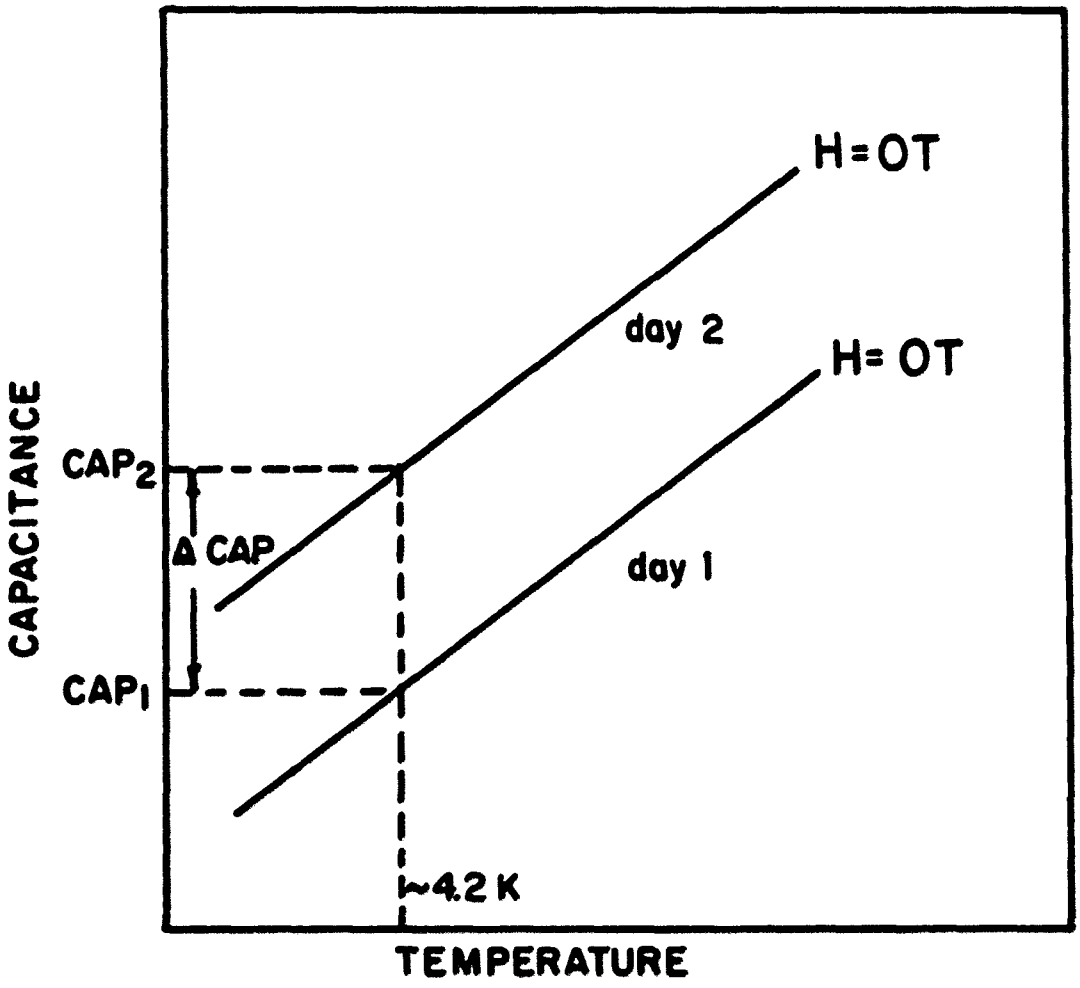

Figure 5. The meaning of the ΔCAP shown schematically

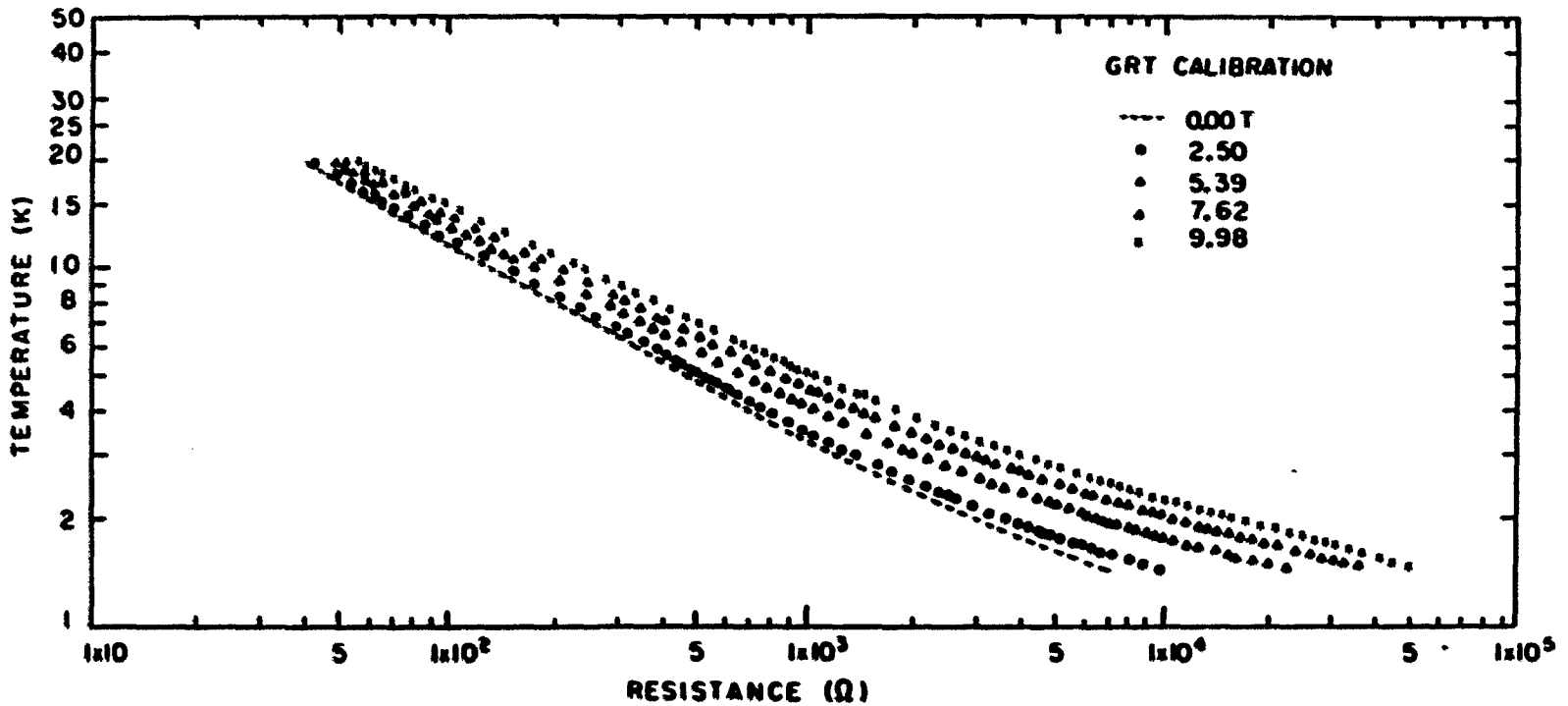

Figure 6. The temperature vs. resistance plot of the GRT thermometry

initial germanium resistance thermometer was replaced by a new one in 1981 and the new GRT had to be calibrated as described in the previous section.

The calorimeter was designed for accurate measurements of small samples in the temperature range of 1.4 to 20 K. A superconducting solenoid made of Nb_3Sn by Intermagnetics Corporation was used to generate magnetic fields up to 10 T. This would enable us to study the heat capacity of superconductors in magnetic fields. Because the superconducting transition temperature is suppressed by the magnetic field, the normal state properties, such as γ and θ_D, are more accessible, and the field dependence of T_c, and the $H_{c2}(T)$ can be determined.

The calorimeter was of the isolation heat-pulse type and it consisted of three parts: the cryogenic system, the heater circuit and the temperature measurement circuit. The first part consists of the dewars to cool the system and the sample chamber. The outermost dewar contained liquid nitrogen which could cool the system to 77 K if sufficient time was allowed. Inner dewar contained liquid helium and in which the sample chamber and a liquid helium pot attached to the chamber could be inserted. The helium dewar and inner pot were evacuated by a Stokes pump and then filled with a small amount helium as an exchange gas. The sample chamber was evacuated to better than 10^{-7} torr by a diffusion pump with a cold trap and backed by a

mechanical pump. Only after a good vacuum was achieved in the sample chamber, the liquid nitrogen and then liquid helium were transferred. A needle valve immersed in the liquid helium dewar could be opened to fill the inner helium pot if necessary. The inner helium pot could be pumped to reduce the vapor pressure over the liquid to achieve temperatures lower than 4.2 K. An orifice located on a plate ~ 1/3 of the way from the bottom of the pot was used to control the flow of the helium superfluid below the λ point at 2.2 K.

In the sample chamber, a mechanical heat switch was used to control the thermal contact of the addenda and sample to the inner pot. In the close position, the addenda and sample were cooled down to the temperature of the inner pot. In the open position, the addenda and sample were isolated and they could be warmed by a heater. The sample chamber shown in Fig. 7 was similar to the one built by Kienzle. The only difference was in the sample holder. In our holder, a sample is clamped between two copper discs which were tightened by a screw, and the GRT and the CT were sitting on the top disc. In Kienzle's holder, the sample sat on a copper foil container and the GRT was fastened underneath the container.

The second part of the calorimeter was the heater circuit. A 92 % Pt-8 % W was used as the heater wire. The amount of the heat supplied to the addenda and sample was given by

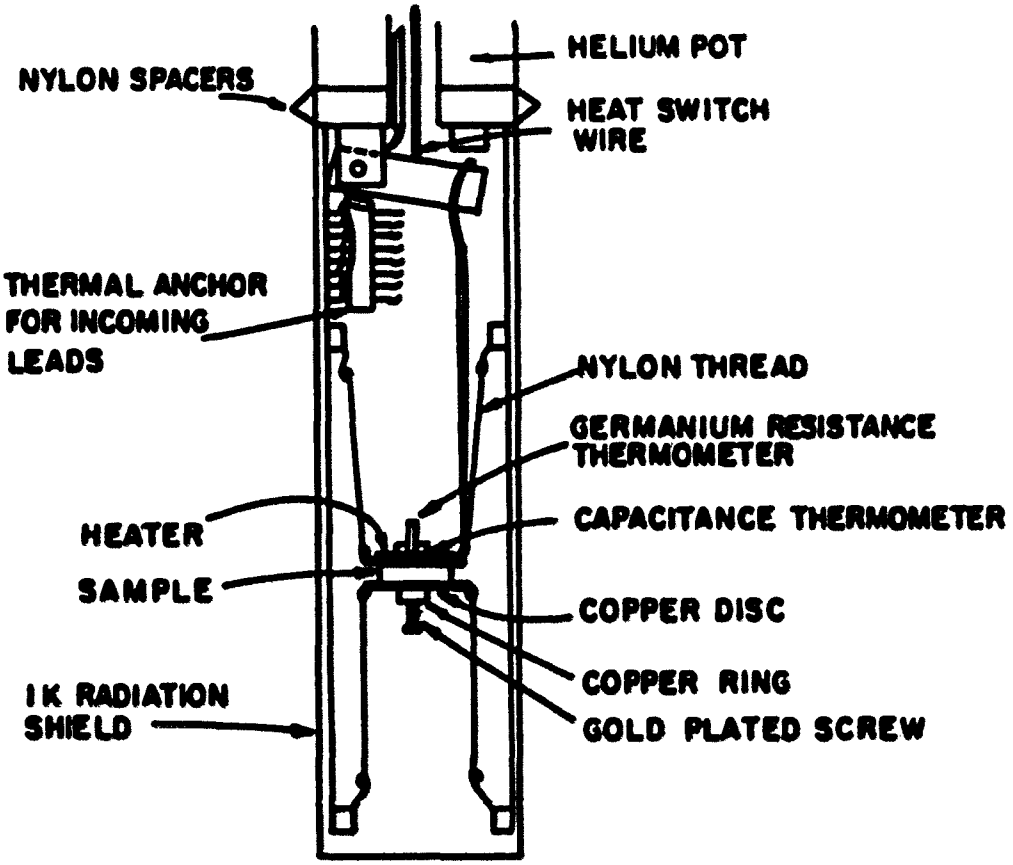

Figure 7. The view of the sample chamber in the calorimeter

$$\Delta Q = I_H V_H \Delta t \qquad (3\text{-}4)$$

where I_H is the current through the heater, V_H is the voltage drop across the heater and Δt is the time interval of the heat pulse. The current I_H was determined by the voltage drop across a 1 kΩ standard resister. This voltage and V_H were measured by a 7500 Data Precision voltmeter. The Δt was recorded by a Monsanto 8510 50 MHz counter/timer.

The third part of the system was the GRT circuit. The GRT resistance was measured by the standard dc four-probe method. Its measurement was described in the previous section of the GRT calibration.

The heat capacity of the sample was found in the following way. A certain amount of the heat, ΔQ_{add} or ΔQ, was supplied to the addenda (consists of sample holder, heater and GRT) or addenda plus sample respectively to raise their temperature by ΔT. The heat capacity of the addenda, C_{add} or sample, C, was found from the relationships

$$C_{add} = \Delta Q_{add} / \Delta T \qquad (3\text{-}5)$$

or

$$C = (\Delta Q / \Delta T - C_{add}(cal)) / X \qquad (3\text{-}6)$$

respectively, where $C_{add}(cal)$ was the calculated heat capacity of the addenda and X is the number of the gram-atoms of the

sample. The C_{add}(cal) term could be found as follows. The C_{add} data and the temperature T were fitted by a least-squares method to the relation

$$C_{add} = \sum_{i=1}^{6} D^0_i \, T^{2i-1} \qquad (3\text{-}7)$$

in different temperature ranges. The term C_{add}(cal) in Eq. (3-6) was then found from Eq. (3-7). The values of γ and Θ_D from the first heat capacity measurements of a Cu-reference standard[1] in five magnetic fields are listed in Appendix B. The temperature range for the least-squares fitting was from 2.5 to 5.0 K. The data for T < 2.5 K were not used because of the poor fit of the addenda data at lower temperatures. The γ and Θ_D values agreed within 15.4 and 1.6 % with the published values respectively. These results indicated that the procedure used for obtaining the addenda heat capacity was not reliable. The poor agreement was mainly due to the small heat content of the addenda. Therefore, a different procedure was used to obtain the addenda value, and is called the revised addenda. The revised addenda data were obtained from the heat capacity data of the addenda plus the Cu standard. Then, by substracting the known heat capacity of Cu one obtains the

---

[1]The Cu-reference standard was measured twice and the raw data were processed twice too. The second raw data which included the lower temperature data were taken by Dr. S. K. Dhar and his raw data were processed and used for the later work.

revised addenda. That is, Eq. (3-5) becomes

$$C_{rev\ add} = \Delta Q / \Delta T - C_{Cu} \times X \qquad (3\text{-}5a)$$

where C_{Cu} is the copper heat capacity from the refernce equation[38] and X was the number of gram-atoms of the Cu. The Cu reference equation was given as

$$C_{Cu} = \sum_{i=1}^{6} A_i T^{2i-1} \qquad (3\text{-}8)$$

in the unit of mJ/(g-atom K) where the coefficients A_i are listed in Appendix B. Fig. 8 (a) and (b) show the C/T vs. T^2 and C vs. T plots of the revised addenda from 1.4 to 20 K and 1.5 to 20 K respectively. In Fig. 9, the $C_{rev\ add}$ was compared to the C_{add} in zero magnetic field. The good agreement indicated that the method of using the revised addenda was reliable. The $C_{rev\ add}$ data were fitted against T by a least-squares method to the equation similar to Eq. (3-7)

$$C_{rev\ add} = \sum_{i=1}^{6} D_i T^{2i-1} \qquad (3\text{-}7a)$$

for different temperature ranges. The coefficients D_i are listed in Appendix B. Then, Eq. (3-6) was modified to give the heat capacity of the sample and was expressed to be

$$C = (\Delta Q / \Delta T - C_{rev\ add}(cal)) / X \qquad (3\text{-}6a)$$

where $C_{rev\ add}(cal)$ was calculated from Eq. (3-7a).

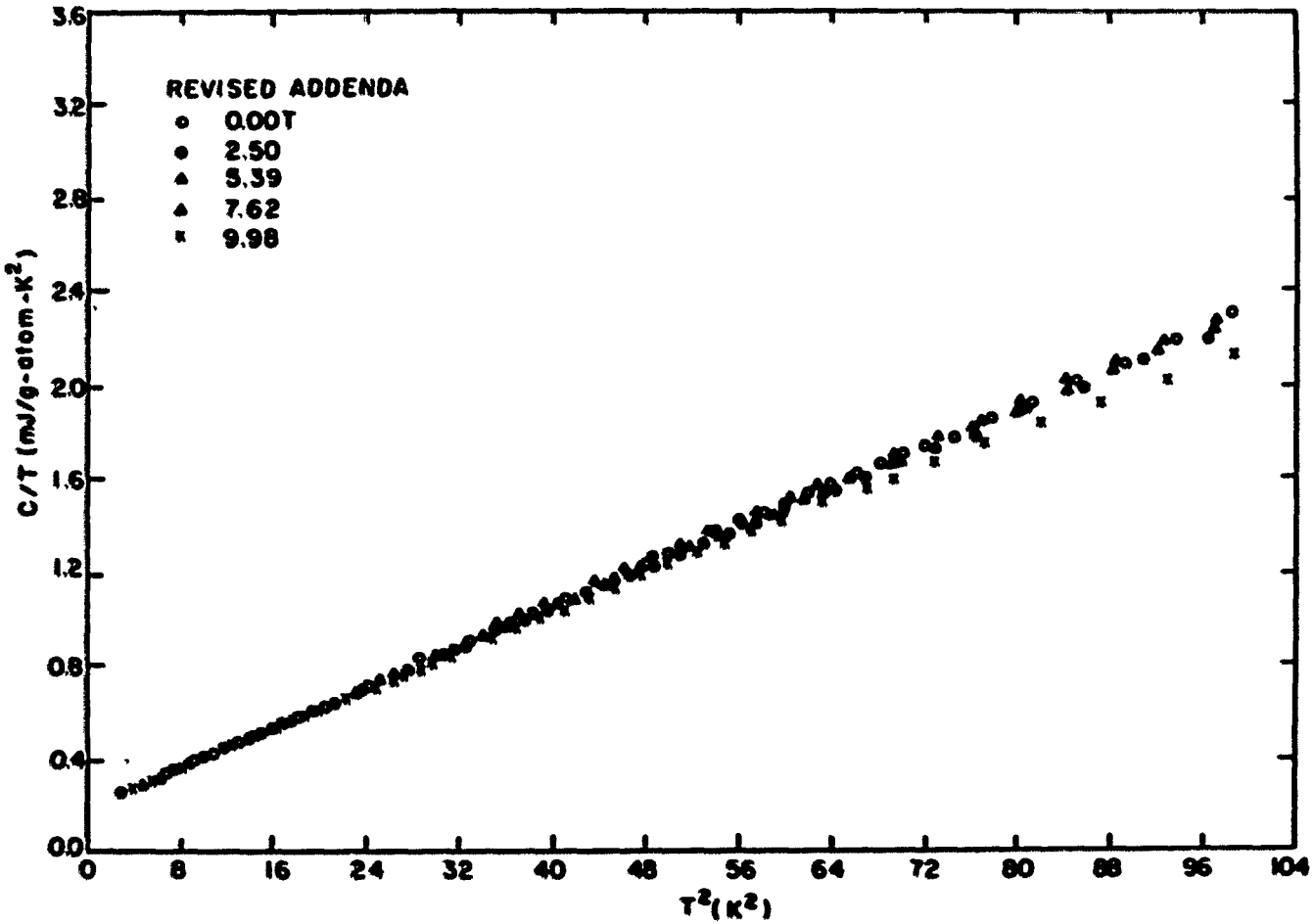

Figure 8(a). The C/T vs. T^2 plot of the heat capacity of the revised addenda from 1.4 to 10 K

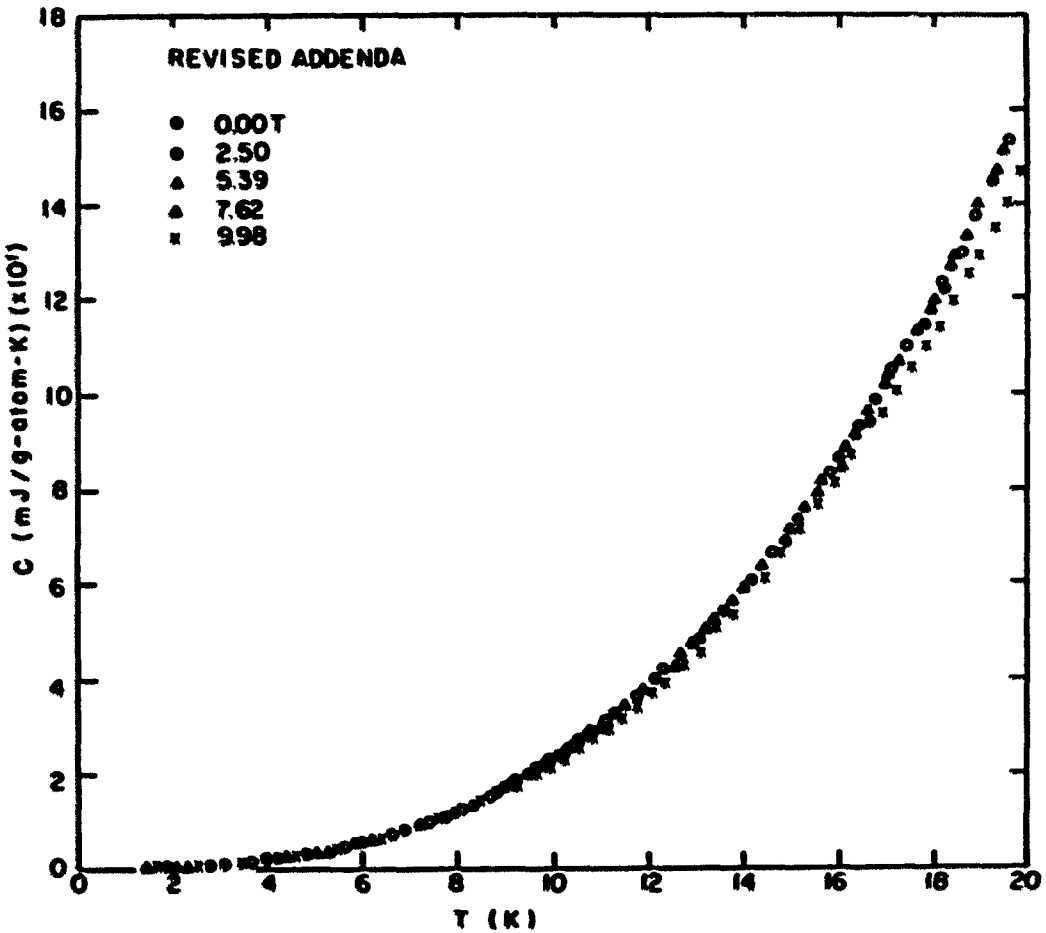

Figure 8(b). The C vs. T plot of the heat capacity of the revised addenda from 1.5 to 20 K

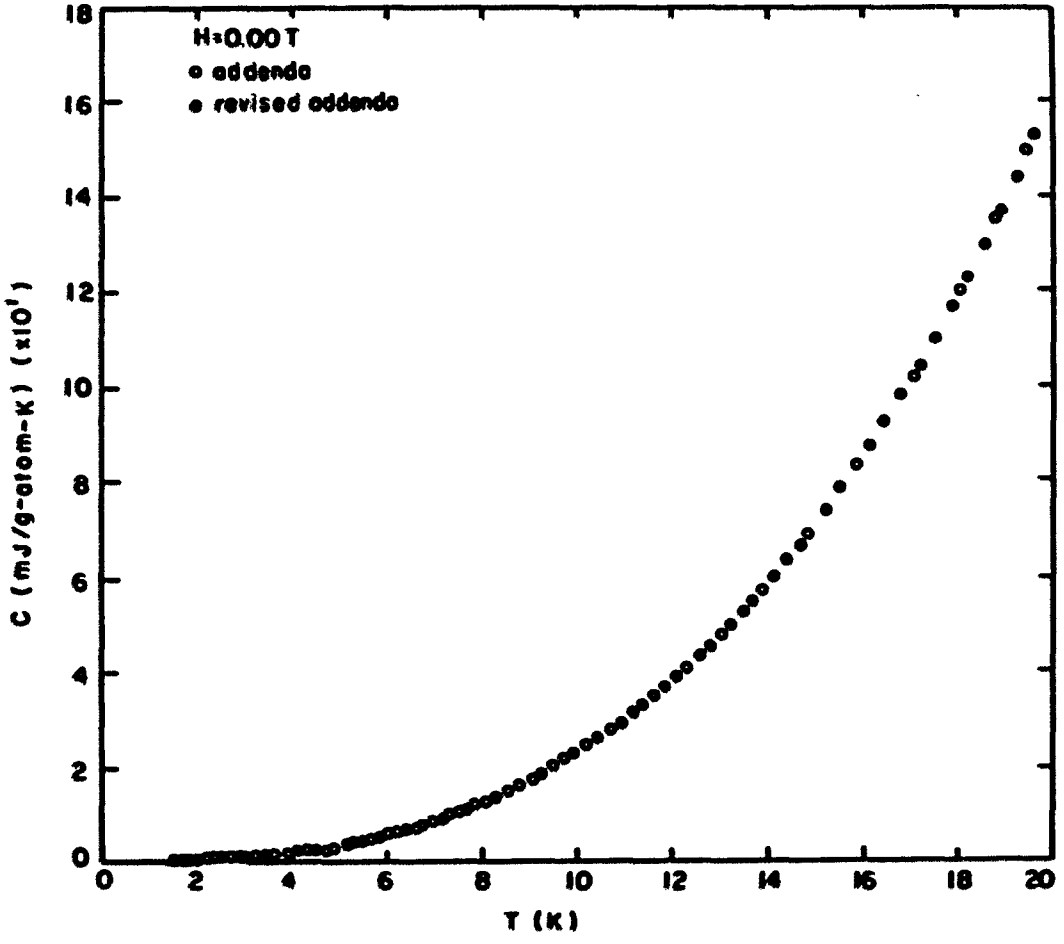

Figure 9. Comparison of the heat capacity of the revised addenda to the addenda in zero magnetic field

The heat capacity of a high purity Sn sample obtained from Dr. R. N. Shelton of the Physics Department was measured to check the thermometry and addenda data. Fig. 10 shows the heat capacity of the Sn from Eq. (3-6a) in H = 0.00 and 2.50 T. The literature data[39,40] were also included in the figure. A good agreement was achieved. Fig. 11 gives the heat capacity of the Sn in five magnetic fields from 1.7 to 10 K. The Sn data showed that our thermometry and revised addenda data are satisfactory.

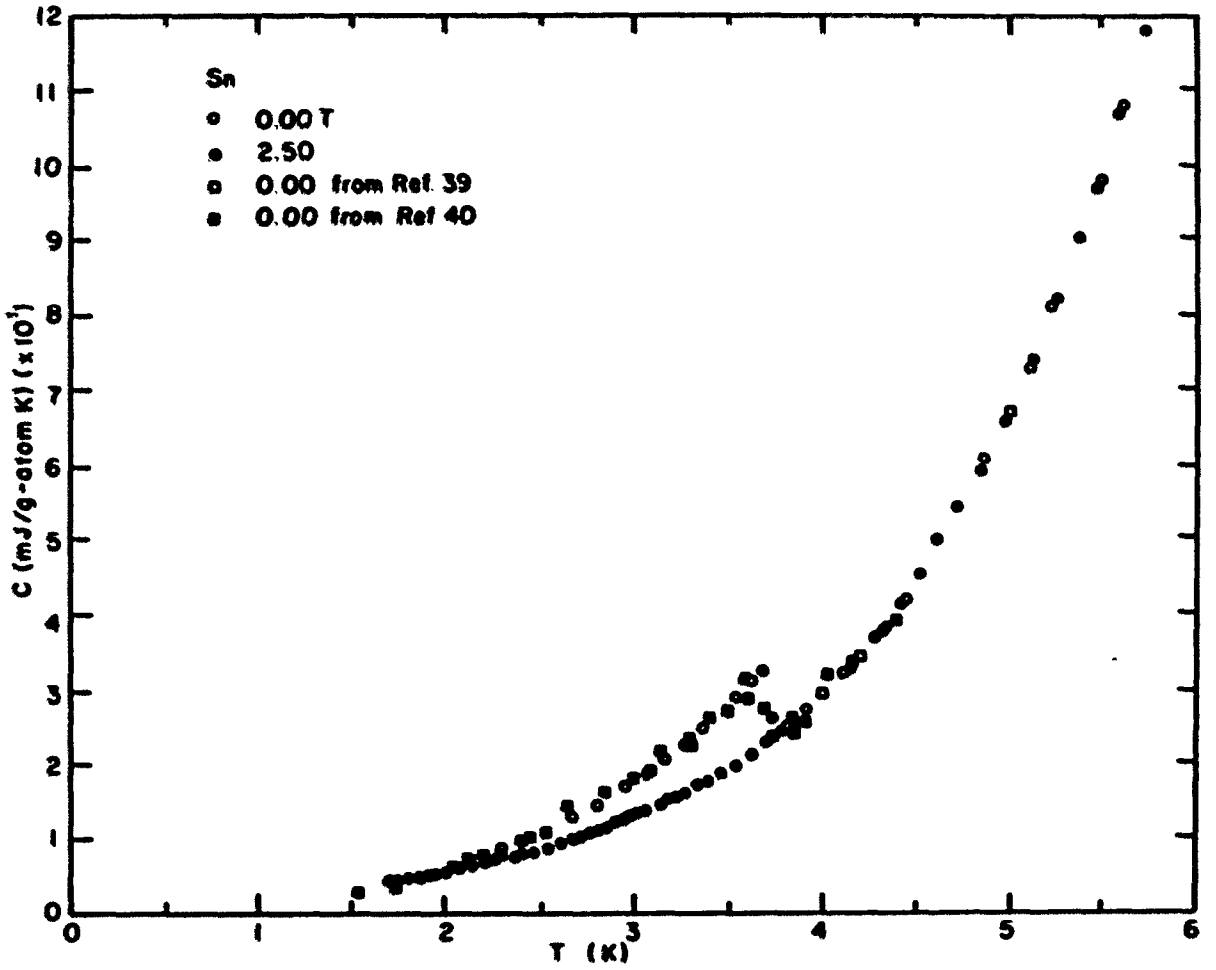

Figure 10. The heat capacity of the Sn sample in H = 0.00 and 2.50 T from 1.7 to 6 K

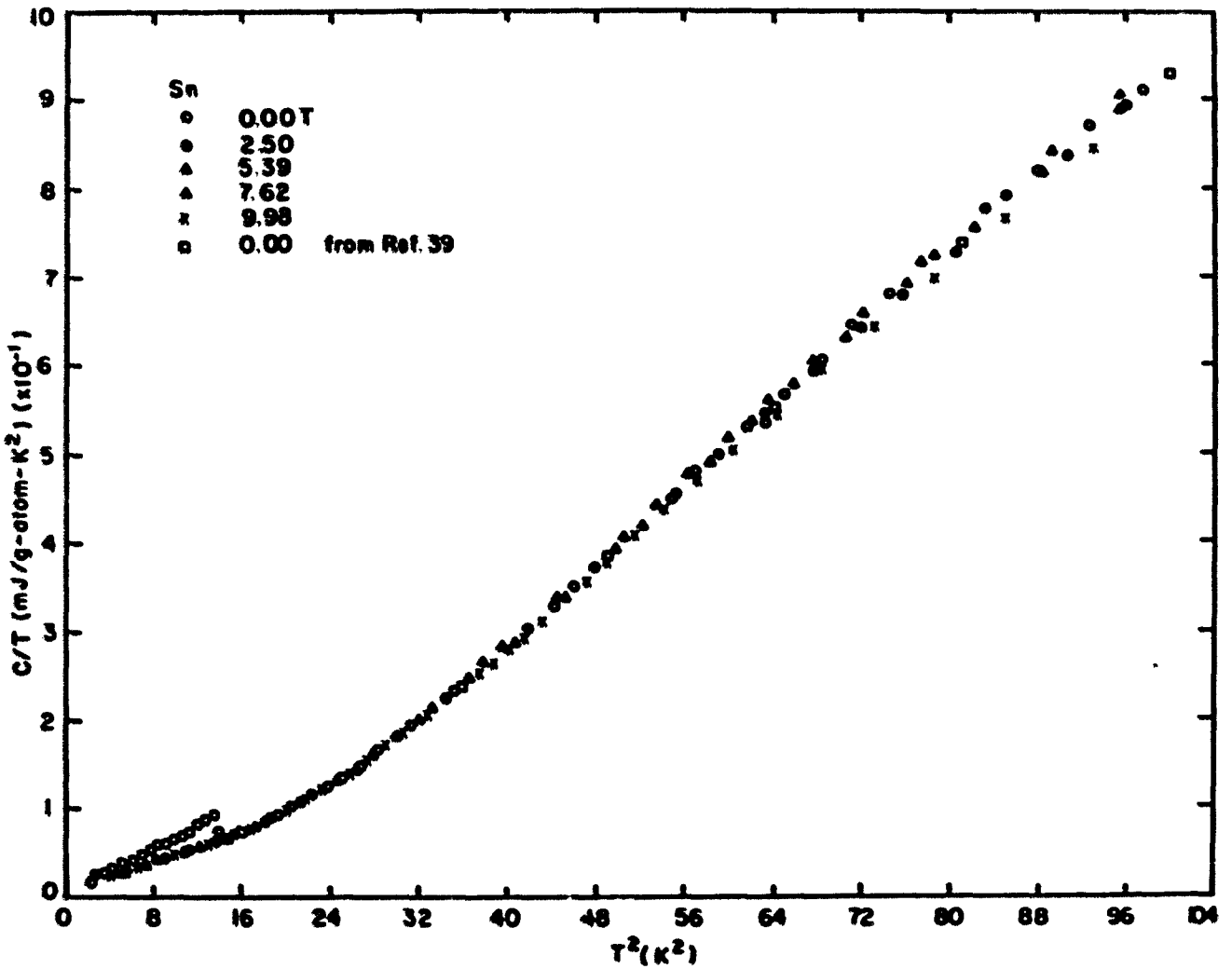

Figure 11. The C/T vs. T^2 plot of the heat capacity of the Sn sample in five magnetic fields from 1.7 to 10 K

IV. RESULTS

A. Electrical Resistivity

The electrical resistivity measurements from 4.2 to 300 K have been made on five $LaSe_x$ alloys (x : 1.334 to 1.387), two pseudobinary $La(S_{1-y}Se_y)_x$ alloys (x = 1.358, y = 0.102 and x = 1.381, y = 0.89), eight $La_{1-y}Th_yS_x$ alloys (x : 1.333 to 1.351 and y : 0.02 to 0.04) and one $La_{0.98}Y_{0.02}S_{1.339}$ alloy. The resistivity of each alloy was calculated from Eq. (2-1). Figs. 12(a)-(c) show the resistivities of some of these alloys as a function of temperatures. The slope changes seen in some of the curves indicate the temperatures at which the alloys transform from the bcc to bct phase, T_M's. The dashed lines extrapolated from T_M to 0 K give the expected values if the alloys remained cubic. For $LaSe_{1.360}$, the slope changes in the cooling and heating curves are not easily seen. Therefore, the slope ($\Delta\rho/\Delta T$) of the resistivity curve of the heating run was calculated and plotted in Fig. 12(d). A peak in the slope vs. T plot indicates that the T_M for this alloy is about 15.7 K upon heating. Table 3 lists the results of the resistivity measurements. Also given in Table 3 are : ρ_{300} - the resistivity value at 300 K; $T_c(\rho)^{max}$ - the maximum superconducting transition temperature from the resistivity measurements; N_e - the concentration of the conduction electrons which is given by

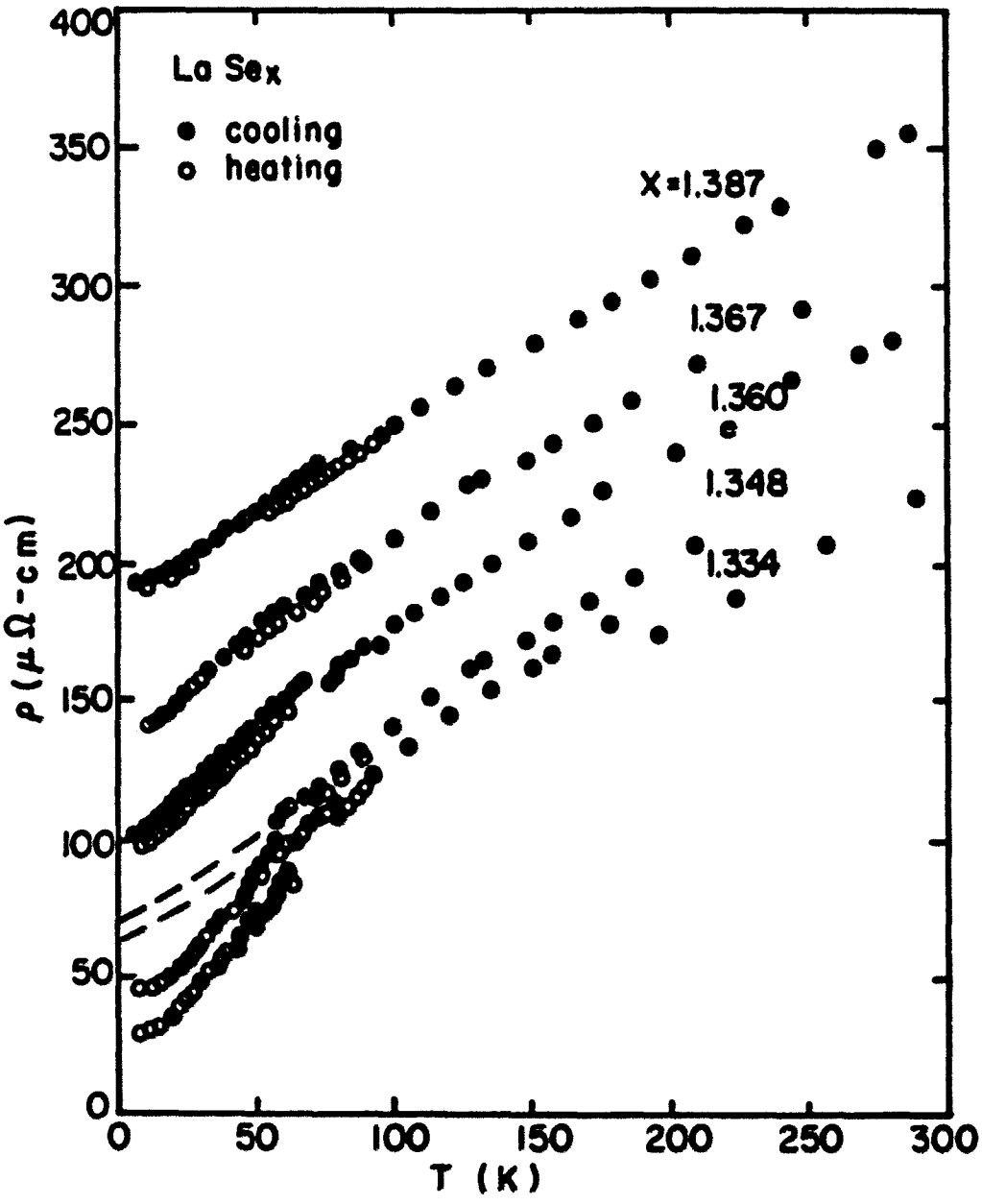

Figure 12(a). The curves of the electrical resistivity of the $LaSe_x$ alloys (x : 1.334, 1.348, 1.360, 1.367 and 1.387)

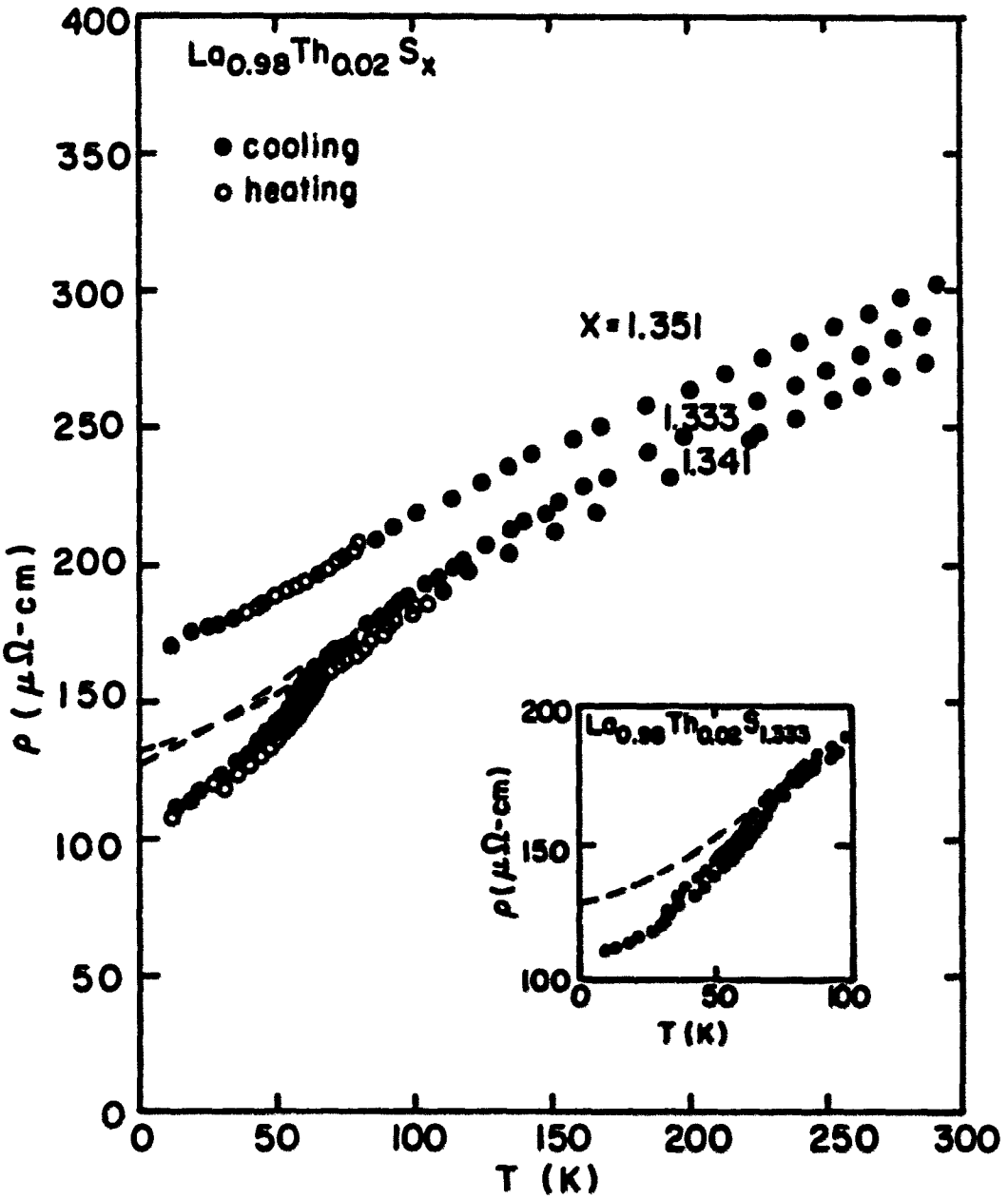

Figure 12(b). The curves of the electrical resistivity of the $La_{.98}Th_{.02}S_x$ alloys

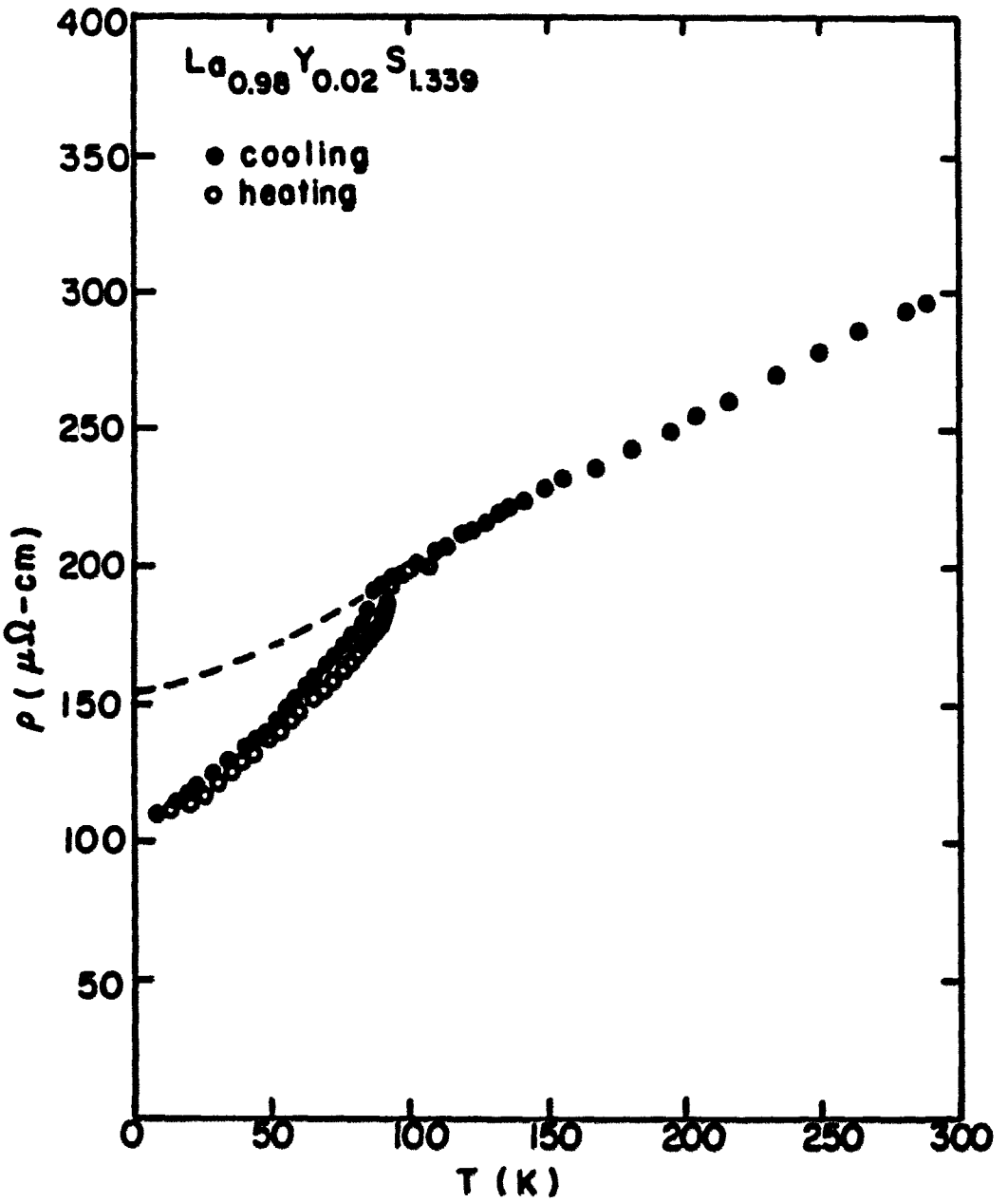

Figure 12(c). The curves of the electrical resistivity of the $La_{.98}Y_{.02}S_{1.339}$ alloy

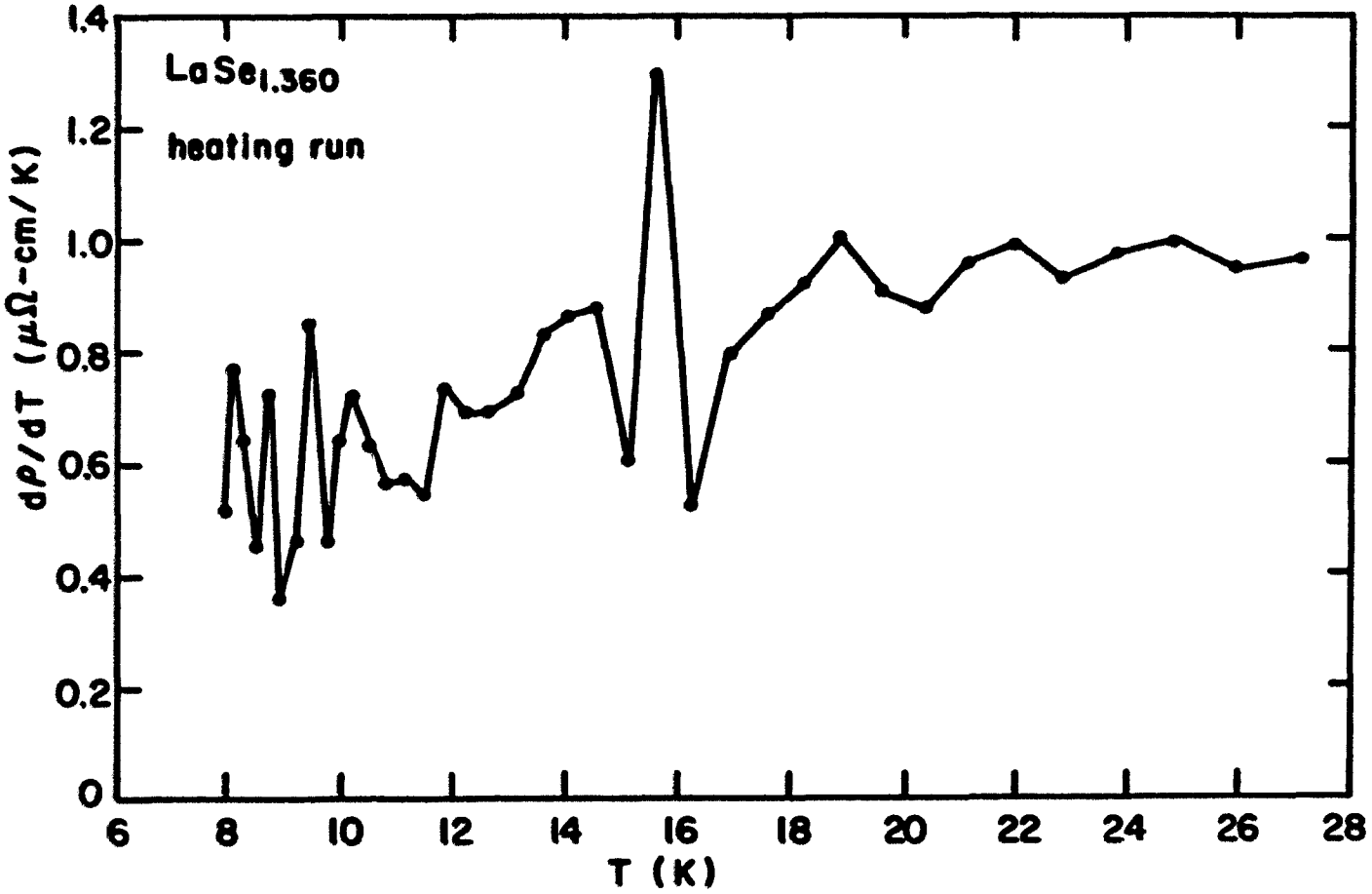

Figure 12(d). The slope of the electrical resistivity vs. T curve for $LaSe_{1.360}$ alloy in the heating run

Table 3. The results of the electrical resistivity measurements for selenides and sulfides

Alloy	T_M[a] (K)	ρ_r (μΩ-cm)	ρ_{300} (μΩ-cm)	$T_c(\rho)^{max}$ (K)	N_e ($atom^{-1}$)	N_v (at.%)
$LaSe_{1.334}$	65(c) 65(h)	30.2	229.3	7.7	0.143	0.021
$LaSe_{1.348}$	57(c) 64(h)	44.1	257.9	7.3	0.130	0.466
$LaSe_{1360}$	14(c) 16(h)	98.4	293.0	7.5	0.119	0.840
$LaSe_{1.367}$	____	140.7	319.1	9.05	0.112	1.056
$LaSe_{1.387}$	____	190.7	362.7	6.50	0.095	1.658
$La(S_{.898}Se_{.102})_{1.358}$	____	199.9	329.1	7.7	0.120	0.779
$La(S_{.11}Se_{.89})_{1.377}$	____	214.5	336.9	7.2	0.104	1.359
$La_{.98}Th_{.02}S_{1.333}$	61(c) 70(h)	108.6	293.0	8.2	0.152	0.000
$La_{.97}Th_{.03}S_{1.333}$	____	199.0	374.5	8.8	0.156	0.000
$La_{.96}Th_{.04}S_{1.333}$	____	174.5	292.5	8.2	0.160	0.000

$La_{.98}Th_{.02}S_{1.341}$	56(c) 65(h)	107.8	278.3	8.4	0.144	0.245
$La_{.96}Th_{.04}S_{1.341}$	———	279.4	404.1	8.3	0.153	0.245
$La_{.98}Th_{.02}S_{1.351}$	———	169.0	306.4	8.2	0.135	0.560
$La_{.97}Th_{.03}S_{1.360}$	———	204.0	324.8	7.5	0.131	0.840
$La_{.98}Y_{.02}S_{1.339}$	88(c) 94(h)	109.0	303.0	6.4	0.138	0.181

[a](c) or (h) after T_M values mean in the cooling or heating run.

$$N_e = (3 - 2x) / (1 + x) \qquad (4\text{-}1)$$

and N_v - the number of vacancies at the lanthanum sites which is given by

$$N_v = (3x - 4) / (7x) \qquad (4\text{-}2)$$

The vacancy or compositional variations of the residual resistivity, ρ_r, in the selenides and sulfides are shown in Figs. 13(a) and (b), respectively. The ρ_r value was found from the extrapolation of the data above T_c to 0 K. The dashed lines in Figs. 13(a) and (b) indicate the expected cubic ρ_r values taken from Fig. 12(a) and Ref. 15 for selenides and sulfides respectively. It is seen that the expected bcc phase would have higher ρ_r values than the bct phase.

The compositional variations of the T_M and the effects of up to 4 % Th and 2 % Y additions to La on T_M are shown in Figs. 14(a) and (b). The results for the LaS_x alloys were again taken from Ref. 15. For x close to 1.333, the alloy always contained a second phase of LaSe or LaS as seen by optical metallography. In Fig. 14(a), the alloy contained two phases, namely LaSe and $LaSe_{1.346}$. The value x = 1.346 was determined from the intersection of the curves (2) and (1). Curve (1) is the expected curve if a single phase alloy existed at that composition. From the level law, the

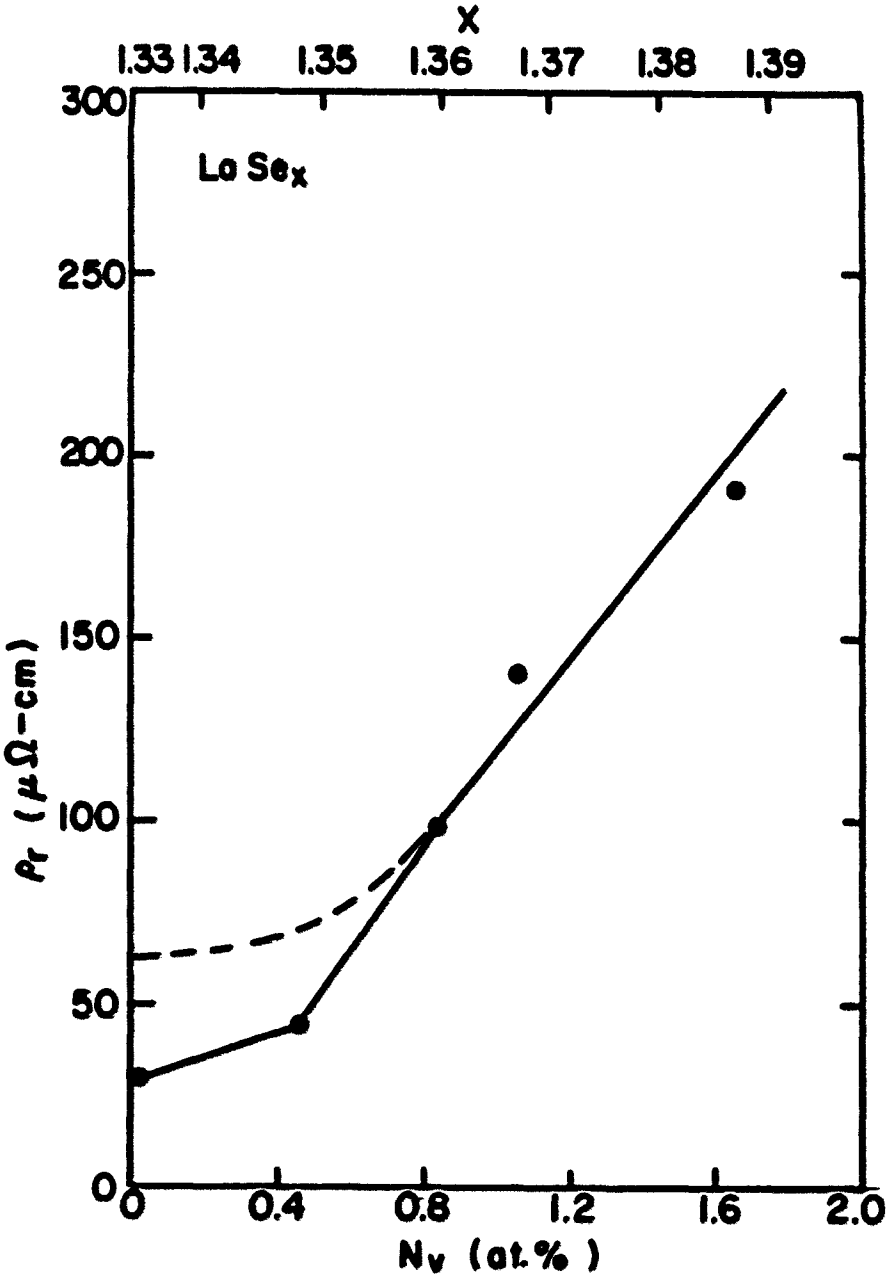

Figure 13(a). The electrical residual resistivity in the selenides

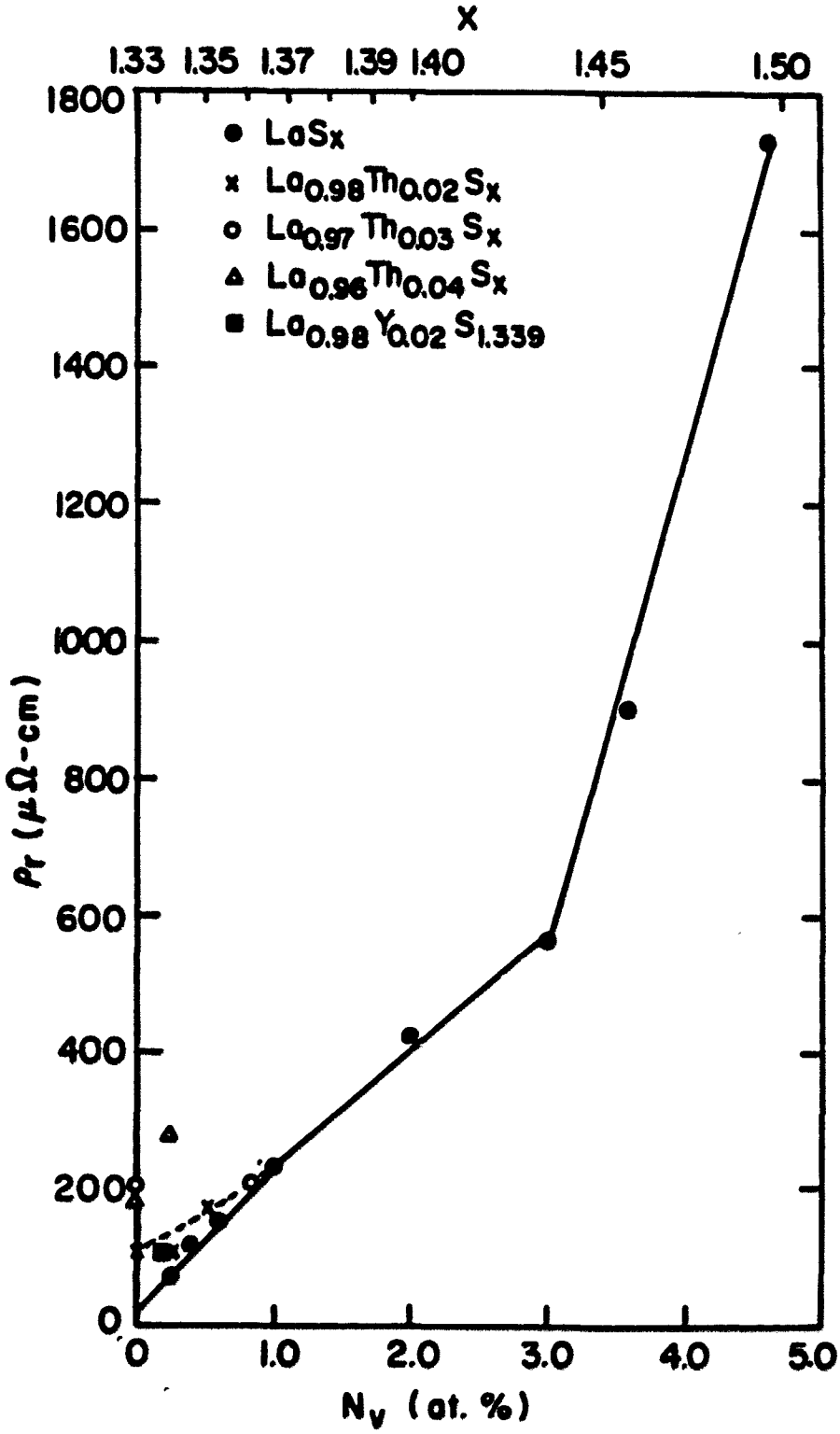

Figure 13(b). The electrical residual resistivity in the sulfides

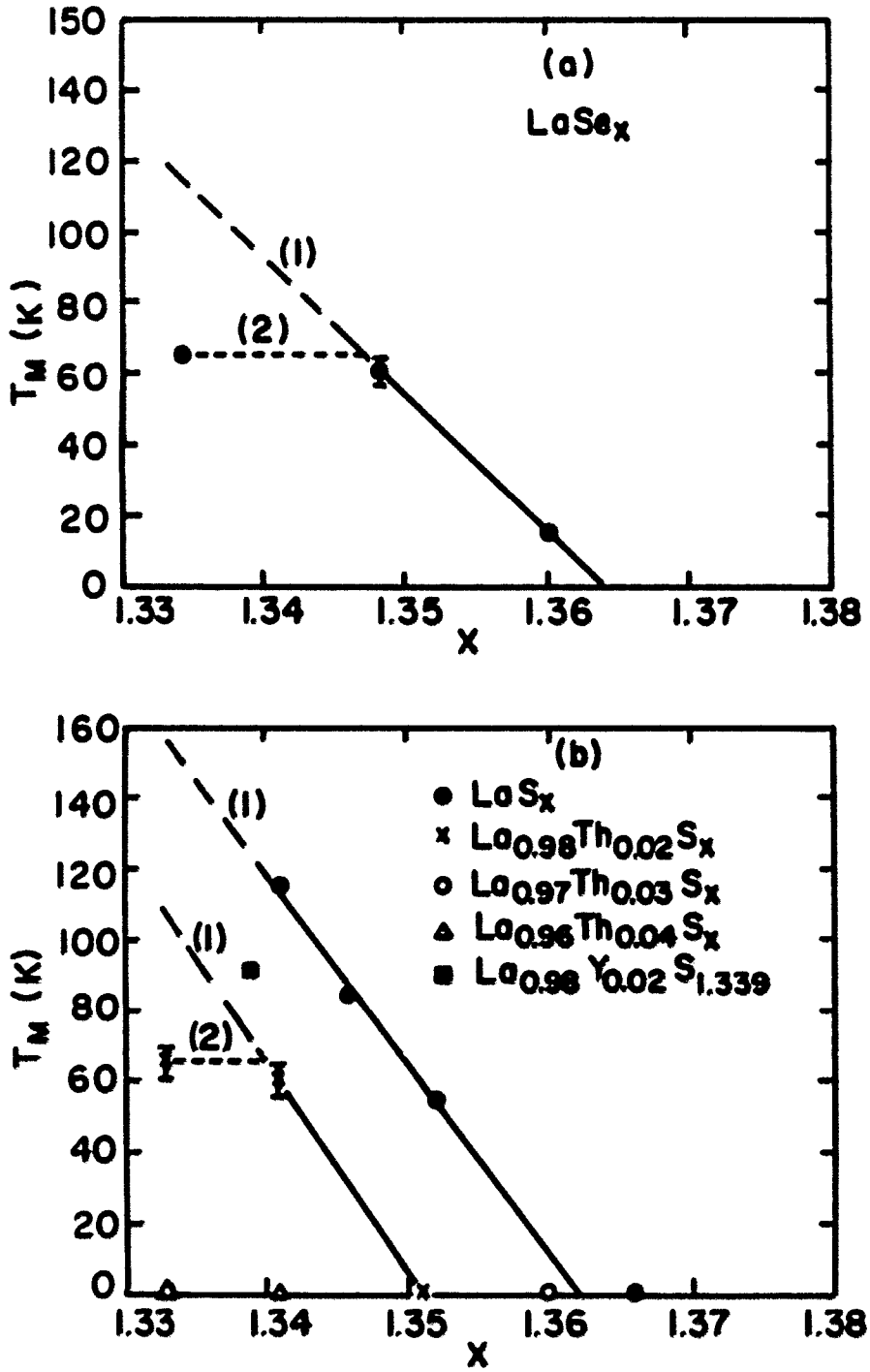

Figure 14. The compositional dependences of the T_M in (a) the selenides and (b) the sulfides

$LaSe_{1.334}$ alloy contained 3.6 % of the LaSe phase. In Fig. 14(b), the dashed line marked with (1) also showed the expected curve if the single phase alloy existed. The $La_{.98}Th_{.02}S_{1.333}$ alloy had its main component as $La_{.98}Th_{.02}S_{1.340}$. Again, from the level law, the $La_{.98}Th_{.02}S_{1.333}$ alloy contained 2.1 % of the LaS phase. It is seen that the Th additions lower T_M. The $La_{.98}Y_{.02}S_{1.339}$ alloy also had a small amount of the LaS phase on the top surface of the bulk sample. However, the quantity of the second phase could not be determined due to insufficient number of samples. It seemed that the Y addition had less effect on T_M than the Th addition. The relationship between N_e and T_M in selenides and sulfides is shown in Fig. 15. The curves (1) had same meanings as those in Figs. 14(a) and (b). It is interesting that the three curves for binary selenides, sulfides and pseudobinary $La_{.98}Th_{.02}S_x$ alloys are essentially parallel.

B. A. C. Magnetic Susceptibility

Figs. 16(a) and (b) show the T_c^{mid} values obtained from the a. c. magnetic susceptibility measurements. The values are also listed in Table 4. The T_c values for LaS_x alloys were taken from the Ref. 16 which were obtained from the heat capacity measurements. It was found that the T_c values from the heat capacity and a. c. magnetic susceptibility

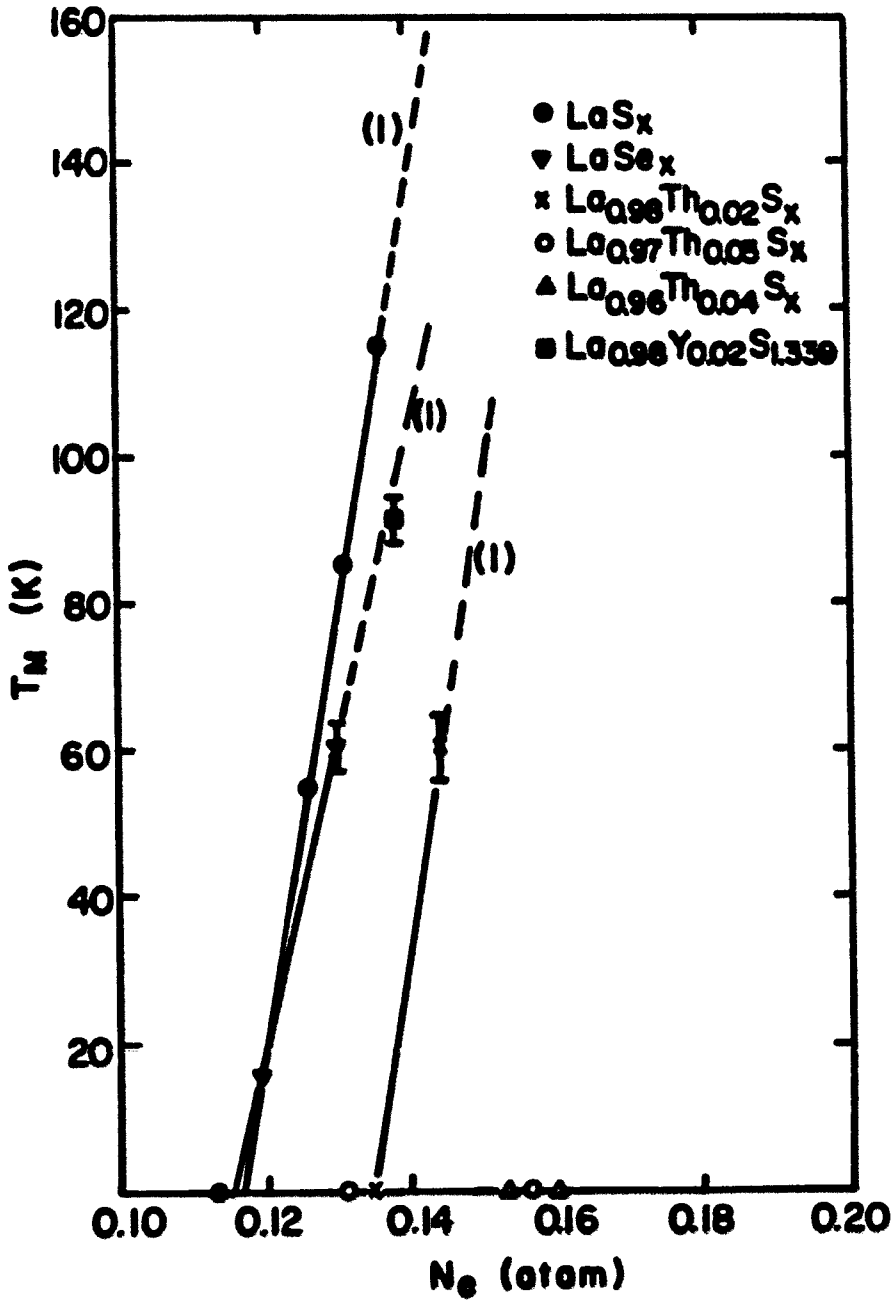

Figure 15. The conduction electron concentration dependences of the T_M. The dashed lines marked with (1) were drawn from the data in the dashed lines marked with (1) in Figure. 14

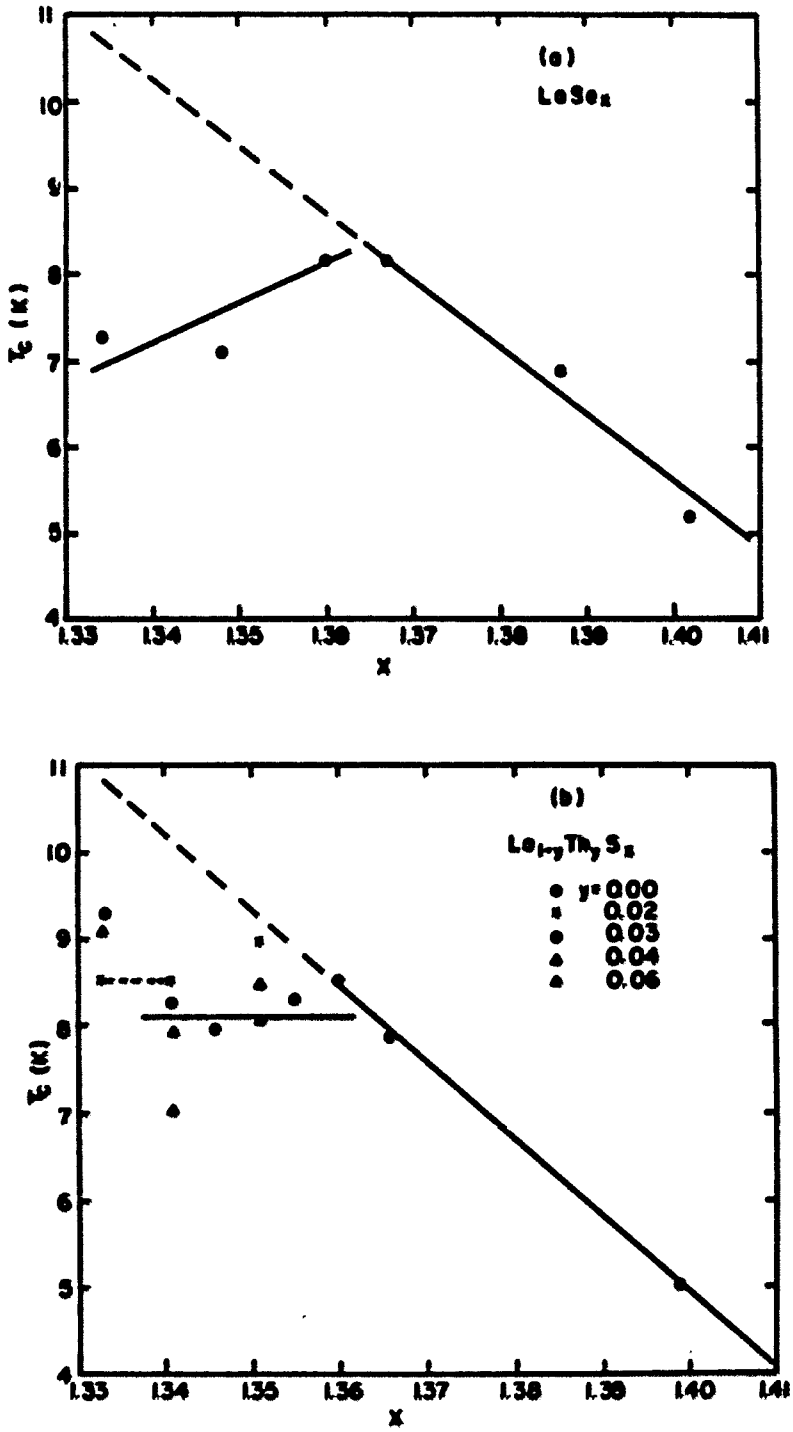

Figure 16. The T_c^{mid} values determined from the a. c. magnetic susceptibility measurements for (a) the selenides and (b) the sulfides

Table 4. The results of the a. c. magnetic susceptibility measurements in the selenides and sulfides

Alloy	phase[a] C or T	T_c^{max} (K)	T_c(10%) (K)	T_c^{mid} (K)	T_c(90%) (K)	ΔT[b] (K)
$LaSe_{1.334}$	T	7.47	7.35	7.26	7.19	0.16
$LaSe_{1.348}$[c]	T	7.10	7.10	7.10	7.10	0.00
$LaSe_{1.360}(1)$[c,d]	T	7.90	7.90	7.80	7.70	0.20
$LaSe_{1.360}(2)$[d,e]	T	9.42 8.79	9.05 8.37	8.94 8.14	8.91 8.06	0.04 0.31
$LaSe_{1.360}(3)$[d]	T	8.94	8.77	8.64	8.57	0.20
$LaSe_{1.367}$	C	8.34	8.21	8.16	8.11	0.10
$LaSe_{1.387}$	C	6.97	6.90	6.89	6.84	0.06
$LaSe_{1.402}$	C	5.29	5.23	5.19	5.06	0.17
$La(S_{.898}Se_{.102})_{1.358}$	C	8.24	8.18	8.11	8.05	0.13
$La(S_{.51}Se_{.49})_{1.373}$	C	5.40	5.35	5.32	5.26	0.09
$La(S_{.11}Se_{.89})_{1.377}$	C	6.44	6.38	6.35	6.28	0.10
$La_{.98}Th_{.02}S_{1.333}$	T	8.70	8.60	8.54	8.46	0.14

$La_{.97}Th_{.03}S_{1.333}$	C	9.38	9.31	9.28	9.24	0.07
$La_{.96}Th_{.04}S_{1.333}$	C	9.37	9.25	9.09	8.94	0.31
$La_{.98}Th_{.02}S_{1.341}$	T	8.70	8.57	8.50	8.44	0.13
$La_{.96}Th_{.04}S_{1.341}$	C	8.42	8.22	7.92	7.84	0.38
$La_{.94}Th_{.06}S_{1.341}$	C	7.43	7.20	7.04	6.92	0.28
$La_{.98}Th_{.02}S_{1.351}$	C	9.07	9.01	8.96	8.93	0.08
$La_{.96}Th_{.04}S_{1.351}$	C	8.75	8.55	8.47	8.35	0.20
$La_{.94}Th_{.06}S_{1.351}$	C	8.35	8.24	8.06	7.90	0.34
$La_{.97}Th_{.03}S_{1.360}$[c]	C	8.60	8.50	8.50	8.50	0.00
$La_{.98}Y_{.02}S_{1.339}$	T	7.91	7.81	7.76	7.68	0.13

[a]Phase C or T indicates that the low temperature phase of the alloy is in bcc or bct phase.

[b]ΔT is the width of the transition from 10 to 90 % of the superconducting phase.

[c]The T_c values of these samples were measured in Dr. R. N. Shelton's apparatus.

[d]Three portions (1), (2) and (3) of a sample were measured for the T_c values.

[e]Portion (2) of the $LaSe_{1.360}$ alloy had two peaks in the transition curve. Also, this sample was the resistivity sample.

measurements were nearly the same. In Figs. 16(a) and (b), the dashed lines indicate the expected cubic values for binary selenides and sulfides respectively. The effect of substituting M for La on T_c was shown in Fig. 17. The values for binary LaS_x alloys (for which y = 0) were taken from the Fig. 16(b) of the cubic alloys. The T_c values of three alloys, $La_{.98}Ca_{.03}S_{1.333}$, $La_{.97}Mg_{.03}S_{1.333}$ and $La_{.97}Ca_{.03}S_{1.333}$ prepared by B. J. Beaudry in the Ames Laboratory were also measured and included in Fig. 17.

From the T_c data, it is seen that the metastable bcc phase would have a higher T_c value than the corresponding bct phase. The effect of alloying of tetravalent, trivalent and bivalent metals for La metal on T_c was always to decrease the T_c values. For the Th additions, the smaller the sulfur to metal ratio the greater the suppresion of T_c.

The $La_{.98}Ce_{.02}S_{1.333}$ alloy in which the phase transformation was not studied has a lower T_c value than either bct or bct phase $LaS_{1.333}$. The presence of the magnetic Ce atoms tends to break or weaken the Cooper pairs. Since T_c value was not increased, this alloy system was not studied in any detail. The three percent Mg and Ca alloys decrease T_c substantially due to a smaller conduction electron concentration than the corresponding $LaS_{1.333}$ alloy. Therefore, no further study was conducted on these two alloy systems.

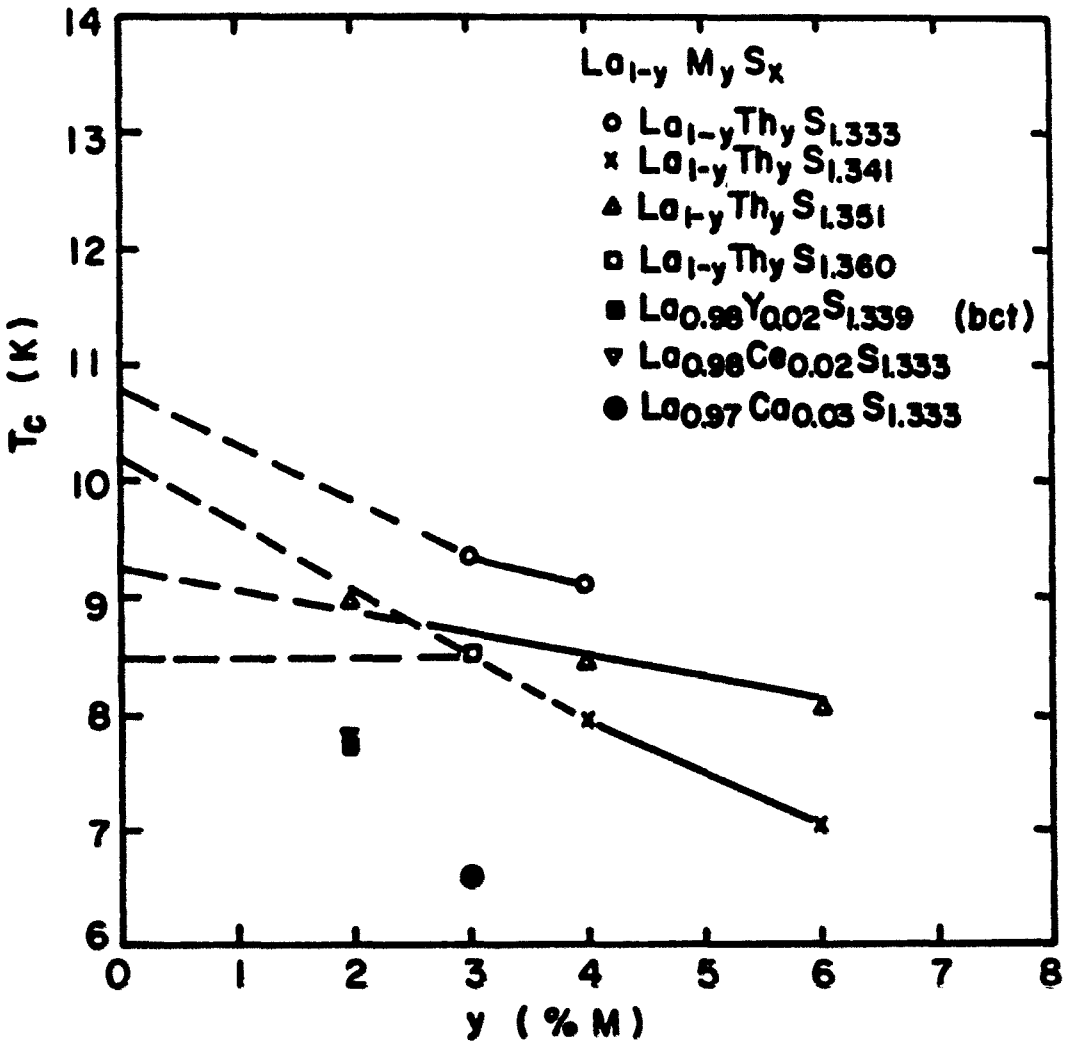

Figure 17. The effect of the alloying on T_c values in pseudobinary sulfides. The $La_{.97}Mg_{.03}S_{1.333}$ alloy whose T_c is not shown in the plot is not superconducting down to 1.37 K

C. Heat Capacity

The heat capacity measurements from 1.4 to 20 K have been made on three $LaSe_x$ alloys (x = 1.334, 1.360 and 1.367), one $La(S_{1-y}Se_y)_x$ alloy (x = 1.358 and y = 0.102) and four $La_{1-y}Th_yS_x$ alloys (x : 1.333 to 1.360 and y : 0.02 to 0.03). The plot of the C/T vs. T^2 for temperatures below 10 K is shown in Fig. 18 for $LaSe_{1.367}$. Other alloys exhibit similar plots which are not shown here. The effect of the applying magnetic field on T_c is to suppress the value of T_c. In Fig. 18, it is seen that above T_c^* (maximum superconducting temperature) at each field, the alloy becomes a normal conductor and its plot of C/T vs. T^2 is linear. The values of γ and β were obtained from the least-squares fitting of the normal state data in five fields to the Eq. (2-10). The temperature range was selected in the linear region of the C/T vs. T^2 plot. The Debye temperature was calculated from the Eq. (2-9). The values of γ, β, θ_D, and the temperature range over which the data were fitted are listed in Table 5. The $La_{.97}Th_{.03}S_{1.333}$ alloy after first heat-treatment had two peaks in C/T vs. T^2 plots at zero and the various magnetic fields. The alloy was homogenized by a second heat-treatment at 1700 C for three weeks. The heat capacity measurement was made again.

Fig. 19 shows schematically the method used to determine the jump in the heat capacity at the superconducting

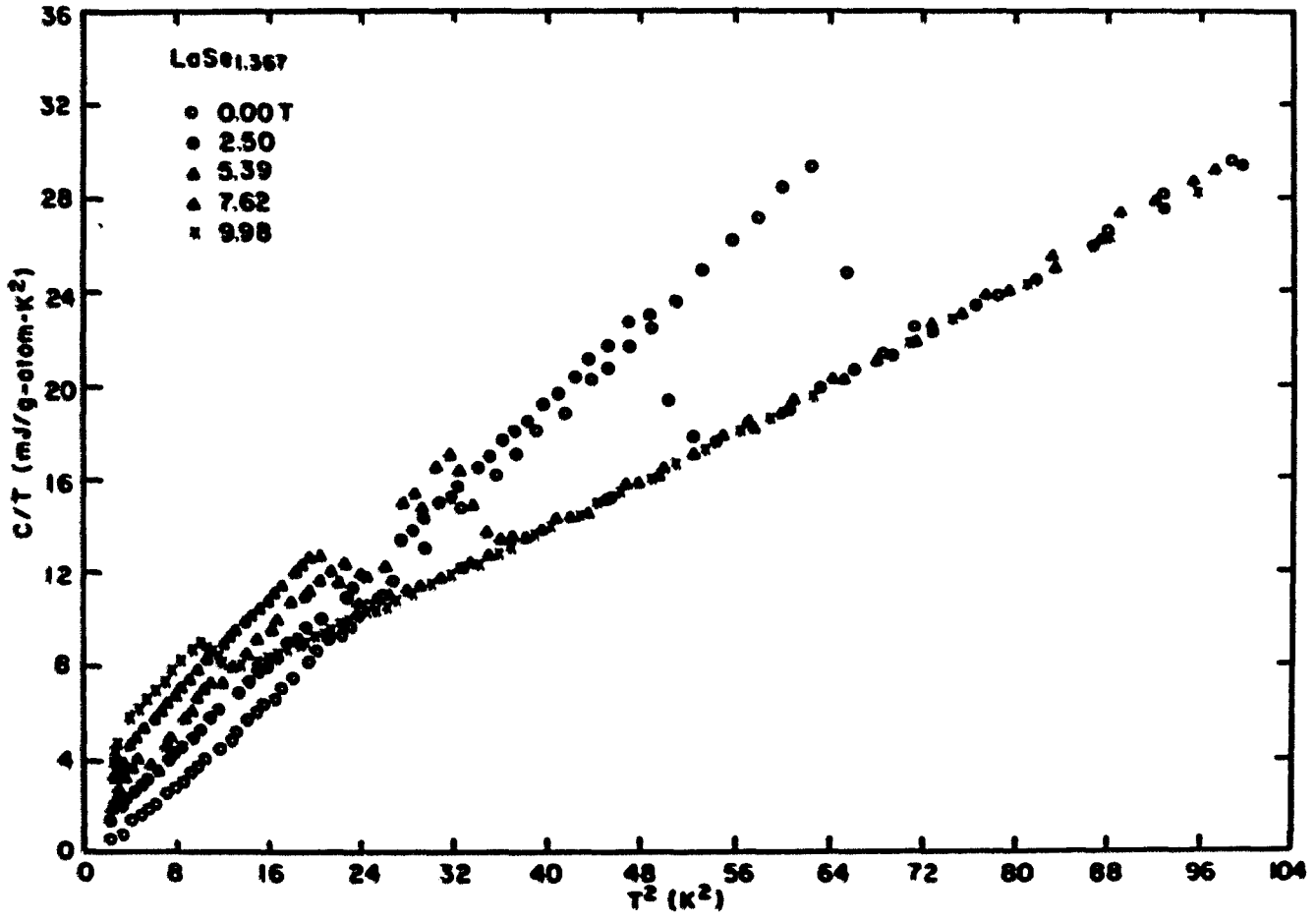

Figure 18. The plot of C/T vs. T^2 from 1.4 to 10 K for $LaSe_{1.367}$

Table 5. The results of the heat capacity measurements : the values of the γ, β, θ_D, $T_c \pm \Delta T_c$ (in zero magnetic field) and the temperature range for the least-squares fitting

Alloy	phase[a] C or T	γ $(\frac{mJ}{g\text{-at. } K^2})$	β $(\frac{mJ}{g\text{-at. } K^4})$	θ_D (K)	$T_c \pm \Delta T_c$ (K)	temp. range (K)
$LaSe_{1.334}$	T	2.93	0.236	202	7.18±0.15	3.8-7.0
$LaSe_{1.360}$	T	3.63	0.273	192	8.15±0.25	2.8-5.4
$LaSe_{1.367}$	C	4.50	0.235	202	8.08±0.29	2.4-4.5
$La(S_{.898}Se_{.102})_{1.358}$	C	4.24	0.188	218	8.15±0.20	5.1-7.0
$La_{.98}Th_{.02}S_{1.333}$	T	3.62	0.164	228	8.44±0.33	3.0-6.0
$La_{.97}Th_{.03}S_{1.333}$	C	4.64	0.194	216	9.24±0.29	6.2-7.6
$La_{.98}Th_{.02}S_{1.341}$	T	3.34	0.185	219	8.45±0.21	3.5-6.4
$La_{.97}Th_{.03}S_{1.360}$	C	3.92	0.162	229	8.05±0.41	5.3-7.0

[a]See the footnote a in Table 4.

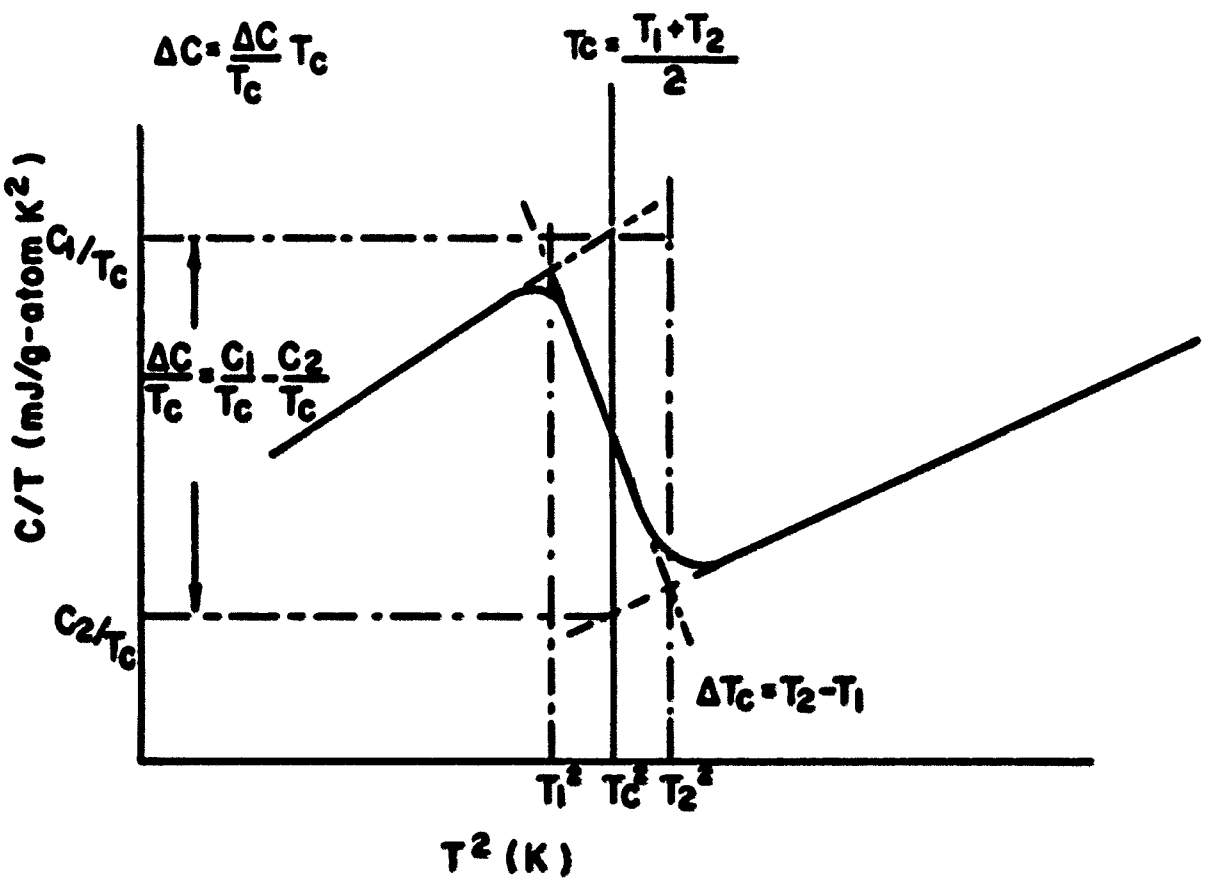

Figure 19. Method shown schematically to determine the jump in the heat capacity at the superconducting temperature, ΔC, the superconducting temperature, T_c and the width of the transition, ΔT_c

temperature (ΔC) the superconducting transition temperature, T_c and the width of the transition (ΔT_c). The values of T_c and ΔT_c are also listed in Table 5. The ΔC(obs) values for the alloys are given in Table 6. Table 6 also lists the values of $\Delta C/\gamma T_c$. All of which are larger than 1.43 from the BCS prediction.

As described in the previous background theory chapter (II), the entropy, S, at T can be obtained from the integration of the C/T with T as expressed in the Eq. (2-16). An example of the C_i vs. T plot where i = s or n for $LaSe_{1.367}$ is given in Fig. 20. The normal state data above T_c^* (in 9.98 T) was taken from the data in 9.98 T and below T_c^* (in 9.98 T) was taken from the Eq. (2-10). At T_c^*, S_n should equal to S_s. An example of the entropy vs. T plot is given in Fig. 21 for $LaSe_{1.367}$. The S_n and S_s at T_c^* and the percentage difference between them for each of the alloys is listed in Table 7. A good agreement (< 1 %) is found for the bcc alloys and a fair agreement (< 7 %) for the bct alloys. The entropy agreements prove that the method of obtaining the γ and β values is reliable.

The electronic heat capacity in the superconducting state, C_{es}, can be determined from Eq. (2-11). The semi-log plots of the reduced superconducting electronic heat capacity, $C_{es}/\gamma T_c$, vs. T_c/T (from 1 to 4.5) are shown in Figs. 22(a) and (b) for selenides and sulfides respectively. The experimental

Table 6. Thermodynamic critical field at 0 K, $H_c(0)$; jump in the heat capacity at T_c in zero filed, $\Delta C(obs)$; $\Delta C(cal)$ obtained from the Rutger's relation; the percentage difference between $\Delta C(obs)$ and $\Delta C(cal)$; and the reduced jump in the heat capacity at T_c, $\Delta C/\gamma T_c$ in which $\Delta C(obs)$ was used for the selenides and sulfides

Alloy	phase[a] C or T	$H_c(0)$ (T)	$\Delta C(obs)$ $(\frac{mJ}{g\text{-at. } K^2})$	$\Delta C(cal)$ $(\frac{mJ}{g\text{-at. } K^2})$	$\Delta(\Delta C)$ %	$\Delta C/\gamma T_c$
$LaSe_{1.334}$	T	0.080	71.76	56.59	21.2	3.41
$LaSe_{1.360}$	T	0.111	79.90	77.72	2.7	2.70
$LaSe_{1.367}$	C	0.115	84.61	83.42	1.4	2.33
$La(S_{.898}Se_{.102})_{1.358}$	C	0.113	77.02	71.96	6.6	2.23
$La_{.98}Th_{.02}S_{1.333}$	T	0.113	79.72	68.78	13.7	2.61
$La_{.97}Th_{.03}S_{1.333}$	C	0.140	91.23	96.09	5.1	2.13
$La_{.98}Th_{.02}S_{1.341}$	T	0.111	77.90	65.92	15.4	2.76
$La_{.97}Th_{.03}S_{1.360}$	C	0.111	70.06	69.35	1.0	2.22

[a]See the footnote a in Table 4.

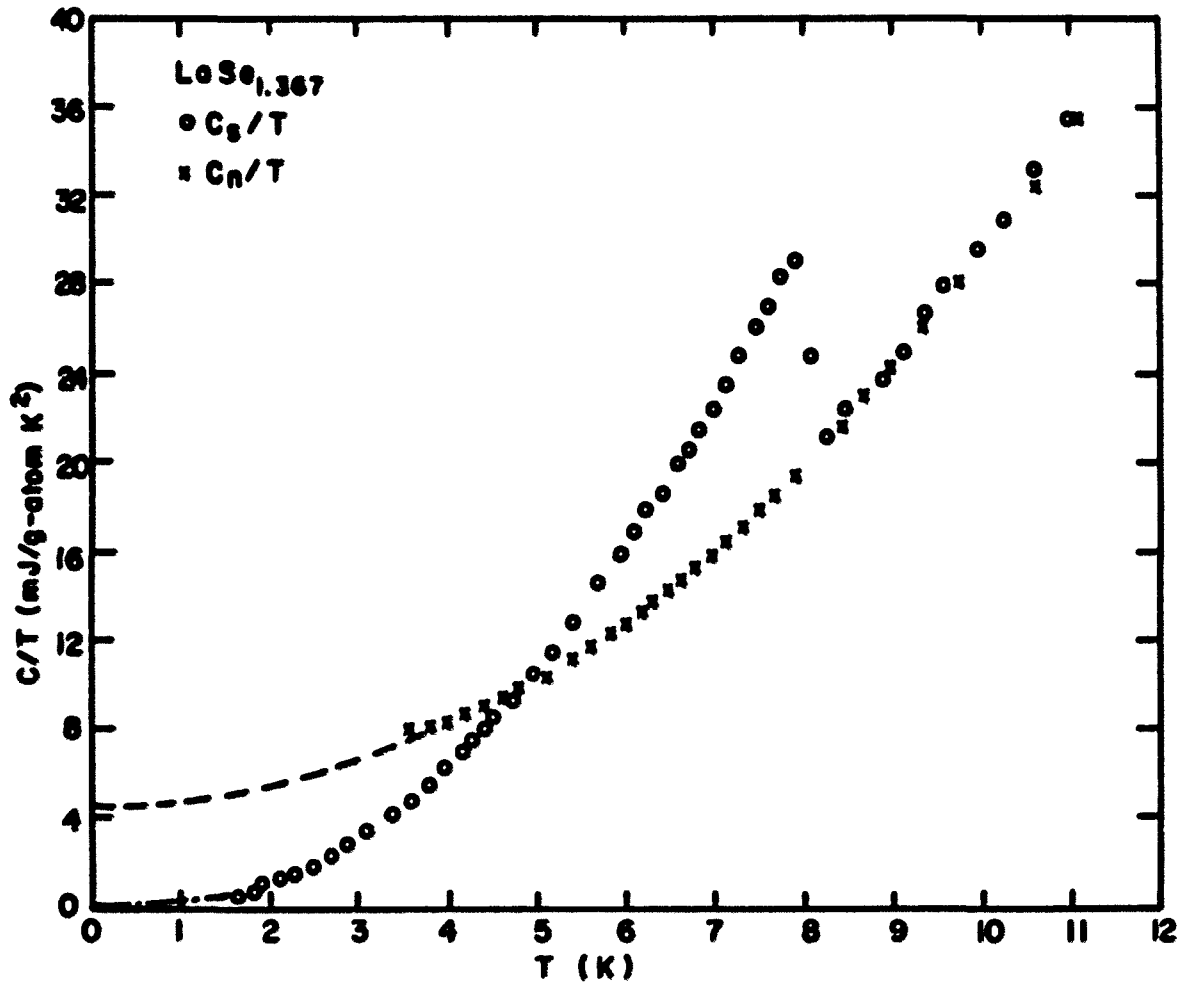

Figure 20. The plot of C_i/T vs. T in which i = s or n for $LaSe_{1.367}$

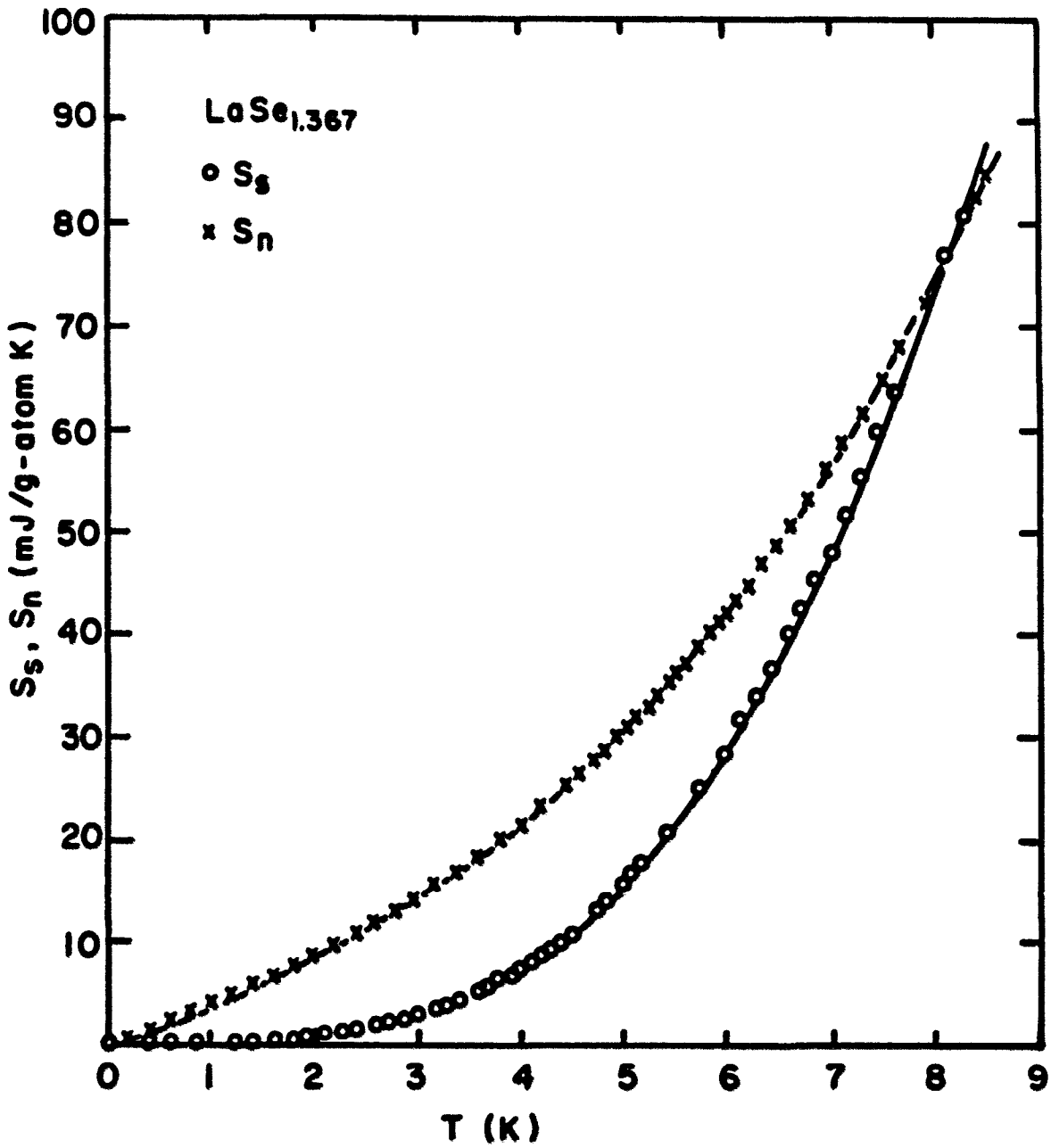

Figure 21. The plot of entropy vs. T for $LaSe_{1.367}$

Table 7. The maximum superconducting temperature, T_c^*; the entropy values at T_c^* in the normal and superconducting states, S_n and S_s respectively; and the percentage difference between S_n and S_s, ΔS

Alloy	phase[a] C or T	T_c^* (K)	S_n $(\frac{mJ}{g\text{-at. } K})$	S_s $(\frac{mJ}{g\text{-at. } K})$	ΔS (%)
$LaSe_{1.334}$	T	7.2	53.5	57.6	7.0
$LaSe_{1.360}$	T	8.3	83.5	81.6	2.2
$LaSe_{1.367}$	C	8.3	81.5	81.5	0.0
$La(S_{.898}Se_{.102})_{1.358}$	C	8.3	70.9	71.5	0.8
$La_{.98}Th_{.02}S_{1.333}$	T	8.7	69.1	71.7	3.7
$La_{.97}Th_{.03}S_{1.333}$	C	9.4	98.2	97.8	0.4
$La_{.98}Th_{.02}S_{1.341}$	T	8.6	68.8	71.1	3.2
$La_{.97}Th_{.03}S_{1.360}$	C	8.3	63.5	64.1	0.9

[a]See the footnote a in Table 4.

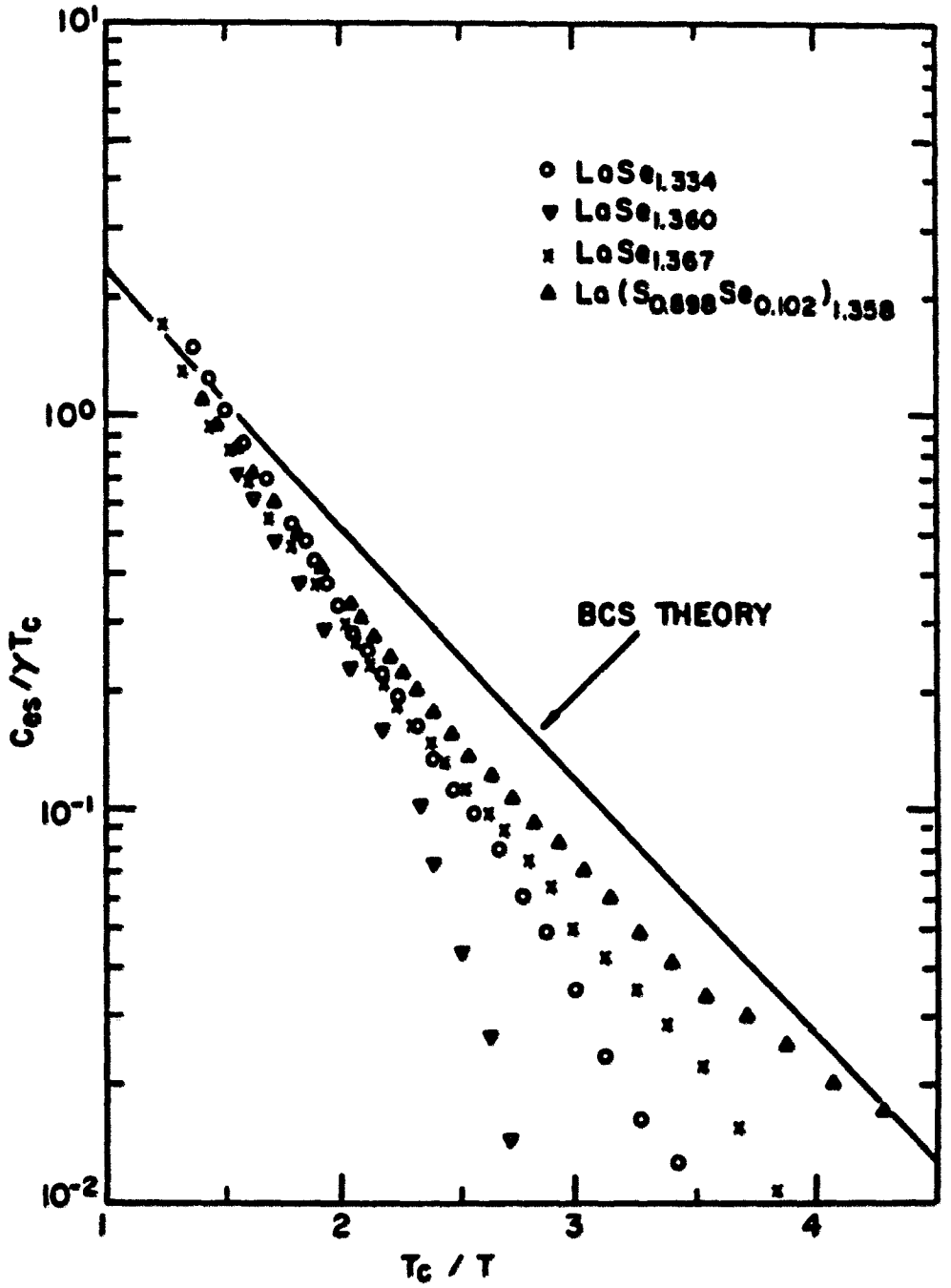

Figure 22(a). Reduced superconducting electronic heat capacity of $LaSe_x$ (x : 1.334, 1.360 and 1.367) and $La(S_{.898}Se_{.102})_{1.358}$ alloys

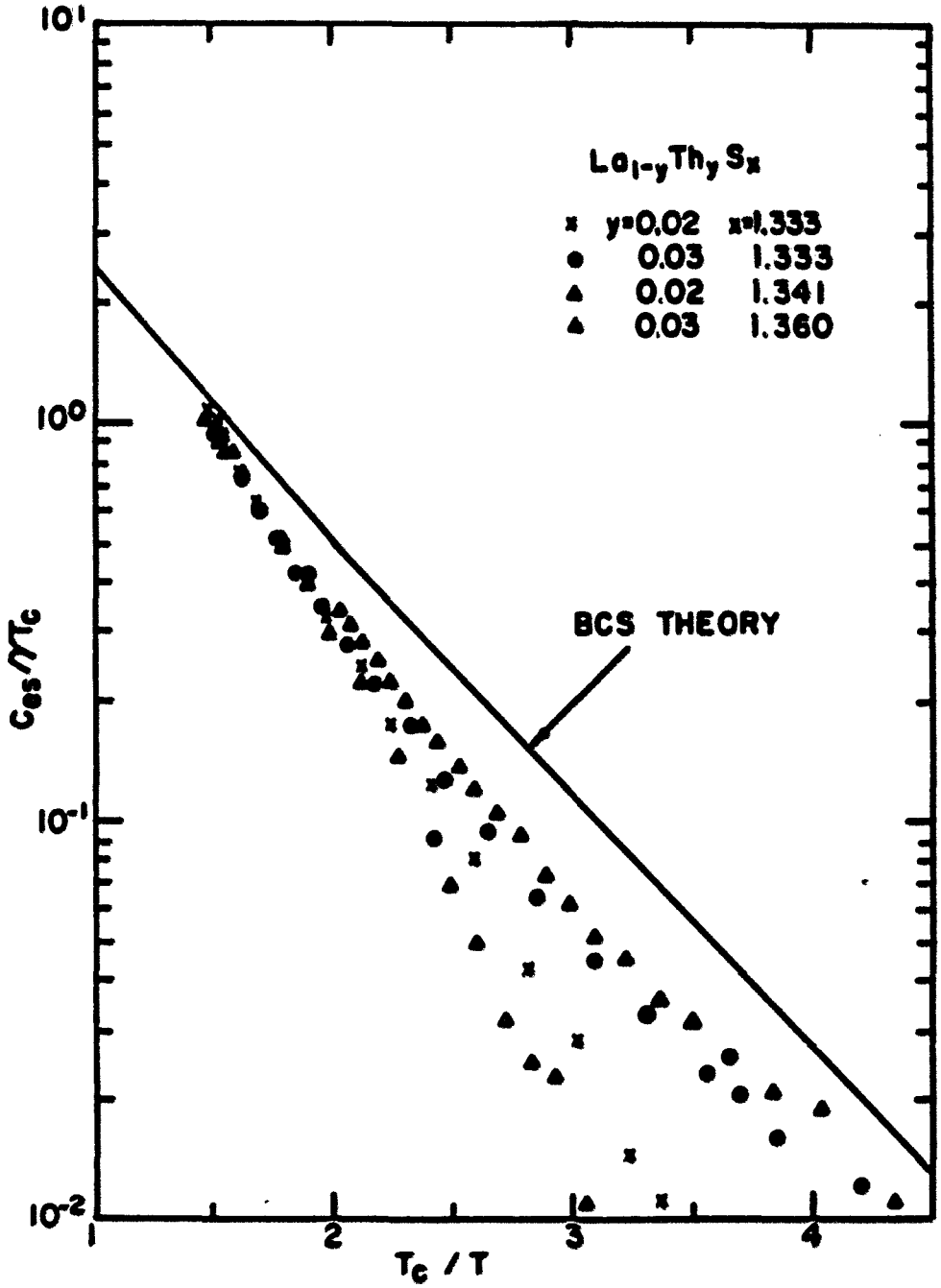

Figure 22(b). Reduced superconducting electronic heat capacity of the $La_{1-y}Th_yS_x$ alloys ($0 < y < 0.03$, $1.333 \leq x \leq 1.360$)

values do not agree well with the BCS theory prediction for a weak-coupling superconductor. The value of the energy gap ($2\Delta(0)$) can be obtained based on the assumptions[41] : (1) $\Delta(T)$ is independent of the energy and isotropic and (2) $\Delta(T)/\Delta(0)$ is identical to that given by BCS. Therefore, the BCS gap is scaled by a constant factor to find the gap of superconductors studied, i. e., $\Delta(T)/\Delta^{BCS}(T)$ = constant. The values of the reduced energy gap, $2\Delta(0)/kT_c(1)$, can be determined from the slopes of the curves in Figs. 22(a) and (b) by the relation

$$2\Delta(0)/kT_c(1) = 3.52 \times b / 1.44$$

$$= 2.44 \times b \qquad (4\text{-}3)$$

where b is the negative of the slope value and was defined in Eq. (2-12), 3.52 is the value from the BCS theory and 1.44 is taken from Eq. (2-13). The ranges of T_c/T for the slope determination, the values of the reduced energy gap obtained from Eq. (4-3), a (defined in Eq. (2-12)) and b are listed in Table 8. It is seen that the values of the reduced energy gap are larger than the BCS prediction of 3.53. Also seen in Table 8, the bct alloys have larger a values than the BCS prediction of 8.5.

The Gibbs free energy can be obtained from the Eq. (2-17). Its values in the normal and superconducting states are plotted in Fig. 23 in which the U + (P V) terms are neglected since they remain the same in both states. From the

Table 8. The constants a and b defined in Eq. (2-12); the range of T_c/T; the values of the reduced energy gap, $2\Delta(0)/kT_c(1)$ and $2\Delta(0)/kT_c(2)$ obtained from Eqs. (4-3) and (4-6) respectively

Alloys	phase[a] C or T	a	b	range of T_c/T	$2\Delta(0)/kT_c$ (1)	$2\Delta(0)/kT_c$ (2)
$LaSe_{1.334}$	T	22.5	2.13	2.0-2.7	5.20	3.74
$LaSe_{1.360}$	T	58.4	2.78	1.5-2.7	6.79	4.16
$LaSe_{1.367}$	C	9.2	1.73	2.0-4.0	4.23	3.88
$La(S_{.898}Se_{.102})_{1.358}$	C	7.4	1.52	1.5-4.0	3.71	3.70
$La_{.98}Th_{.02}S_{1.333}$	T	35.9	2.38	1.5-3.4	5.81	3.85
$La_{.97}Th_{.03}S_{1.333}$	C	10.8	1.74	1.5-4.0	4.25	3.84
$La_{.98}Th_{.02}S_{1.341}$	T	63.6	2.74	1.5-2.8	6.69	3.92
$La_{.97}Th_{.03}S_{1.360}$	C	8.9	1.63	1.5-4.0	3.98	3.80

[a]See the footnote a in Table 4.

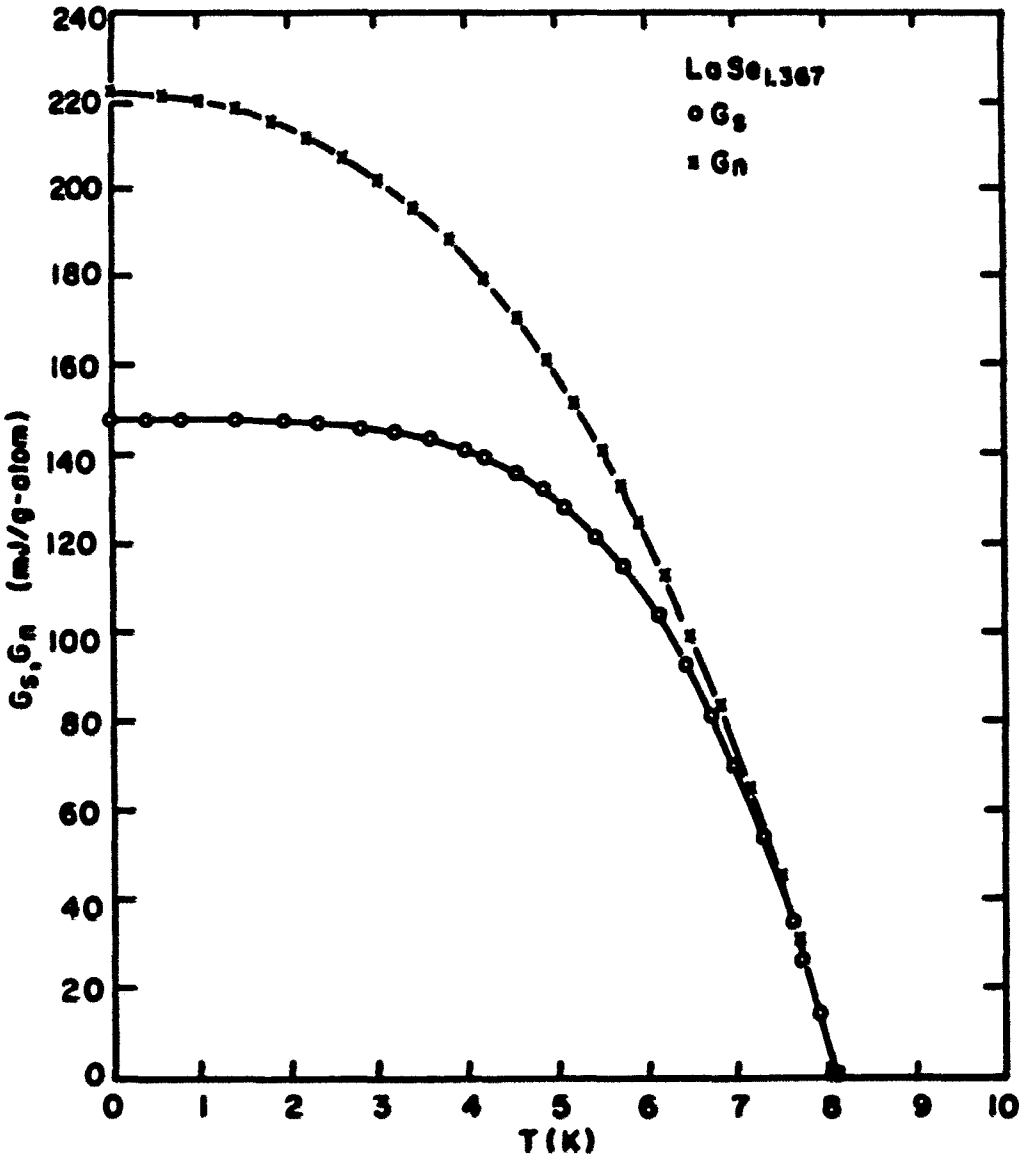

Figure 23. The plot of Gibbs free energy vs. T for $LaSe_{1.367}$

Eq. (2-20c), $H_c(T)$ can be calculated from the difference between $G_n(T)$ and $G_s(T)$. Table 6 lists the $H_c(0)$ values. For each of the alloys measured, the $H_c(0)$ value is small as compared to the corresponding $H_{c2}(0)$ value since the alloys are still superconducting at 2.50 T or above.

According to Eq. (2-21), the relationship between the $H_c(t)$ ($t = T/T_c$) and t^2 is linear. It is obeyed rather well for the selenides and sulfides as shown in Figs. 24(a) and (b) for the selenides and sulfides respectively. The deviation function, D(t) is defined as follows.

$$D(t) = H_c(t)/H_c(0) - [1 - t^2] \qquad (4\text{-}4)$$

The D(t) vs. t^2 plot is shown in Figs. 25(a) and (b) for the selenides and sulfides respectively. The plots of the D(t) from the BCS prediction[42] and for Sn[43] (weak coupling) and Hg[43] (strong coupling) are also included in the plots. It is seen that the selenides and sulfides with $x \lesssim 1.370$ are strong-coupling superconductors. The shapes of the D(t) curves, especially the initial changes in the D(t) values, show the systematic changes in the reduced energy gap values in each alloy system.

The jump in the heat capacity, ΔC at T_c in zero field can be calculated by using the Rutger's relation[30]

$$\Delta C(\text{cal}) = (V\, T_c/4\pi)\, (dH_c(T)/dT)^2_{T=T_c} \qquad (4\text{-}5)$$

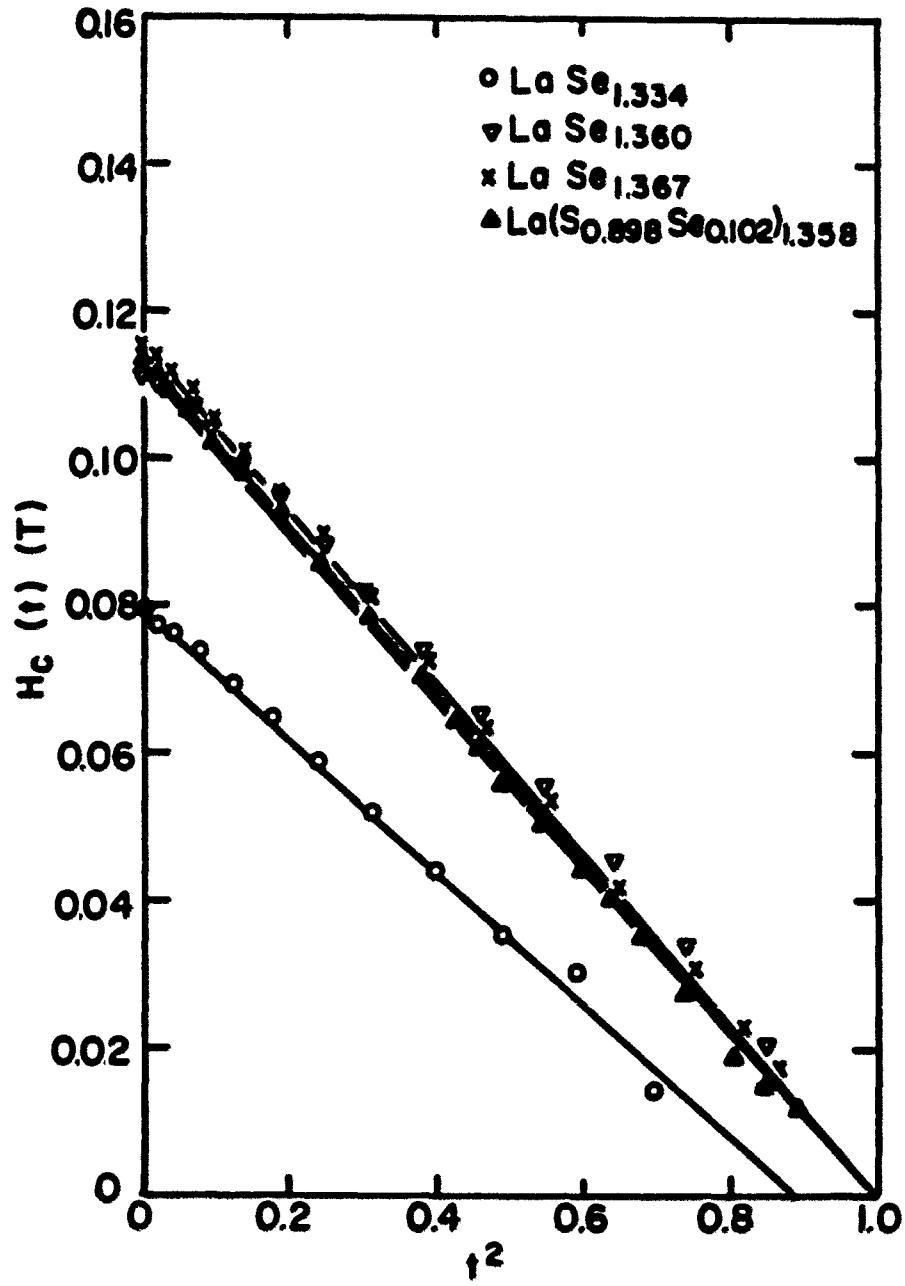

Figure 24(a). The $H_c(t)$ vs. t^2 plot for the selenides

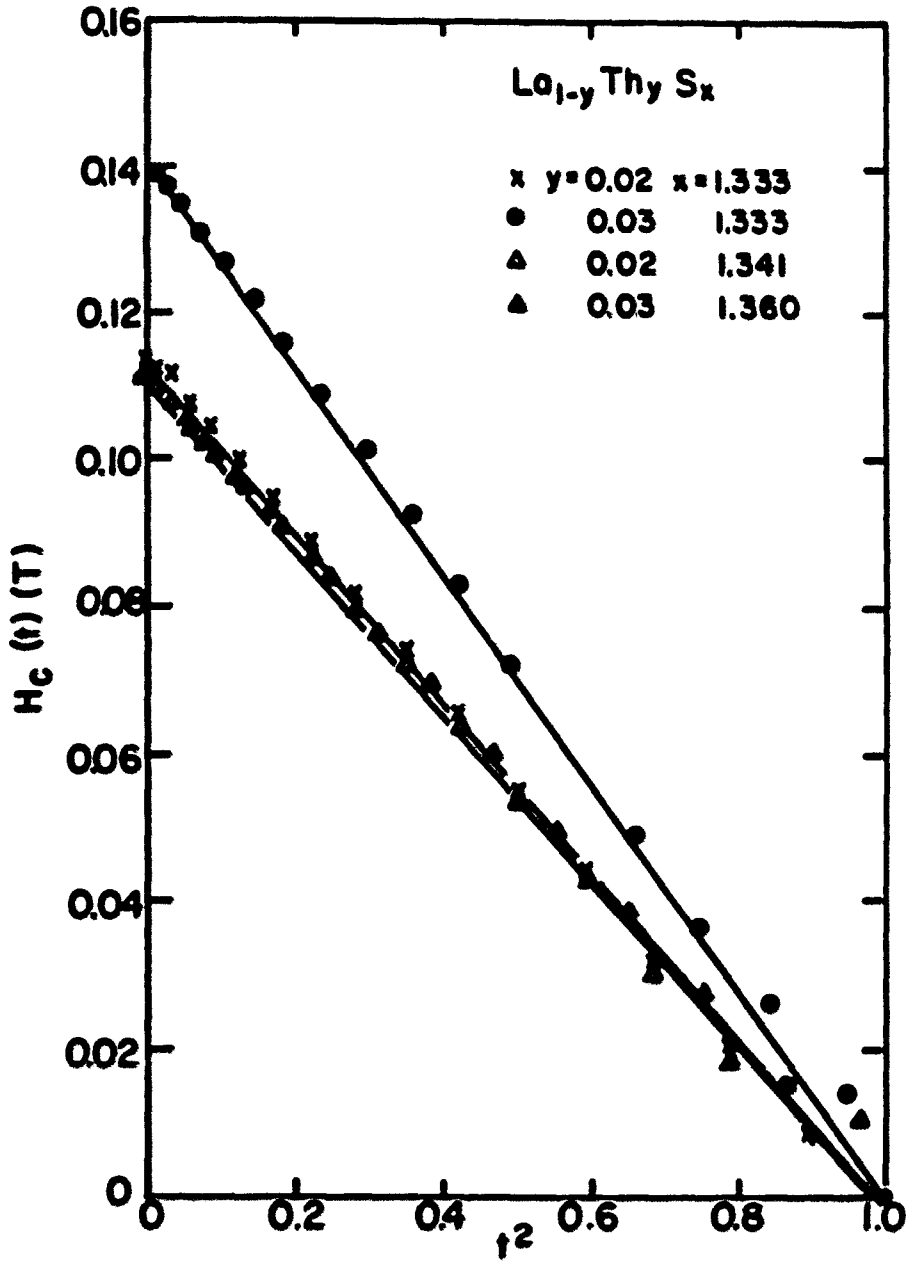

Figure 24(b). The $H_c(t)$ vs. t^2 plot for the sulfides

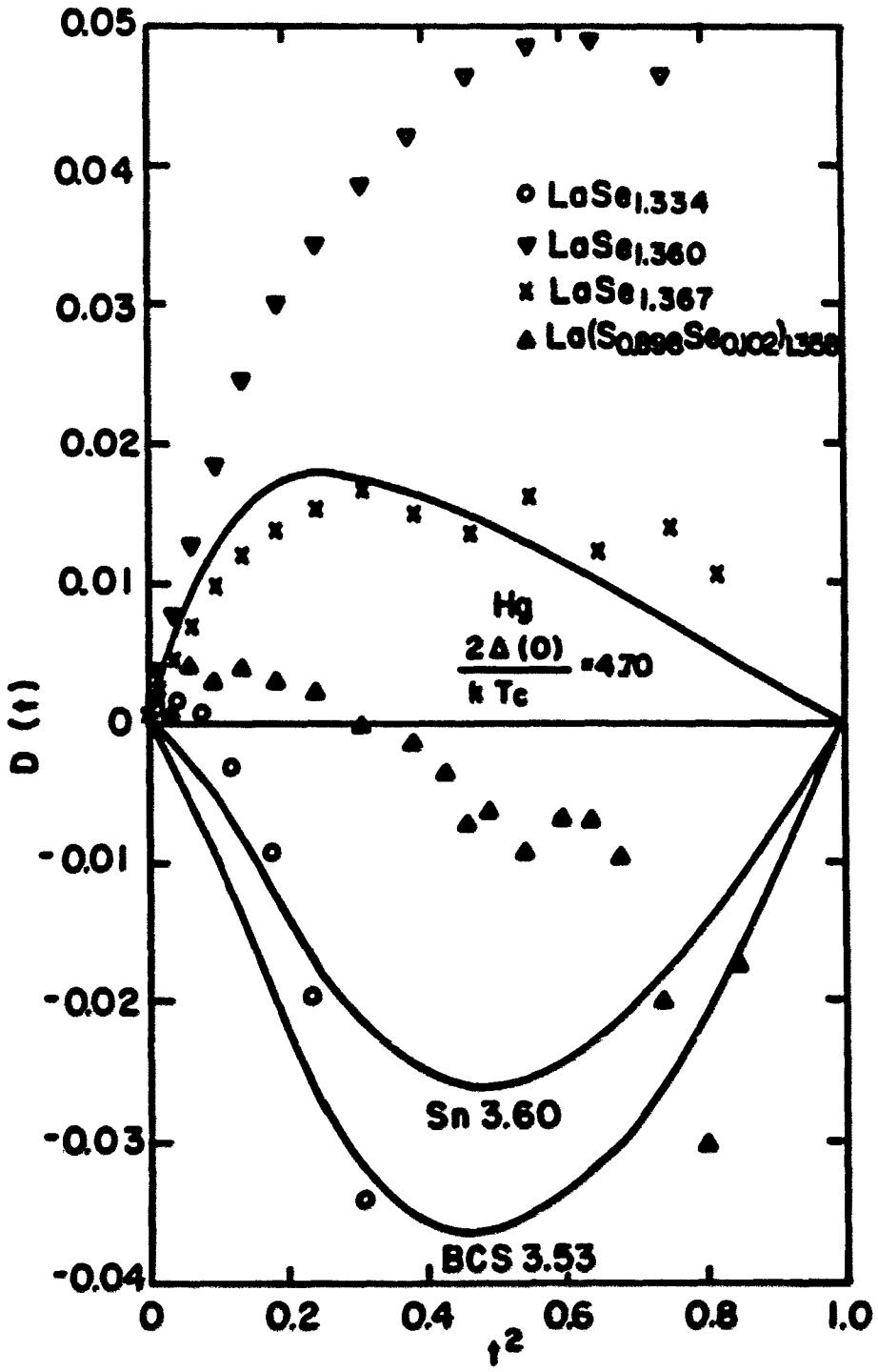

Figure 25(a). The D(t) vs. t^2 plot for selenides

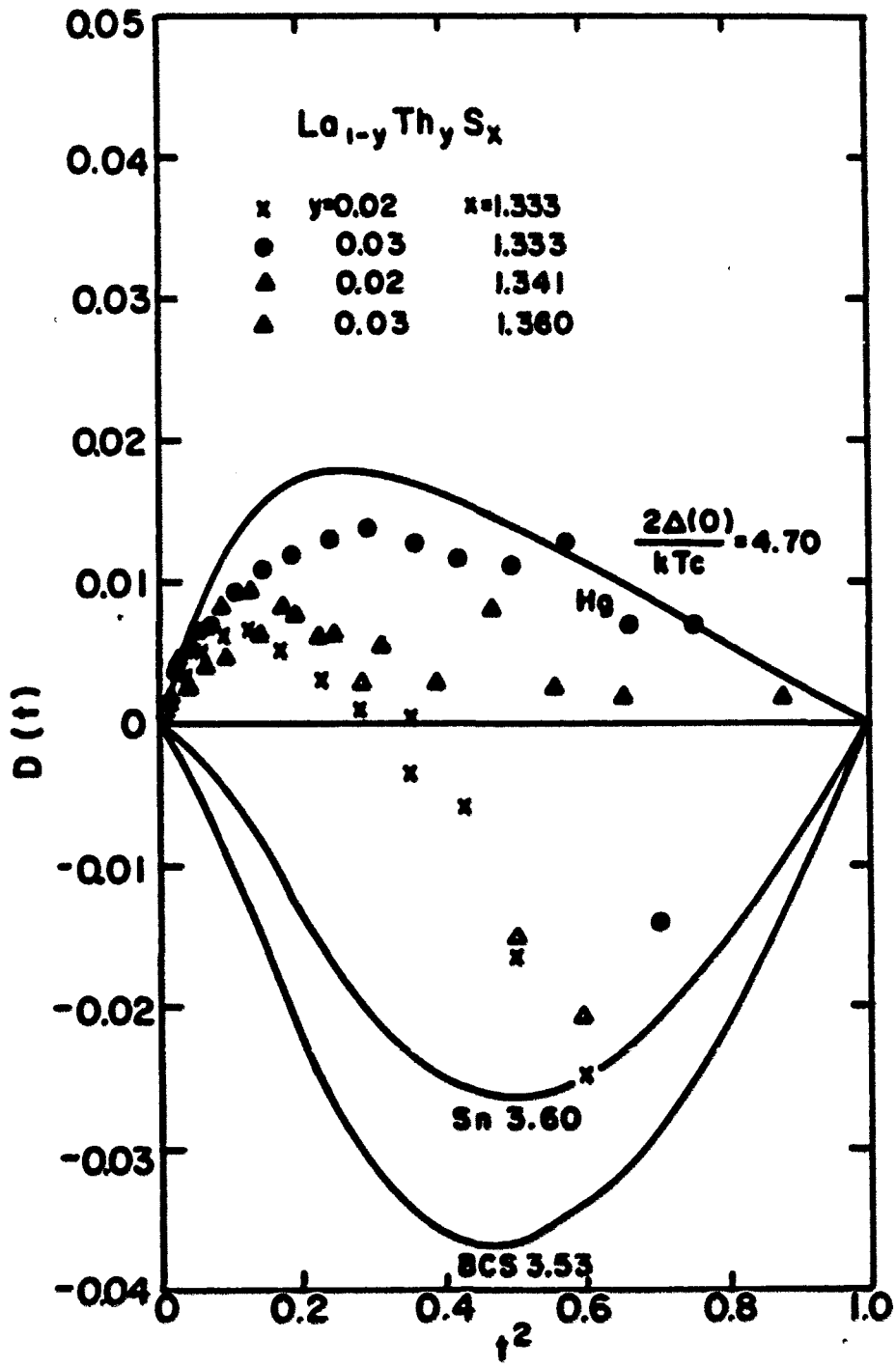

Figure 25(b). The D(t) vs. t^2 plot for sulfides

Eq. (2-21) has been used to calculate the slope of the $H_c(T)$ vs. T at T_c. For $LaSe_{1.334}$ alloy, $H_c(t) = H_c(0)\,[1 - t^2/0.89]$ was used. The factor of 0.89 was taken from the $H_c(t)$ vs. t^2 plot in Fig. 24(a). The ΔC(cal) values are compared to the ΔC(obs) found experimentally and are given in Table 6. It is seen that the bcc alloys are in better agreement (< 7 %) in ΔC values than the bct alloys(< 21 %).

According to Goodman[44], the values of the reduced energy gap at T = 0 can be obtained from the relation

$$2\Delta(0)/kT_c(2) = 4\pi/\sqrt{3}\,[H_c^2(0)\,V / 8\pi\gamma T_c^2]^{1/2} \qquad (4\text{-}6)$$

The values of the reduced energy gap obtained from Eq. (4-6) are compared to the values obtained from Eq. (4-3) and listed in Table 8. Again, a better agreement (< 10 %) is seen for the bcc alloys than the bct alloys (< 41 %). The reduced energy gap values obtained from both Eqs. (4-3) and (4-6) are larger than the BCS prediction of 3.53 especially for the bct alloys.

According to Hohlfeld and Pietrass[45], Eq. (4-6) valid for a weak-coupling superconductor should be modified for a strong-coupling superconductor. A correction factor[45] arising from the characteristic phonon spectrum was included in Eq. (4-6). Using this factor, the correction would increase the

reduced energy gap value by about 5 %. As discussed in Ref. 45, the determination of the energy gap from the $H_c(0)$ gives more reliable results than the plot of $\ln C_{es}/\gamma T_c$ vs. T_c/T.

McMillan[46] explained theoretically that the transition temperature of a strong-coupling superconductor is related to the Debye temperature and the electron-phonon coupling parameter, λ, by

$$T_c = \Theta_D / 1.45 \exp \{- 1.04 (1+\lambda)/[\lambda - \mu^* (1 + 0.62 \lambda)]\} \quad (4-7)$$

where μ^* is the repulsive electron-electron interaction parameter. The value of the μ^* can be taken to be the same as that of lanthanum metal - 0.08[47]. The value of λ for each of the alloys is given in Table 9. Now, the density of states at the Fermi energy at 0 K, N(0), can be calculated from Eq. (2-8). The N(0) values are listed in Table 9. From the plots of λ and N(0) vs. x in the $LaSe_x$ alloys (which are not shown here), the largest values of λ and N(0) are obtained at x_c, the critical phase transformation temperature. Same behavior has been found for the LaS_x system in Ref. 16. The largest N(0) value at $x_c = 1.363$ in the $LaSe_x$ system lies between 2.3 and 2.6 states/eV-atom which is close to the value for β-La (fcc) metal (2.44[48] states/eV-atom).

Table 10 lists the superconducting transition temperatures at different magnetic fields for each alloy. It

Table 9. The electron-phonon coupling parameter (λ); and the electronic density of states at the Fermi surface (N(0)) for the selenides and sulfides

Alloy	phase[a] C or T	λ	N(0) ($\frac{\text{states}}{\text{eV-at.}}$)	N(0) ($\frac{\text{states}}{\text{eV-La at.}}$)
$LaSe_{1.334}$	T	0.72	0.724	1.690
$LaSe_{1.360}$	T	0.78	0.864	2.039
$LaSe_{1.367}$	C	0.76	1.086	2.571
$La(S_{.898}Se_{.102})_{1.358}$	C	0.74	1.036	2.443
$La_{.98}Th_{.02}S_{1.333}$	T	0.73	0.886	2.067
$La_{.97}Th_{.03}S_{1.333}$	C	0.79	1.102	2.571
$La_{.98}Th_{.02}S_{1.341}$	T	0.75	0.812	1.901
$La_{.97}Th_{.03}S_{1.360}$	C	0.72	0.970	2.289

[a]See the footnote a in Table 4.

Table 10. The superconducting transition temperatures in magnetic fields of 0.00, 2.50, 5.39, 7.62 and 9.98 T for the selenides and sulfides

Alloy / T_c (K)	phase[a] C or T	H 0.00 (T)	2.50 (T)	5.39 (T)	7.62 (T)	9.98 (T)
$LaSe_{1.334}$	T	7.18	3.38	none	none	none
$LaSe_{1.360}$	T	8.15	6.79	5.03	3.57	none
$LaSe_{1.367}$	C	8.08	7.08	5.81	4.70	3.42
$La(S_{.898}Se_{.102})_{1.358}$	C	8.15	7.37	6.42	5.59	4.67
$La_{.98}Th_{.02}S_{1.333}$	T	8.44	7.14	5.53	4.17	2.41
$La_{.97}Th_{.03}S_{1.333}$	C	9.24	8.50	7.49	6.66	5.81
$La_{.98}Th_{.02}S_{1.341}$	T	8.45	7.26	5.82	4.52	3.22
$La_{.97}Th_{.03}S_{1.360}$	C	8.05	7.33	6.41	5.66	4.75

[a]See the footnote a in Table 4.

is seen that the upper critical field at 0 K, $H_{c2}(0)$, is much larger than 10 T for most alloys, suggesting that the selenides and sulfides are high field superconductors. The functional dependences of the $H_{c2}(T)$ can be determined in the following way.

The $H_{c2}(T)$ is related to the $H_c(T)$ by the parameter κ_1 defined in Eq. (2-22). The $H_{c2}(T)$ data in Table 10 and a parabolic form for $H_c(T)$ have been used to obtain the $\kappa_1(T)$ values. The $\kappa_1(T)$ values are shown in Figs. 26(a) and (b) for the selenides and sulfides respectively. In Figs. 26(a) and (b), the solid lines are the results of the least-squares fitting of the data to the relationship

$$\kappa_1(t) = D_0 - D_1 t^2 \qquad (4\text{-}8)$$

where $t = T/T_c$ and D_0 and D_1 are the fitting constants and their values are listed in Table 11. For selenides and sulfides, the changes in the reduced values of $\kappa_1(t)$ over the whole temperature range do not exceed 40 % which is comparable to the theoretical calculation of 25 %.[49]

The upper critical field, $H_{c2}(T)$, is then calculated from Eq. (2-22) by using the parabolic form of $H_c(T)$ and the one degree best-fitting of $\kappa_1(T)$, i. e.,

$$H_{c2}(T) = \sqrt{2}\, H_c(0)\, (1- t^2)\, (D_0 - D_1 t^2) \qquad (4\text{-}9)$$

The values of $H_{c2}(T)$ are plotted in Figs. 27(a) and (b) for

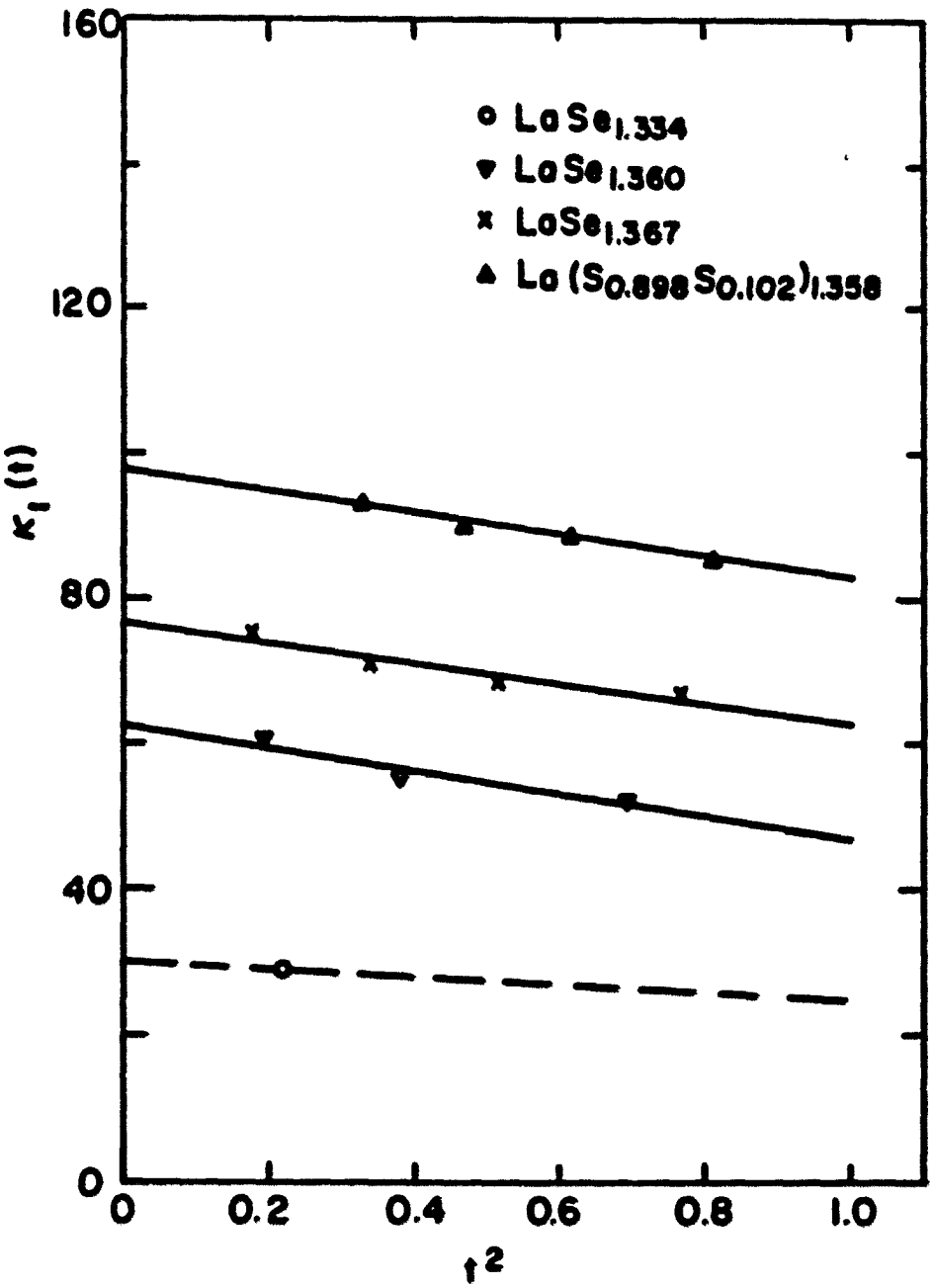

Figure 26(a). Generalized Ginzburg-Landau parameter $\kappa_1(t)$ vs. t^2, where $t = T/T_c$ for the selenides. The solid lines are the results of least-squares fitting against $\kappa_1(t) = D_0 - D_1 t^2$. The slope for $LaSe_{1.334}$ (dashed line) was estimated, see the footnote b in Table 11

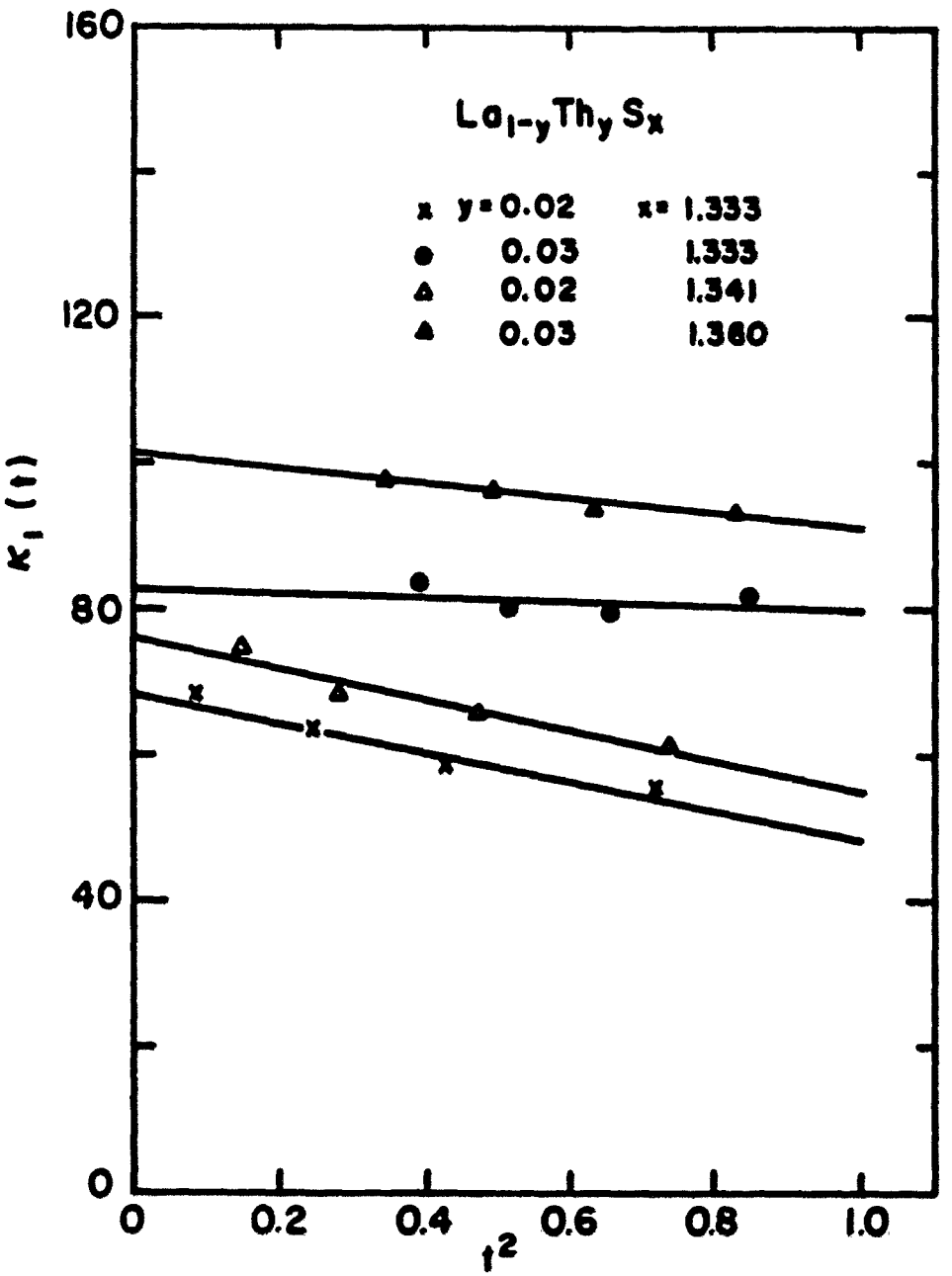

Figure 26(b). Generalized Ginzburg-Landau parameter $\kappa_1(t)$ vs. t^2, where $t = T/T_c$ for the sulfides. The solid lines are the results of least-squares fitting against $\kappa_1(t) = D_0 - D_1 t^2$

Table 11. The values of the constants in Eq. (4-8); generalized Ginzburg-Landau parameters (κ_1, κ_2 and κ); and the upper critical fields at 0 K ($H_{c2}(0)$) for the selenides and sulfides

Alloy	phase[a] C or T	D_0	D_1	κ		$H_{c2}(0)$ (obs) (T)	$H_{c2}(0)$ (cal) (T)
				$\kappa_1(t=1)$	$\kappa_2(t=1)$		
$LaSe_{1.334}$[b]	T	29.7	5.4	24.4	17.9	3.35	1.24
$LaSe_{1.360}$	T	62.3	15.4	46.9	43.0	9.80	5.62
$LaSe_{1.367}$	C	76.6	14.0	62.6	57.8	12.42	9.89
$La(S_{.898}Se_{.102})_{1.358}$	C	97.7	14.8	82.9	74.6	15.55	14.75
$La_{.98}Th_{.02}S_{1.333}$	T	68.6	20.0	48.6	42.0	10.98	7.25
$La_{.97}Th_{.03}S_{1.333}$	C	82.9	3.1	79.7	75.5	16.41	18.67
$La_{.98}Th_{.02}S_{1.341}$	T	76.0	21.1	54.9	46.8	11.90	6.63
$La_{.97}Th_{.03}S_{1.360}$	C	101.3	10.3	91.0	83.9	15.83	13.93

[a]See the footnote a in Table 4.
[b]For $LaSe_{1.334}$ alloy, a ratio of 1.22 has been assumed for $\kappa_1(t=0)/\kappa_1(t=1)$.

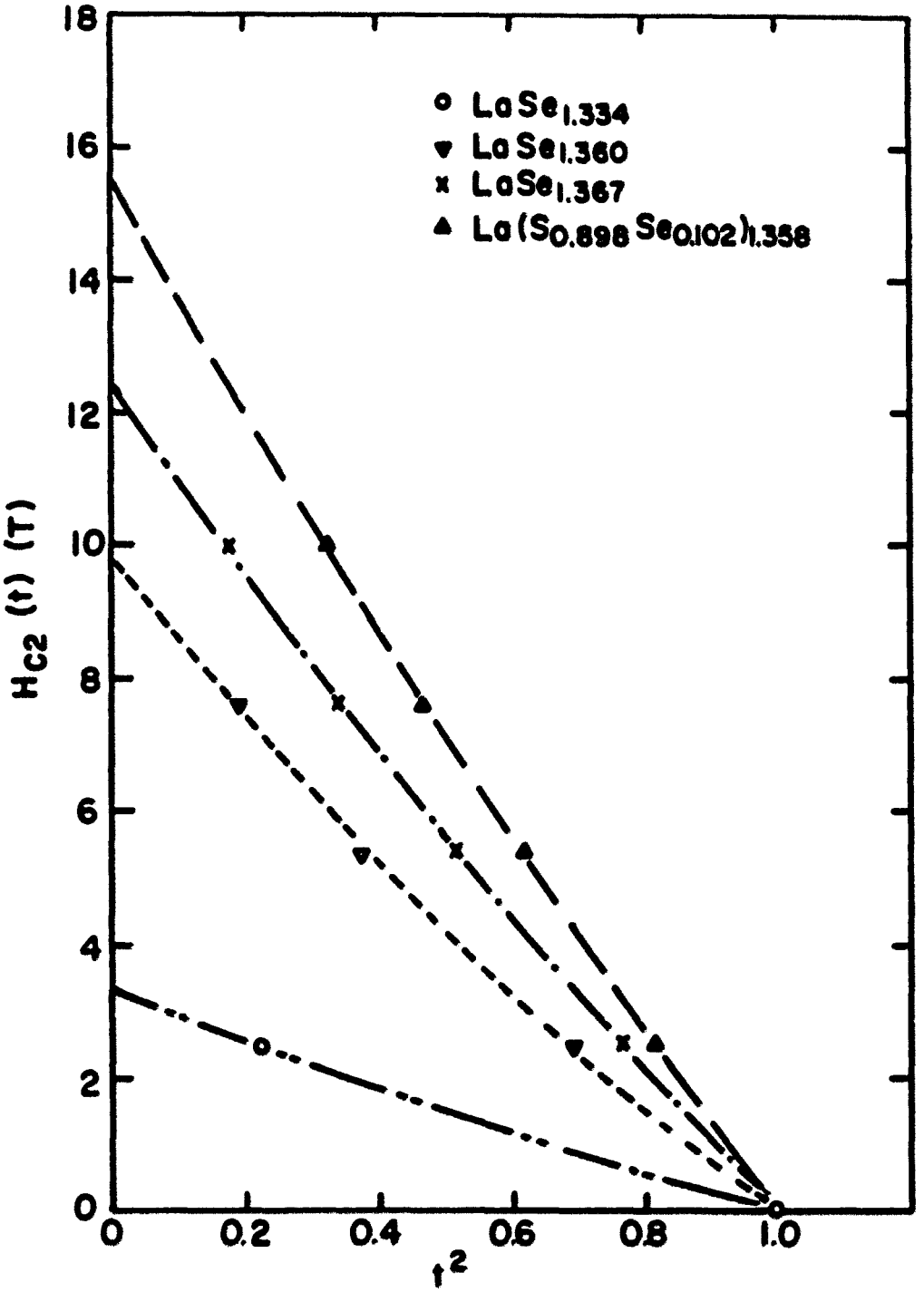

Figure 27(a). Upper critical field $H_{c2}(t)$ vs. t^2 for the selenides, where $t = T/T_c$. The dashed lines are the results from Eq. (4-8) and the points are the experimental values

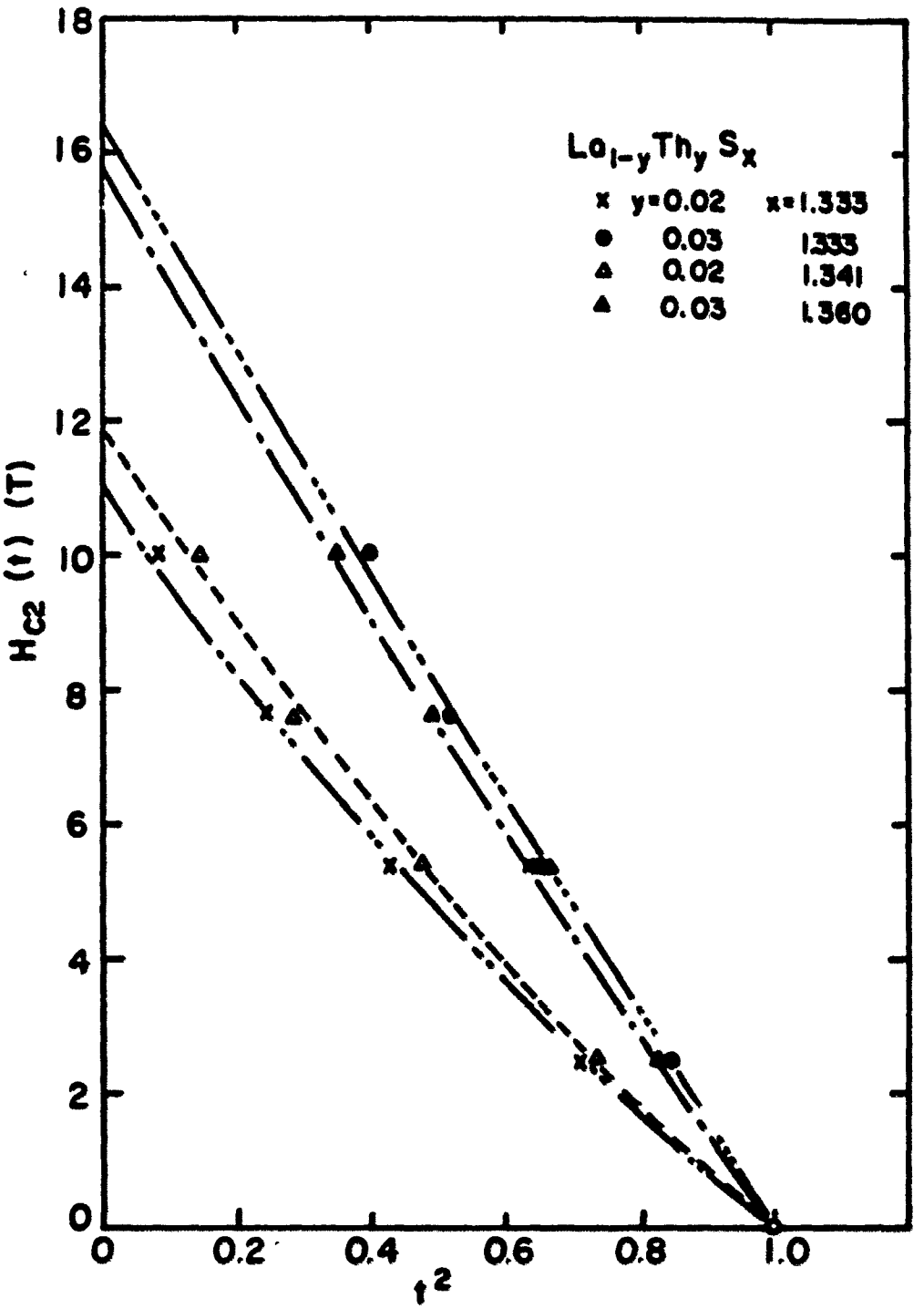

Figure 27(b). Upper critical field $H_{c2}(t)$ vs. t^2 for the sulfides, where $t = T/T_c$. The dashed lines are the results from Eq. (4-8) and the points are the experimental values

each of the alloys. The $H_{c2}(0)$ determined in this way are listed as $H_{c2}(0)(obs)$ in Table 11. Note that the bcc alloys have larger $H_{c2}(0)$ values than the bct alloys.

The $H_{c2}(0)$ value can also be calculated by using Eq. (2-26) proposed by Kim et al.[33] Table 11 also lists the $H_{c2}(0)(cal)$ values. The comparison of $H_{c2}(0)(obs)$ vs. $H_{c2}(0)(cal)$ is shown in Fig. 28. The data points would be expected to lie on the dotted line if Eq. (2-26) holds for the $LaSe_x$ alloys. The calculated values are too small in comparison with the observed values, especially for the bct alloys. The deviation is larger as the composition decreases.

The $\kappa_2(T)$ values can be determined from Eqs. (2-23) and (2-25) in which Eq. (4-9) was used in Eq. (2-25) to find the slope of the $H_{c2}(T)$ at T_H. The $\kappa_2(T)$ values are shown in Figs. 29(a) and (b) for the selenides and sulfides respectively. The solid lines in the plots are the results of the least-squares fitting to the relation

$$\kappa_2(t) = E_0 + E_1 t^2 + E_2 t^4 + E_3 t^6 \qquad (4\text{-}10)$$

where E_0 to E_3 are the fitting constants. According to Eq. (2-24), the κ values can be determined from $\kappa_1(t = 1)$ or $\kappa_2(t = 1)$. The κ values are listed in Table 11. As seen in the Table, the bcc alloys have higher κ values than the bct alloys.

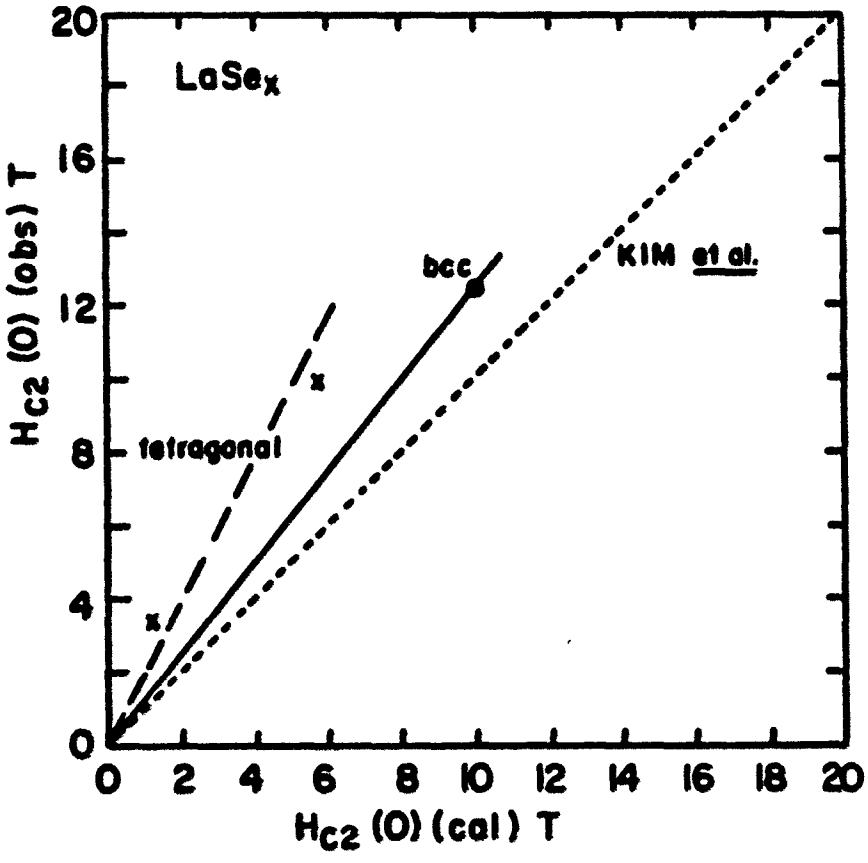

Figure 28. Comparison of $H_{c2}(0)$ (obs) vs. $H_{c2}(0)$ (cal) in the selenides. The points would be expected to lie on the dotted line if Eq. (2-26) holds for the selenides

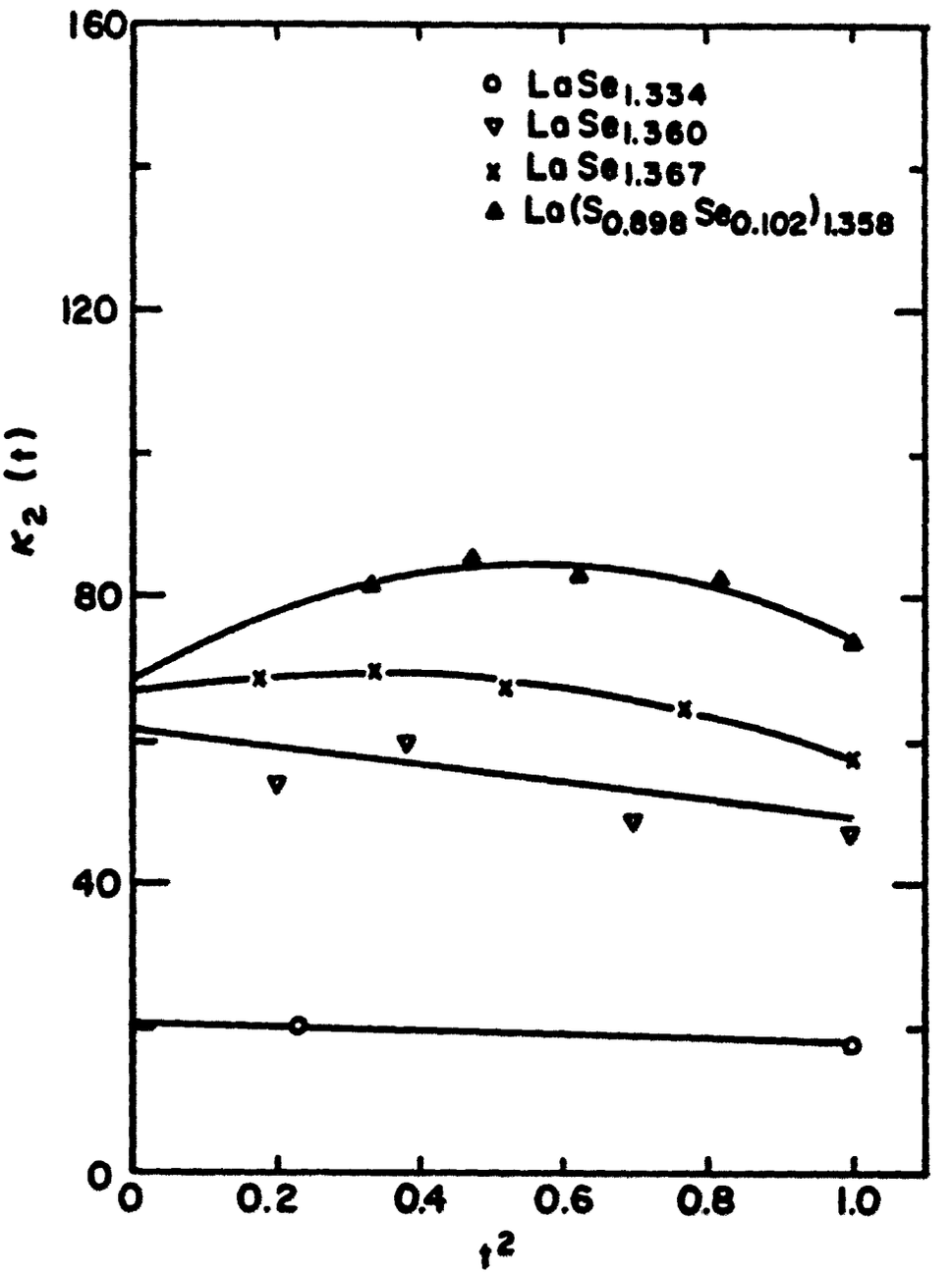

Figure 29(a). The $\kappa_2(t)$ vs. t^2 plot for the selenides. The solid lines are the results of least-squares fitting against $\kappa_2(t) = E_0 + E_1 t^2 + E_2 t^4 + E_3 t^6$

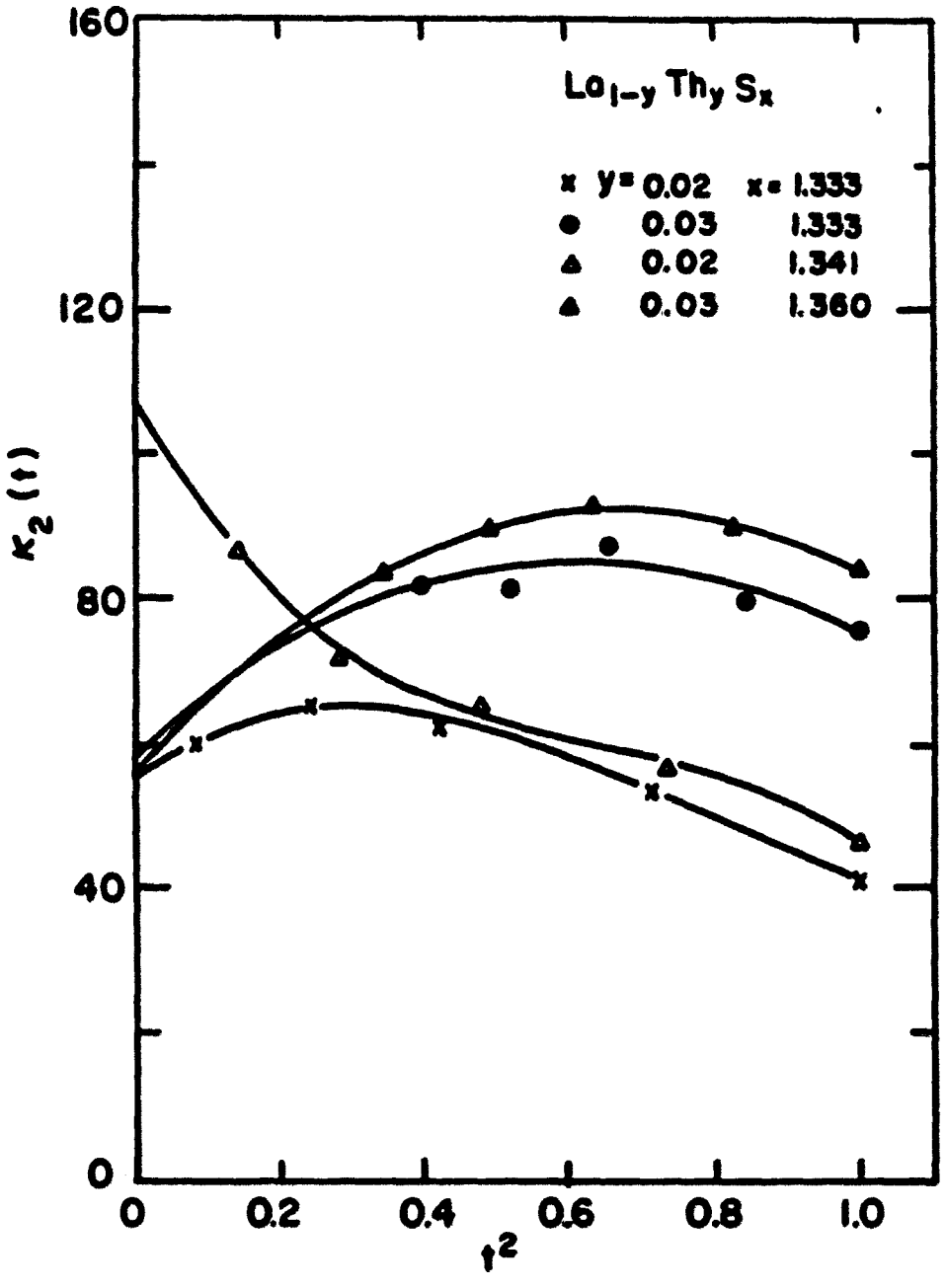

Figure 29(b). The $\kappa_2(t)$ vs. t^2 plot for the sulfides. The solid lines are the results of least-squares fitting against $\kappa_2(t) = E_0 + E_1 t^2 + E_2 t^4 + E_3 t^6$

V. DISCUSSION

A. Influence of the Phase Transformation on Superconductivity

The results of the heat capacity and the electrical resistivity measurements for the selenides are summarized in Figs. 14(a), 15 and 30. In Fig. 30, the expected cubic values for $H_{c2}(0)$ were calculated by Eq. (2-26) in which the expected cubic values for γ, ρ_r and T_c were used and a constant of 5.41 was used instead of 3.11 so that the $H_{c2}(0)$ (cal) value agreed with $H_{c2}(0)$ (obs) for $LaSe_{1.360}$. The effect of alloying with Th in the sulfides is shown in Figs. 14(b), 15, 16(b), 17 and 31. In Fig. 31 only the cubic phase data are used. The data for y = 0 are taken from Ref. 16. For Th alloys, a constant of 3.35 was used in Eq. (2-26) to calculate $H_{c2}(0)$ values so that the $H_{c2}(0)$ (cal) value agreed with $H_{c2}(0)$ (obs) value for $La_{.97}Th_{.03}S_{1.360}$. The results of the replacement of S by Se are shown in Figs. 32 and 33.

As shown in Figs. 1 and 30 and also 14(a),(b) and 15, the sulfides and selenides behave similarly with respect to the superconductivity and the phase transformation. In fact, the solid lines for θ_D, γ and $H_{c2}(0)$ in the cubic phase in Fig. 30 were drawn based on the results of sulfides. The θ_D values are expected to decrease with increasing conduction electron concentration (i. e., decreasing x) due to the increasing

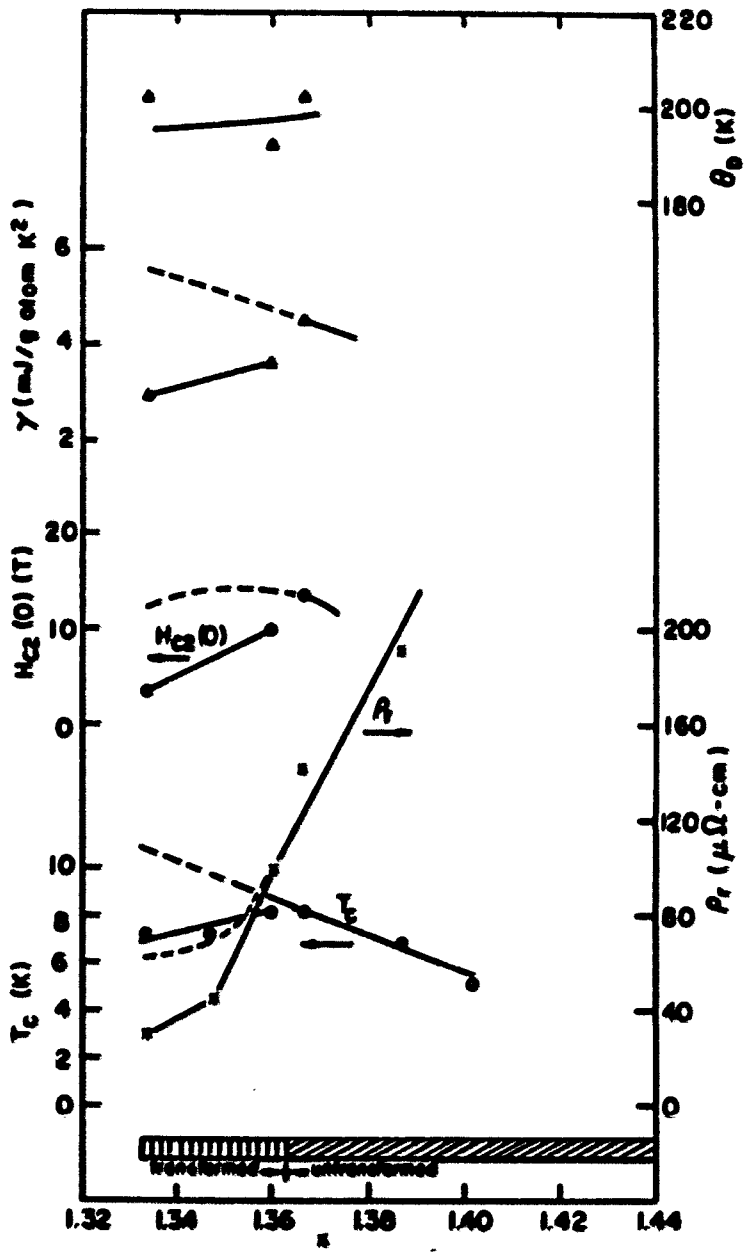

Figure 30. Summary of the results of the heat capacity and electrical resistivity measurements for the $LaSe_x$ alloys ($1.333 < x < 1.410$). The dashed lines are the expected values if the alloys remained cubic at low temperatures

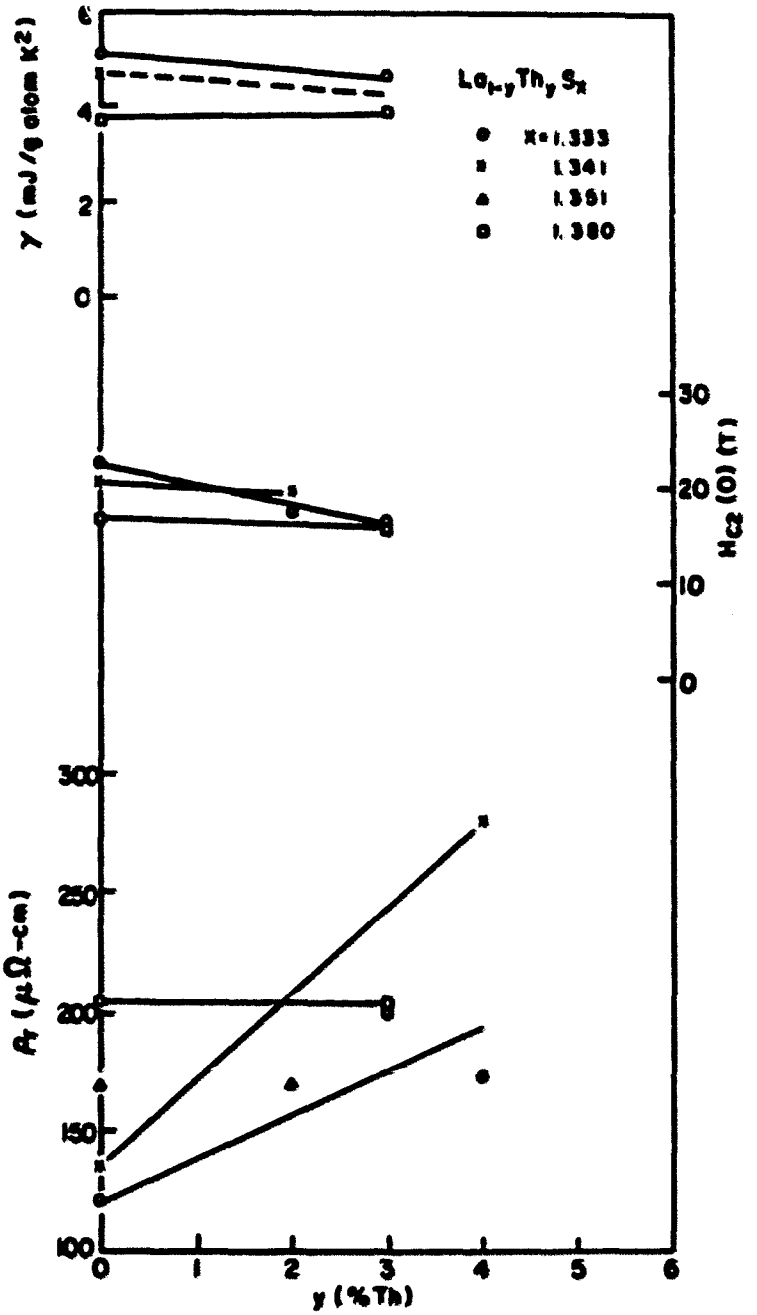

Figure 31. The effect of the Th additions on γ, $H_{c2}(0)$ and ρ_r in the metastable bcc phase of the pseudobinary sulfides

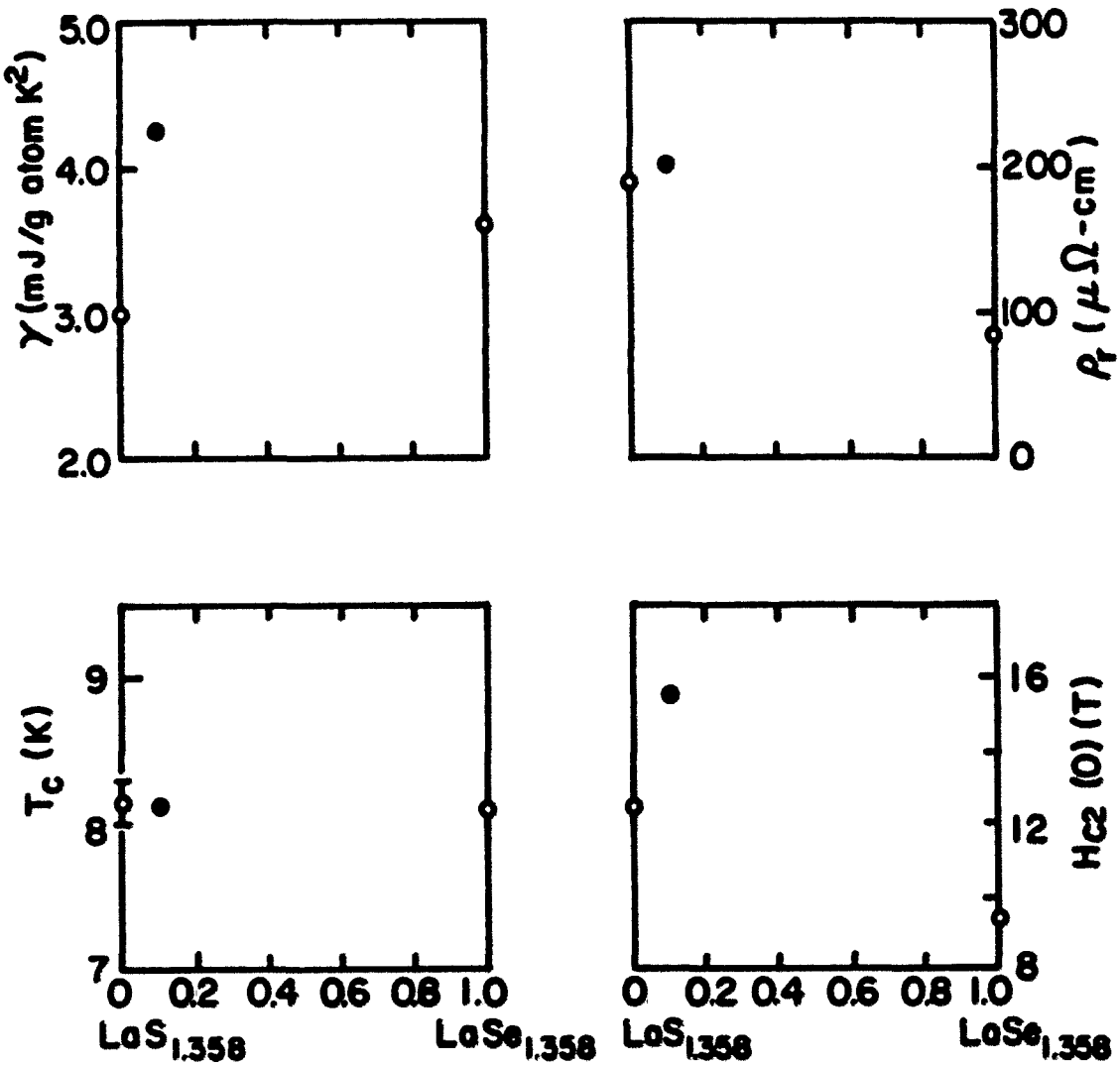

Figure 32. The effect of the replacement of 10 % S by Se on γ, ρ_r, T_c and $H_{c2}(0)$ in $La(S_{1-y}Se_y)_{1.358}$ alloys (y = 0.0, 0.102 and 1.0). The open and solid circles indicate that the alloys are in bct and bcc phases at low temperatures respectively

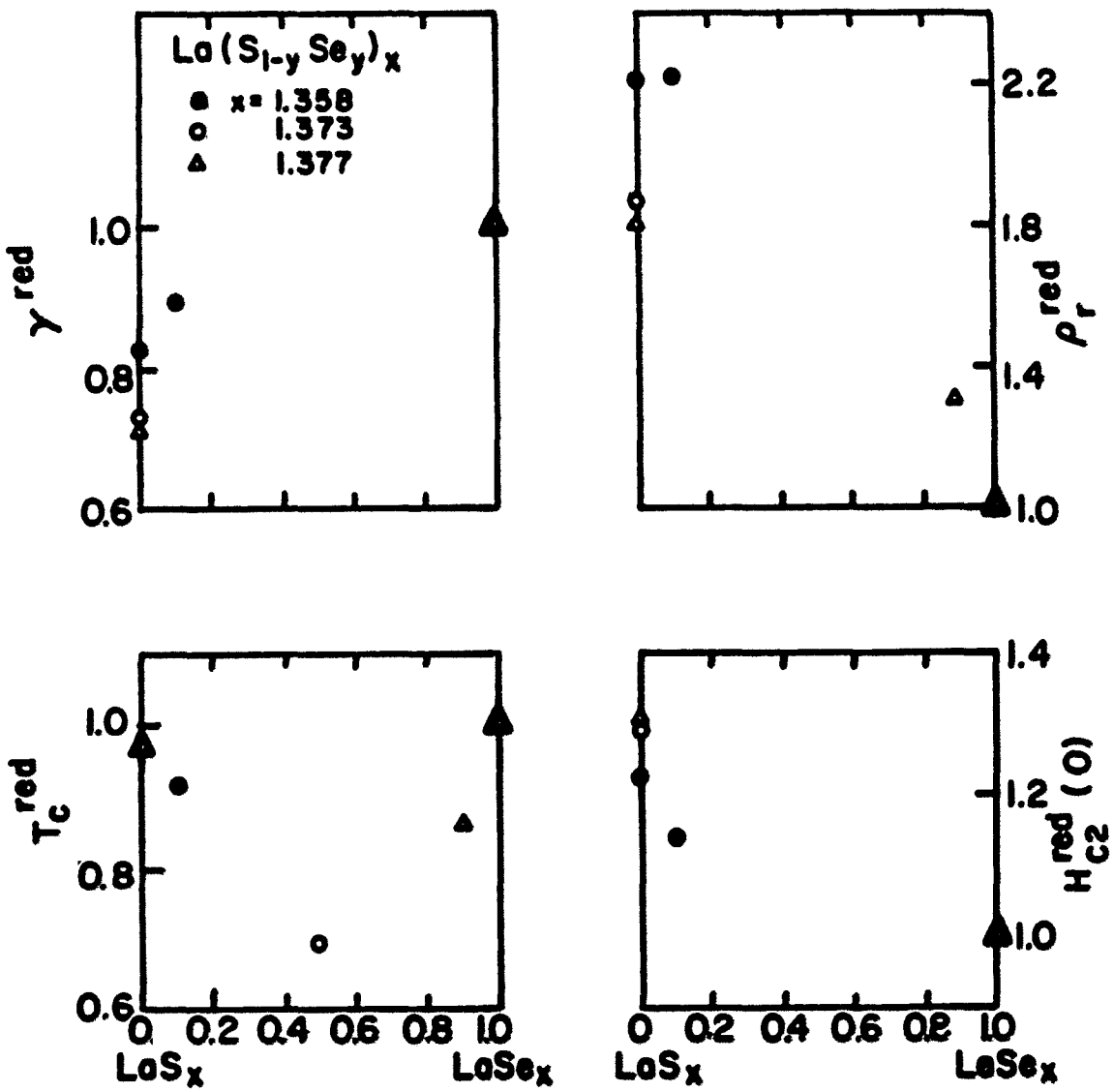

Figure 33. The effect of the substitution of S by Se on γ, ρ_r, T_c and $H_{c2}(0)$ in the metastable bcc phase of $La(S_{1-y}Se_y)_x$ alloys ($0.0 \leq y \leq 1.0$ and $1.358 \leq x \leq 1.377$). The data are reduced with respect to the $LaSe_x$ data

conduction electron screening of the ionic potential. The structural phase transformation with a c/a of 1.009[9] should not have too much effect on Θ_D. The scatter in the Θ_D values for $LaSe_{1.334}$ and $LaSe_{1.360}$ are due to the small samples for the heat capacity measurements. The heat capacities of the addenda were about 86 and 77 % of the total heat capacities for $LaSe_{1.334}$ and $LaSe_{1.360}$ respectively. This also accounts to some extent for the large entropy difference, ΔS, at T_c^*. The solid line for Θ_D in Fig. 30 was drawn to show the trend of the variation of the Θ_D values with the composition.

As seen in Fig. 30 for the selenides, the optimum superconducting properties, such as the highest T_c, γ, and $H_{c2}(0)$ values, are obtained at the critical composition (x_c = 1.363) of the structural phase transformation. Below x_c, the T_c values are not sensitive to the composition (see Figs. 16(a) and 30) while T_M values are strongly composition dependent (see Fig. 14(a)). Above x_c, the composition (or the conduction electron concentration) has a strong effect on T_c as seen in Figs. 16(a) and 30. For $x < x_c$, the metastable bcc phase would have better superconducting properties. For example, the expected values are 10.8 K and 12.5 T for $LaSe_{1.334}$ which compare to the observed values of 7.3 K and 3.4 T respectively.

In Figs. 14(b) and 16(b), for x less than x_c of the sulfides (x_c = 1.362) the Th atoms tend to stabilize the bcc

phase at low temperatures, i. e., T_M is lowered and T_c consequently increases. As a critical amount of Th for inhibition of the phase change is exceeded, the Th addition will have a little effect on T_c. Further Th additions will decrease the T_c value. The effect of Th addition on T_c in the metastable bcc phase is shown in Fig. 17. With a smaller x value, i. e. with fewer vacancies, the substitution of Th for La degrades the T_c value rapidly, with initial Th concentrations. With a larger x value, e. g. x = 1.360, the Th addition up to 3 % increases the T_c value slightly. It is expected that the further Th addition will decrease the T_c value. The shape of the curves is thought to be due to two competing effects.[50] The increase in T_c is due to the availability of a larger number of conduction electrons as Th is substituted for La. The decrease in T_c is due to the replacement of La by Th which disrupts the superconducting chains of La atoms. The latter effect probably becomes more pronounced at smaller x and y values. At a larger x value, e. g. x = 1.360, the former effect probably becomes more pronounced. The effect of Th additions on γ and $H_{c2}(0)$ values in the metastable bcc phase follows more or less the trend as the effect on T_c. The ρ_r values in the Th alloys follow the Mathiessen's rule for a dilute alloy.

As seen in Figs. 14(b) and 16(b), the maximum in T_c and the inhibition of the transformation for $LaS_{1.333}$ occur at a

change in the electron concentration of about 0.013 electrons/atom ($LaS_{1.333}$ transforms while $La_{.97}Th_{.03}S_{1.333}$ does not). As x increases toward x_c, the inhibition occurs at a smaller change in the electron concentration.

The $La(S_{1-y}Se_y)_x$ alloy system was examined to see whether the La-La separation influences the T_M and T_c to some extent. The lattice parameters of the three $La(S_{1-y}Se_y)_x$ alloys listed in Table 2 follow the Vegard's law for a solid solution system. As seen in Fig. 32 for x = 1.358 alloy, the replacement of 10 % of Se for S stabilizes the bcc phase. This substitution has little or no effect on T_c, as expected for x close to x_c, but increases γ and $H_{c2}(0)$ to values, which are larger than either bct $LaS_{1.358}$ or bct $LaSe_{1.358}$. In the stable or metastable bcc phase as shown in Fig. 33, the pseudobinary alloy has lower T_c value than the corresponding binary alloys. Also, the $H_{c2}(0)$ data point lies below the interpolated line drawn from two end binary alloys. Since the T_c dependence does not interpolate between the binary sulfides and selenides, the La-La separation is not the sole parameter in determining the T_c value.

The values of λ, N(0), $\Delta C/\gamma T_c$, D(t), $H_c(0)$ and κ have been calculated from the heat capacity results and it is found that the values of λ, N(0), $2\Delta(0)/kT_c$ and $H_c(0)$ reach maximum values at x_c for the selenides. The effect of Th additions on the magnitude of these values follows the same trend as the

effect on T_c, γ, and $H_{c2}(0)$. The high values of $\Delta C/\gamma T_c$, $2\Delta(0)/kT_c$ and κ in the selenides and sulfides as compared to the BCS prediction of 1.43, 3.53 and 0.71 for a weak-coupling type-I superconductor make them high field strong-coupling type-II superconductors.

B. Related Phase Transformation in Other Superconductors

The high density of state, N(0), is important for superconductivity in La-chalcogenides. It is thought that the Fermi level is located in the narrow 5d band. The maximum N(0) value is found at the x_c of the phase transformation. Further increasing of the N(0) induces the d-band instability such that the conduction electrons are redistributed in the tetragonal phase to lower the free energy and the density of state is also reduced.[16] The drop of the Pauli susceptibility on cooling[13] as the phase change occurs indicates a lower conduction electron concentration in the bct phase.

The nature of the phase transformations in the sulfide and selenide systems is similar to the one in A-15 high T_c superconductors.[51,52] They both transform from the cubic to the tetragonal phase and have anomalies in the Pauli susceptibilities and the softenings of the phonon modes in some directions at low temperatures for the bct alloys. The band Jahn-Teller model[51,53] has been proposed to explain the phase transformations in these systems. In this model, a

doubly degenerate electronic band is coupled to the shear mode of the cubic lattice by electron-phonon interaction. Exceeding the coupling limit, the doubly degenerate band is split and lattice distorts into the tetragonal phase. A recent paper published by K. Westerholt et al.[10] for the phase transformation in La_3S_4 and La_3Se_4 supports this model based on the magnetic field dependence of the T_M. The difference in phase transformation temperatures in 0 and 9 T (ΔT_M) is about 0.45±0.1 K for La_3Se_4. Ford et al.,[14] based on the phonon softening, a small c/a ratio and no multiplication of the unit cell edges, has suggested the transformation maybe elastic in nature. It could be that both electronic term and lattice strain are responsible for the transformation. Due to complicated crystal structure, the band structure has not been solved. It is hoped that good quality single crystals and experimental data on the materials will assist the theorists for such calculations.

C. Comparison with the Published Results

The comparison of our selenide data with the published results with respect to the T_c[1-5,54], T_M[3-5,9,10], γ[4] and Θ_D[4] values is shown in Fig. 34. The agreement of the magnitude of these values is quite good. For "La_3Se_4" with known T_M values between 60 to 65 K, the reported T_c values[3,4,5] are almost the same (7.4 to 7.8 K) and agree with our results on $LaSe_{1.334}$.

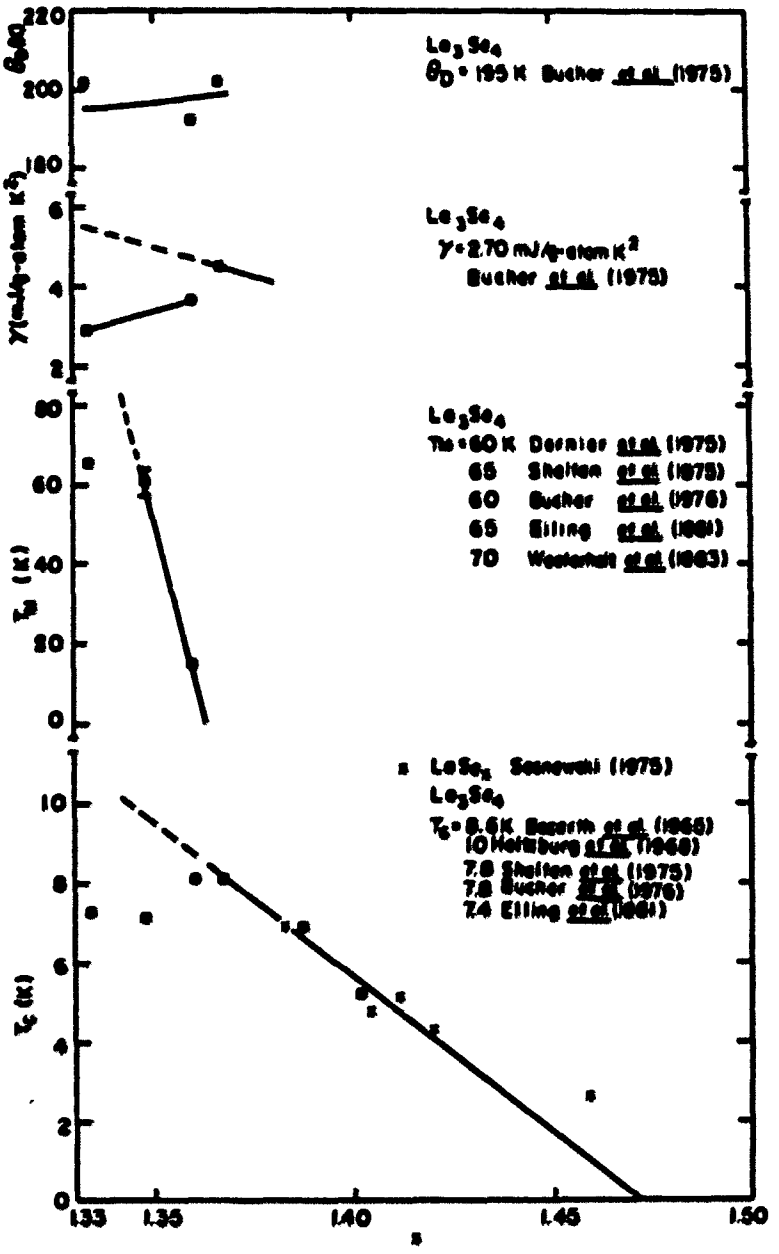

Figure 34. Comparison of the T_c, T_M, γ, θ_D values of the selenides with the published results

However, since our $LaSe_x$ or $La_{1-y}Th_yS_x$ alloys with x close to 1.333 always contain a second phase of LaSe or LaS, we believe that the results published on "La_3Se_4" alloys are also off stoichiometry. From Fig. 14(a), their alloys must have the compositions between 1.346 and 1.348. The difficulty in obtaining the perfectly stochiometric La_3Se_4 probably is because the minimum vapor pressure of the system lies at a sulfur-rich composition of $x > 1.333$. Furthermore, because the T_c of the bcc $LaSe_x$ phase has a strong compositional dependence, the vapor pressure minimum probably lies between 1.333 and the x_c. Ref. 16 reported the similar behavior in the LaS_x alloys.

VI. CONCLUSIONS

The lanthanum selenides and pseudobinary sulfides have been studied to investigate the influence of the bcc to tetragonal phase transformation on their superconducting properties. It was found that the suppression of this phase transformation improves the superconducting properties. The suppression is accomplished in this study by alloying with Th or substitution of S be Se.

From the thermodynamic calculations, the values of $\Delta C/\gamma T_c$, $H_{c2}(0)$ and κ have been estimated. The high values of $\Delta C/\gamma T_c$ indicate that the alloys studied in this work are strong-coupling. The high magnitude of the $H_{c2}(0)$ and κ values shows that the materials are type-II superconductors.

VII. REFERENCES

1. R. M. Bozorth, F. Holtzburg, and S. Methfessel, Phys. Rev. Lett. 14, 952 (1965).

2. F. Holtzburg, P. E. Seiden, and S. Von Molnar, Phys. Rev. 168, 408 (1968).

3. R. N. Shelton, A. R. Moodenbough, P. D. Dernier, and B. T. Mattias, Mat. Res. Bull. 10, 1111 (1975).

4. E. Bucher, J. P. Maita, G. W. Hull, Jr., and L. D. Longinotti, Z. Phys. B 25, 41 (1976).

5. A. Eiling, J. S. Schilling, and H. Bach, Physics of Solid Under Pressure, edited by J. S. Schilling, and R. N. Schelton (North-Holland, Amsterdam, the Netherlands, 1981), p. 385.

6. P. I. Kripyakevich, Soviet Phys.- Crys. 7, 556 (1963).

7. P. J. Flahaut, M. Guittard, M. Patrie, M. P. Pardo, S. H. Golabi, abd L. Domange, Acta Cryst. 19, 14 (1965).

8. W. B. Pearson, The Crystal Chemistry and Physics of Metals and Alloys (John Wiley & Sons, Inc., Canada, 1972).

9. P. D. Dernier, E. Bucher, and L. D. Longinotti, J. Solid State Comm. 15, 203 (1975).

10. K. Westerholt, H. Bach, S. Methfessel, D. K. Ray, and S. K. Ghatak, Solid State Comm. 45, 137 (1983).

11. G. L. Guthrie, and R. L. Palmer, Phys. Rev. 141, 346 (1966).

12. K. Westerholt, H. Bach, R. Wendemuth, and S. Methfessel, Solid State Comm. 31, 961 (1979).

13. K. Westerholt, H. Bach, R. Wendemuth, and S. Methfessel, J. Phys. F 10, 2459 (1980).

14. P. J. Ford, W. A. Lambson, A. J. Miller, G. A. Saunders, H. Bach, and S. Methfessel, J. Phys. C 13, L697 (1980).

15. K.Ikeda, K. A. Gschneidner, Jr., B. J. Beaudry, and T. Ito, Phys. Rev. B 25, 4618 (1982).

16. K. Ikeda, K. A. Gschneidner, Jr., B. J. Beaudry, and U. Atzmony, Phys. Rev. B 25, 4604 (1982).

17. B. W. Batterman, and C. S. Barret, Phys. Rev. Lett. 13, 390 (1964).

18. H. G. Smith, and W. Gläser, Phys. Rev. Lett. 25, 1611 (1970).

19. L. R. Testardi, J. J. Hauser, and M. H. Read, Solid State Comm. 9, 1829 (1971).

20. A. C. Lawson, and N. H. Zachariasen, Phys. Lett. A 38, 1 (1972).

21. E. W. Collings, J. C. Ho, and R. Jaffee, Phys. Rev. B 5, 4435 (1972).

22. V.A. Finkel, and N. A. Pushkarev, Soviet Phys. JETP 46, 1220 (1977).

23. A. Junod, and J. Muller, Solid State Comm. 36, 721 (1980).

24. H. R. Khan, Physica B 107, 483 (1981).

25. R. N. Shelton, and R. P. Dougherty, Physica B 107, 475 (1981).

26. D. W. Harrison, K. C. Lim, J. D. Thompson, C. Y. Huang, P. D. Hambourger, and H. L. Luo, Phys. Rev. Lett. 46, 280 (1980).

27. P. D. Hambourger, J. C. Ho, and H. L. Luo, Phys. Rev. B 26, 1446 (1982).

28. K. Westerholt, H. Bach, and S. Methfessel, Solid State Comm. 36, 431 (1980).

29. G. T. Meaden, Electrical Resistance of Metals (Plenum Press, New York, 1965).

30. E. S. R. Gopal, Specific Heats at Low Temperatures (Plenum Press, New York, 1966).

31. K. Maki, Physics 1, 21 (1964).

32. B. B. Goodman, Phys. Lett. 1, 215 (1962).

33. B. B. Kim, C. F. Hempstead, and A. R. Strnad, Phys. Rev. 139, A1163 (1965).

34. D. W. Mellon, Ph.D. thesis, Iowa State University (1970) (unpublished).

35. T. A. Vyrostek, Ph.D. thesis, Iowa State University (1974) (unpublished).

36. J. R. Hopkins, Ph.D. thesis, Iowa State University (1972) (unpublished).

37. W. E. Kienzle, Ph.D. thesis, Iowa State University (1973) (unpublished).

38. D. W. Osborne, H. E. Flotow, and F. Schreiner, Rev. Sci. Instr. 38, 159 (1967).

39. T. C. Cetas, J. C. Holste, and C. A. Swenson, Phys. Rev. 182, 679 (1969).

40. Thermophysical Properties of Matter, The TPRC Data Series, Vol. 4, edited by Y. S. Touloukian (Plenum, New York - Washington, 1970), p. 252.

41. H. Padamsee, J. E. Neighbor, and C. A. Shiffman, J. of Low Temp. Phys. 12, 387 (1973).

42. J. Bardeen, L. N. Cooper, and J. R. Schrieffer, Phys. Rev. 108, 1175 (1957).

43. D. K. Finnemore, and D. E. Mapother, Phys. Rev. 140, A507 (1965).

44. B. B. Goodman, Compt. Rend. 246, 3031 (1958).

45. C. Hohlfeld, and B. Pietrass, J. of Low Temp. Phys. 48, 503 (1982).

46. W. L. McMillan, Phys. Rev. 167, 331 (1968).

47. K. H. Bennemann, and J. W. Garland, Superconductivity in d- and f- Band Metals (AIP Conf. Proc. No. 4), edited by D. H. Douglass (AIP, New York, 1972), p. 103.

48. D. L. Johnson, and D. K. Finnemore, Phys. Rev. 158, 376 (1967).

49. L. P. Gor'kov, Soviet Phys. JETP 10, 593 (1960).

50. K. A. Gschneidner, Jr., K. Ikeda, Y. -C. S. Yeh, B. J. Beaudry, O. D. McMasters, C. B. Vining, and R. N. Shelton, Superconductivity in d- and f- Band Metals, edited by W. Buckel and W. Weber (Karlsruhe, West Germany, 1982), p. 431.

51. J. Labbé, Phys. Rev. 172, 451 (1968).

52. L. J. Vieland, and A. W. Wicklund, Phys. Lett. 34A, 43 (1971).

53. L. P. Gor'kov, and O. N. Dorokhov, J. of Low Temp. Phys. 22, 1 (1976).

54. J. Sosnowski, Phys. Stat. Sol. (b) 72, 403 (1975).

VIII. ACKNOWLEDGEMENTS

I would like to express my sincere thanks to Dr. Karl A. Gschneidner, Jr., my major professor, for suggesting the project, for his advice and encouragement throughout this project. I am also indebted to Mr. B. J. Beaudry for the preparation of some of the sulfide samples and for his advice on the preparation of selenide samples; to Dr. T. Takeshita for useful discussion on the materials; to Dr. R. J. Stierman, Mr. J. O. Moorman and Dr. S. K. Dhar for their assistance in taking the capacitance and addenda raw data; to Dr. T. -N. E. Tsang for the help with the computer work for the addenda change; to Mr. P. E. Palmer for his assistance in using the resistance furnace for heat treating; and to Mr. O. D. McMasters for loaning the X-ray computer program for the determination of the lattice parameters. I would also like to thank Mr. J. O. Moorman for his expert technical assistance in keeping the calorimeter going, and Mr. R. Whetstone for the usage of the laboratory equipment concerning the material preparation.

I also wish to thank Dr. D. K. Finnemore, Dr. R. N. Shelton and Mr. J. Ostenson for the assistance in using their a. c. magnetic susceptibility units, and Dr. R. N. Shelton for loaning the Sn sample.

IX. APPENDIX

A. GRT Calibration

The constants A_i's in Eq. (3-1) for H = 0.00 T are listed rowwise.

For temperatures between 0.8 and 6.5 K :

0.793482552115 60D 03	-0.945879990977 80D 03
0.496219354184 60D 03	-0.149944219980 60D 03
0.287929500933 90D 02	-0.364933006388 10D 01
0.305694634772 40D 00	-0.163371111542 80D-01
0.505868131068 20D-03	-0.691919453505 40D-05

For temperatures between 4.0 and 21 K :

0.544468929257 30D 02	-0.106129813517 30D 03
0.952898720938 60D 02	-0.483179266907 70D 02
0.153330543834 90D 02	-0.318654128279 00D 01
0.436848601379 40D 00	-0.382996561056 70D-01
0.195516362532 50D-02	-0.443460625382 10D-04

The constants a_i's in Eq. (3-2) for T vs. CAP are listed rowwise.

For temperatures between 1.5 and 5.1 K :

-0.346734320928 21D 04	0.466903334243 42D 00
-0.210789141573 29D-04	0.319383533987 04D-09

For temperatures between 4.0 and 8.0 K :

0.604598917769 28D 02	-0.833212982625 99D-02
0.26-292218489 30D-06	

For temperatures between 7.0 and 20.2 K :

0.193373737844 06D 04	-0.975402852982 36D-01
-0.156485657148 25D-04	0.155597478992 35D-08
-0.492152896770 19D-13	0.533722987492 43D-18

The constants b_i's in Eq. (3-3) for CAP vs. T are listed rowwise.

For temperatures between 1.5 and 5.1 K :

0.212465593596350 05	-0.172324268064930 00
0.166235910569780 03	-0.426461916579260 02
0.538208550782160 01	-0.276515703531630 00

For temperatures between 4.0 and 8.0 K :

0.209112627849750 05	0.377587300444960 03
-0.104363337928250 02	0.258830941415080 00

For temperatures between 7.0 and 20.2 K :

0.210506417905680 05	0.309251499345290 03
0.294526383837920 01	-0.106358167068100 01
0.654815324611740-01	-0.121923113727090-02

The constants B_i's (derived in the same manner as A_i's in Eq. (3-1)) in magnetic fields are listed rowwise.

H = 2.50 T, for temperatures between 1.6 and 6.5 K :

0.481094837221460 04	-0.520798619427620 04
0.245296211962510 04	-0.656079366120540 03
0.108980566026810 03	-0.115129510216060 02
0.755415353959430 00	-0.281471840562810-01
0.455980493580860-03	

H = 2.50 T, for temperatures between 4.0 and 21 K :

-0.176186335716680 03	0.279438489410890 03
-0.188691562129460 03	0.726195840578180 02
-0.174844406605280 02	0.269856295242640 01
-0.260677684255910 00	0.143969881032660-01
-0.347623773024270-03	

H = 5.39 T, for temperatures between 1.6 and 6.5 K :

0.215522144104020 04	-0.229548134248790 04
0.106366100288600 04	-0.279673817782500 03
0.456426179777910 02	-0.473601949115250 01
0.305240285662430 00	-0.111760041307220-01
0.178032337674810-03	

H = 5.39 T, for temperatures between 4.0 and 21 K :

0.738565040972530 02	-0.119380057837210 03
0.878197287999460 02	-0.362853469826410 02
0.917907369879820 01	-0.145815665559980 01

0.142337554950620 00 -0.782286364230290-02
0.185742949686340-03

H = 7.62 T, for temperatures between 1.6 and 6.5 K :

0.265159933392160 04 -0.272192880890110 04
0.121567467147950 04 -0.308154379192260 03
0.484871841493740 02 -0.485041588150140 01
0.301318987549180 00 -0.106304545270530-01
0.163104271369780-03

H = 7.62 T, for temperatures between 4.0 and 21 K :

0.129177488115700 03 -0.200425371779180 03
0.139146644366720 03 -0.546341474356700 02
0.132279596318430 02 -0.202233068375830 01
0.190735306285000 00 -0.101537308292760-01
0.233802061217060-03

H = 9.98 T, for temperatures between 1.6 and 6.5 K :

0.215426037679870 04 -0.207091515981380 04
0.867002658378930 03 -0.206078973081170 03
0.304032084042130 02 -0.285044039662610 01
0.165833661800000 00 -0.547327394441190-02
0.784525723132540-04

H = 9.98 T, for temperatures between 4.0 and 21 K :

-0.263883633028880 03 0.394926390706890 03
-0.251826308924000 03 0.907689554160990 02
-0.202693162759350 02 0.287373311754120 01
-0.252782052368890 00 0.126196004450800-01
-0.273850884665360-03

B. Heat Capacities of Cu and the Revised Addenda

The γ and Θ_D values from first heat capacity measurement of the Cu-reference standard were obtained by a least-squares fitting of the normal state data in five fields and are listed below.

γ = 0.8068 mJ/(g-atom K^2)
Θ_D = 354.58 K.

The published values for Cu are :

γ = 0.689 - 0.699 mJ/(g-atom K^2)
Θ_D = 343 - 349 K.

The coefficients A_i in the Cu-reference equation (Eq. (3-8)) in units of mJ/(g-atom K) are listed rowwise.

6.9434×10^{-1}	4.7548×10^{-2}	1.6314×10^{-6}
9.4786×10^{-8}	-1.3639×10^{-10}	5.3898×10^{-14}

The coefficients D_i in Eq. (3-7a) for the revised addenda are listed rowwise.

H = 0.00 T, for temperatures between 1.4 to 2.0 K :

-0.8787666617704406D 01	0.150627731979944D 02
-0.1002277476256820 02	0.3316754808445800 01
-0.5445897362793900 00	0.3546177659934310-01

H = 0.00 T, for temperatures between 1.7 to 2.8 K :

0.1474606534792380 01	-0.1216787627461200 01
0.4637826479446670 00	-0.8472712732507910-01
0.7556385413109220-02	-0.2635755800745870-03

H = 0.00 T, for temperatures between 2.0 to 5.0 K :

0.1720130173109900 00	0.2976139235205420-01
-0.1811674896151270-02	0.1704909873747470-03
-0.7100517460375500-05	0.1083912217002200-06

H = 0.00 T, for temperatures between 3.5 to 9.0 K :

0.1700389652525220 00	0.2342746865971130-01
-0.9499038669205250-04	0.3035475552374540-05
-0.4290059252090700-07	0.2073973309938990-09

H = 0.00 T, for temperatures between 7.0 to 20.0 K :

0.1913119515799040-01	0.2838931649492310-01
-0.8463094051449750-04	0.4034048909082330-06
-0.9683897540958920-09	0.9069909734446290-12

H = 2.50 T, for temperatures between 1.3 to 2.0 K :

0.4654664063668120 01	-0.9108565677563680 01
0.6959704978447120 01	-0.2522353475196600 01

```
 0.440550949759021D 00    -0.299302274542148D-01

H = 2.50 T, for temperatures between 1.7 to 2.8 K :

-0.181530141012730D 00     0.4596434937825910 00
-0.180144357481286D 00     0.339603204591079D-01
-0.302858676544922D-02     0.104032720205822D-03

H = 2.50 T, for temperatures between 2.0 to 5.0 K :

 0.2244106155180610 00     0.262136361042719D-02
 0.313079664546344D-02    -0.228152540050019D-03
 0.737779776936793D-05    -0.863639032121533D-07

H = 2.50 T, for temperatures between 3.5 to 9.0 K :

 0.2508349503153520 00     0.123396055122017D-01
 0.409144005217045D-03    -0.781153932689791D-05
 0.641000773957753D-07    -0.182002201157961D-09

H = 2.50 T, for temperatures between 7.0 to 20.0 K :

 0.2916913582954690 00     0.177460211715159D-01
 0.469770828285048D-04    -0.314042800799386D-06
 0.777495778499626D-09    -0.646231180555299D-12

H = 5.39 T, for temperatures between 1.4 to 2.0 K :

 0.534361210554974D 02    -0.834441500215243D 02
 0.521497635750089D 02    -0.162264789729587D 02
 0.251400526137987D 01    -0.155157330982037D 00

H = 5.39 T, for temperatures between 1.7 to 2.8 K :

-0.162298357706754D 01     0.2029950509973420 01
-0.850650084574790D 00     0.173454949719788D 00
-0.171258851992561D-01     0.657059954865263D-03

H = 5.39 T, for temperatures between 2.0 to 5.0 K :

 0.2220514825534680 00     0.688102959073851D-02
 0.184497350094451D-02    -0.890304077188339D-04
 0.136044105647191D-05     0.391208862193470D-08

H = 5.39 T, for temperatures between 3.5 to 9.0 K :

 0.2966943501391560 00     0.543510733847096D-02
 0.810691643312082D-03    -0.178596474815841D-04
 0.181760495567521D-06    -0.709840938371594D-09
```

H = 5.39 T, for temperatures between 7.0 to 20.0 K :

 0.1698092192664800 00 0.2278783010526350-01
-0.1689155267252530-04 0.5462572567689040-07
-0.1534894472067330-09 0.2066147490446670-12

H = 7.62 T, for temperatures between 1.4 to 2.0 K :

 0.3883163208174430 02 -0.5837177009586890 02
 0.3524194587184170 02 -0.1062819177674030 02
 0.1602342143550400 01 -0.9661301295917410-01

H = 7.62 T, for temperatures between 1.7 to 2.8 K :

-0.4502680016229170 01 0.4731088974534750 01
-0.1827378104876230 01 0.3415931154706280 00
-0.3064930594754600-01 0.1054903870188350-02

H = 7.62 T, for temperatures between 2.0 to 5.0 K :

 0.2423542332629720 00 0.2297684986642070-02
 0.1933886170035260-02 -0.3126875532312610-04
-0.3084702910507520-05 0.9472161925805310-07

H = 7.62 T, for temperatures between 3.5 to 9.0 K :

 0.3691895493362280 00 -0.2942322380218370-02
 0.1175274491892320-02 -0.2383431681852030-04
 0.2162174732381250-06 -0.7246159501605070-09

H = 7.62 T, for temperatures between 7.0 to 20.0 K :

 0.4805328296147840 00 0.1253109477666480-01
 0.1077764076849460-03 -0.5710088178136400-06
 0.1230275176761590-08 -0.9395731339057500-12

H = 9.98 T, for temperatures between 1.3 to 2.0 K :

-0.8904642168911850 00 0.1999517625720810 01
-0.1694834967717880 01 0.7295332770900750 00
-0.1507652251934040 00 0.1193047296542940-01

H = 9.98 T, for temperatures between 1.7 to 2.8 K :

-0.9558886336684060 00 0.9389273491845390 00
-0.2716621588361420 00 0.3661623767542690-01
-0.2159682717985790-02 0.3886647634231450-04

H = 9.98 T, for temperatures between 2.0 to 5.0 K :

```
 0.3718098761321300 00    -0.6290795757512000-01
 0.1404425907129690-01    -0.1091093952972920-02
 0.3976440450654880-04    -0.5500453778435970-06
```

H = 9.98 T, for temperatures between 3.5 to 9.0 K :

```
 0.1768040880916850 00     0.2592528619925030-01
-0.4752771533374170-03     0.1638090397629060-04
-0.2340387610283350-06     0.1161065286573690-08
```

H = 9.98 T, for temperatures between 7.0 to 20.0 K :

```
 0.2581774992154790 00     0.2215727231973770-01
-0.7269212425001840-04     0.5785651485732000-06
-0.1815961548382820-08     0.1899689740885460-11
```